The teratogenicity and cardiotoxicity of phenanthrene in zebrafish, *Danio rerio*

by

Chloe Reves

BSc (Biology), Trinity Western University, 2015

Project Submitted in Partial Fulfillment of the
Requirements for the Degree of
Master of Environmental Toxicology

in the
Department of Biological Sciences
Faculty of Science

© Chloe Reves 2024
SIMON FRASER UNIVERSITY
Summer 2024

Copyright in this work is held by the author. Please ensure that any reproduction or re-use is done in accordance with the relevant national copyright legislation.

Declaration of Committee

Name:	**Chloe Reves**
Degree:	**Master of Environmental Toxicology**
Title:	**The teratogenicity and cardiotoxicity of phenanthrene in zebrafish, *Danio rerio***
Committee:	**Chair:** **Bernie Crespi** Professor, Biological Sciences
	Chris Kennedy Supervisor Professor, Biological Sciences
	Glen Tibbits Committee Member Professor, Biomedical Physiology and Kinesiology
	Layne Myhre Committee Member Faculty Instructor, Biology Kwantlen Polytechnic University
	Ebi Lari Examiner Adjunct Professor, Biological Sciences

Ethics Statement

The author, whose name appears on the title page of this work, has obtained, for the research described in this work, either:

a. human research ethics approval from the Simon Fraser University Office of Research Ethics

or

b. advance approval of the animal care protocol from the University Animal Care Committee of Simon Fraser University

or has conducted the research

c. as a co-investigator, collaborator, or research assistant in a research project approved in advance.

A copy of the approval letter has been filed with the Theses Office of the University Library at the time of submission of this thesis or project.

The original application for approval and letter of approval are filed with the relevant offices. Inquiries may be directed to those authorities.

Simon Fraser University Library
Burnaby, British Columbia, Canada

Update Spring 2016

Abstract

Phenanthrene, classified as a tricyclic polycyclic aromatic hydrocarbon (PAH) and listed as a priority pollutant by the US Environmental Protection Agency, poses a potential hazard to fish. This study evaluated the effects of phenanthrene on the early development of zebrafish (*Danio rerio*) using an innovative passive dosing system. This system maintained consistent concentrations of phenanthrene below water solubility limits through a 5-d acute exposure period, allowing for an accurate assessment of its potential lethal, teratogenic, and cardiotoxic effects. Concentrations up to solubility limits did not result in sufficient mortality to calculate LC50 values, however, the derived 5-d LOEC (lowest-observed-effect concentration) and NOEC (no-observed-effect concentration) values for mortality were 110 and 50 µg/L, respectively. Following exposure, the maximal prevalence of teratogenic effects observed above the controls was 17 % pericardial edema, 15 % yolk edema, 18 % tail kinking and 15 % delayed hatching. Edemas showed evidence of reversibility. The cardiotoxic effects of phenanthrene in isolated adult zebrafish hearts exposed in situ (< 2 h) were examined using an optical mapping technique. Phenanthrene (110 µg/L) induced significant tachycardia (170 % ± 19.3 compared to control), shorter action potential durations (73.7 % ± 19.1) and calcium transient durations (89.2 % ± 30.0). A drug washout effect showed potential reversibility for the effects on heart rate, action potential, and calcium transient. The identified lethal, teratogenic, and cardiotoxic impacts arising from exposures to environmentally relevant concentrations of phenanthrene indicate possible implications for the overall survival and fitness of fish in phenanthrene contaminated environments.

Keywords: polycyclic aromatic hydrocarbons; phenanthrene; passive dosing; teratogenesis; development; cardiotoxicity; lethality; zebrafish

Acknowledgements

I would like to thank my senior supervisor, Dr. Chris Kennedy, for his guidance and support throughout this project. The valuable research skills I have learned from him have helped me critically evaluate my project and furthered my practices in science. I have gleaned a wealth of knowledge on many aspects of research including troubleshooting, refinement and thesis writing. I would like to thank Dr. Layne Myhre, who was instrumental on the creation of this project. Thank you for allowing me to work in your zebrafish research lab at Kwantlen Polytechnic University and for constantly checking in to ensure I had the resources I needed. Your feedback and support were very helpful in this process. I would like to thank Dr. Glen Tibbits, who also contributed to the creation of this project. Thank you for giving a MET student the opportunity to merge toxicology with cardiovascular physiology through the application of your research facility.

Thank you to the many people who assisted in this project in various capacity. A special thank you to Haruyo Kashihara, who put in many hours facilitating cardiac lab tests. Your diligence and patience were invaluable and I am extremely grateful for your contributions. I would also like to thank Eric Lin and Kaveh Rayani for their contributions to cardiac software training and support. Thank you to Ian Bercovitz, the statistics master. Thank you to the undergrad researchers at KPU- Jake Miller, Krista Warzel, Jaden Lewis and Kat Su- and their support with the aquatic facilities and fish husbandry at KPU. Thank you to the undergrad researchers at SFU- Charanveer Sahota, Farhang Tandas and Paolo Orosa- and their support with the spectrophotometry assays. Thank you to Mackenzie Edgar and Feng Lin for the instruction and troubleshooting of some experiments. Thank you to Elaine Taylor for the support with the aquatic facilities and fish husbandry at SFU.

Thank you to my MET peers in both the Kennedy and Marlatt. Karan, Isabella, Hannah, Manpreet, Hannah and Stephanie, your friendship and support enriched my SFU experience. A special thank you to Karan whose assistance in statistics was extremely helpful.

To my parents and family, thank you for your constant love and support through my academic ventures; I could not have done it without you. I am thankful to God for the many blessings in my life.

Table of Contents

List of Tables

List of Figures

List of Acronyms

AhR	Aryl hydrocarbon receptor
ARNT	AhR nuclear translocator
APD	Action potential duration
°C	Celsius
CT	Calcium transient
CaTD	Calcium transient duration
D	Days
DH	Delayed hatching
ENA	Erythrocytic nuclear abnormalities
ER	Estrogen receptor
H	Hours
HMW	High molecular weight
HOC	Hydrophobic organic compound
HPF	Hours post fertilization
HPLC	High performance liquid chromatographic
HR	Heart rate
I_{CaL}	L-type Ca^{2+} channel
I_{Kr}	Rapid delayed rectifier potassium channel
I_{Ks}	Slow-activating delayed rectifier potassium channel
K_{OW}	Octanol-water partition coefficient
LMW	Low molecular weight
OECD	Organization for Economic Cooperation and Development
OM	Optical mapping
PAC	Polycyclic aromatic compound
PAH	Polycyclic aromatic hydrocarbon
PD	Passive dosing
PDMS	Polydimethylsiloxane
PE	Pericardial edema
POP	Persistent organic pollutant
PP	Priority pollutant
SR	Sarcoplasmic reticulum
TK	Tail kinking

TPAHs	Concentrations of total PAHs
WAFs	Water accommodated fractions
XRE	Xenobiotic response element
YE	Yolk edema
ZEM	Zebrafish embryo medium

Chapter 1.

General Introduction

1.1. Polycyclic Aromatic Hydrocarbons

1.1.1. PAH Distribution and Sources

The major sources of polycyclic aromatic hydrocarbons (PAHs) are biological, pyrogenic, and petrogenic (Patel et al., 2020). Biologically-sourced PAHs are produced through long, slow processes that transform organic matter to PAHs by algae, plants, phytoplankton, and microbes (Rocha and Palma, 2019). Biogenic PAHs are also derived from diagenesis, the physicochemical processes that alter sediment profile after deposition (Lourenço et al., 2023). The compaction of sediment exposed to the effects of temperature and pressure leads to the gradual release of fossil fuels through this process. Due to their slow formation, biologically-produced PAHs are not considered a significant source of PAHs to the environment unlike pyrogenic and petrogenic PAHs (Abdel-Shafy and Mansour, 2016; Honda and Suzuki, 2020).

Pyrogenic sources of PAHs stem from the partial combustion of organic materials and includes both anthropogenic and natural production (Patel et al., 2020). These compounds have distinctive chemical characteristics and compositions that differ from other mixtures of PAHs. Pyrogenic PAHs predominantly include high molecular weight (HMW) PAHs like benzo[a]pyrene, benzo[b]fluoranthene, and benzo[k]fluoranthene; however, phenanthrene is a low molecular weight (LMW) included among them (Patel et al., 2020).

Pyrogenic PAHs have a number of major anthropogenic sources but are from three major areas including the metal industry, residential/commercial/institutional sources, and transportation (Environment and Climate Change Canada, 2022). For the metal industries, PAHs are released through processes such as iron casting, sintering, coal tar distillation, coal gasification, and coke manufacturing (Yang et al., 2002; CAREX Canada, 2023). For residential/commercial/institutional sources, PAH production is often attributed to heating and cooking whereas commercial and institutional sources stem from products like resins, wood-tar creosote, pesticides and paint (Abdel-Shafy and Mansour, 2016). For

transportation sources, PAHs are commonly released in automobile exhaust (Marr et al., 1999).

There are several natural sources of pyrogenic PAHs; however, their contribution to the overall presence of PAHs in aquatic environments is relatively small compared to anthropogenic sources. The significance of natural sources lies in their potential to contribute to local or regional variations in PAH concentrations, particularly in areas affected by wildfires or volcanic activity. However, the majority of PAH contamination observed in aquatic environments is attributed to human activities and the combustion of fossil fuels and biomass.

Petrogenic sources of PAHs include any PAH released through the production, handling, transport and storage of petroleum (Abdel-Shafy and Mansour, 2016) and are often released unintentionally into the environment. Petrogenic PAHs predominantly include LMW PAHs (Patel et al., 2020). One of the main avenues for release is through crude oil spills. Due to the nature of crude oil transport being closely associated with water systems, aquatic ecosystems are often most heavily impacted by petrogenic PAHs mainly associated with oil spills. Historically, oil spills have been ranked by size with small spills considered at less than 7 tons and large spills considered exceeding 700 tons (ITOPF, 2023). By volume, some of the most catastrophic oil spills include: Exxon Valdez (1989) – 11 M gallons, Kolva River (1994) – 84 M gallons and Deepwater Horizon (2010) – 134 M gallons (NOAA, 2020). While the annual rate of oil spills has decreased since 2007, oil spills still consistently occur each year. From 2010 – 2019, the global annual rate was 1.8 large oil spills per year (Sönnichsen, 2022). Additionally, oil escapes naturally from oil reservoirs as seepage. Global estimates of the annual oil seepage rate are predicted at approximately 20,000 t (Pampanin and Sydnes, 2013).

1.1.2. Physical and Chemical Properties and Structure

Among the growing concerns regarding environmental contaminants are those from PAHs, a prolific class of organic chemicals generally recognized as detrimental pollutants (Honda and Suzuki, 2020). More broadly, PAHs are considered under the large group of polycyclic aromatic compounds (PACs) which also include the polycyclic heterocycles and nitro-PAHs (Achten and Andersson, 2015). All PACs are defined by a core structure of hydrogen and carbon atoms arranged in at least 2 benzene rings (Lawal, 2017). The sub

groups can further be distinguished by their functional groups. The heterocycles contain an oxygen, nitrogen or sulfur atom their functional groups (Brinkmann et al., 2014) while nitro-PAHs contain a nitrogen-dioxide group (Bandowe and Meusel, 2017).

With over 100 known variants, PAHs are one of the most structurally-diverse groups of PACs (EPA, 2008). Of these, the 16 variants classified among EPA's priority pollutants (PP) are perhaps the most well-studied PAH structures (Figure 1.1). PAHs are broadly categorized into two different sub-groups. Low molecular weight (LMW) PAHs contain 2 to 3 benzene rings; these include bicyclic and tricyclic compounds such as naphthalene and phenanthrene, respectively (Lawal, 2017). Some of the literature considers LMW PAHs to include structures possessing up to 6 benzene rings (Abdel-Shafy and Mansour, 2016); however, the change in physiochemical properties seen in PAHs greater than 4 rings has led others to consider 4-ringed PAHs as intermediate-molecular weight PAHs (Choi et al., 2010). The definition adhered to by both Canadian and U.S regulatory bodies is that LMW PAHs possess 3 or fewer benzene rings. Both the Canadian Council of the Ministers of the Environment (CCME) and U.S EPA (USEPA) support this (CCME, 2010). The CCME defines a high molecular weight (HMW) PAH to possess 4 or more rings (CCME, 2010).

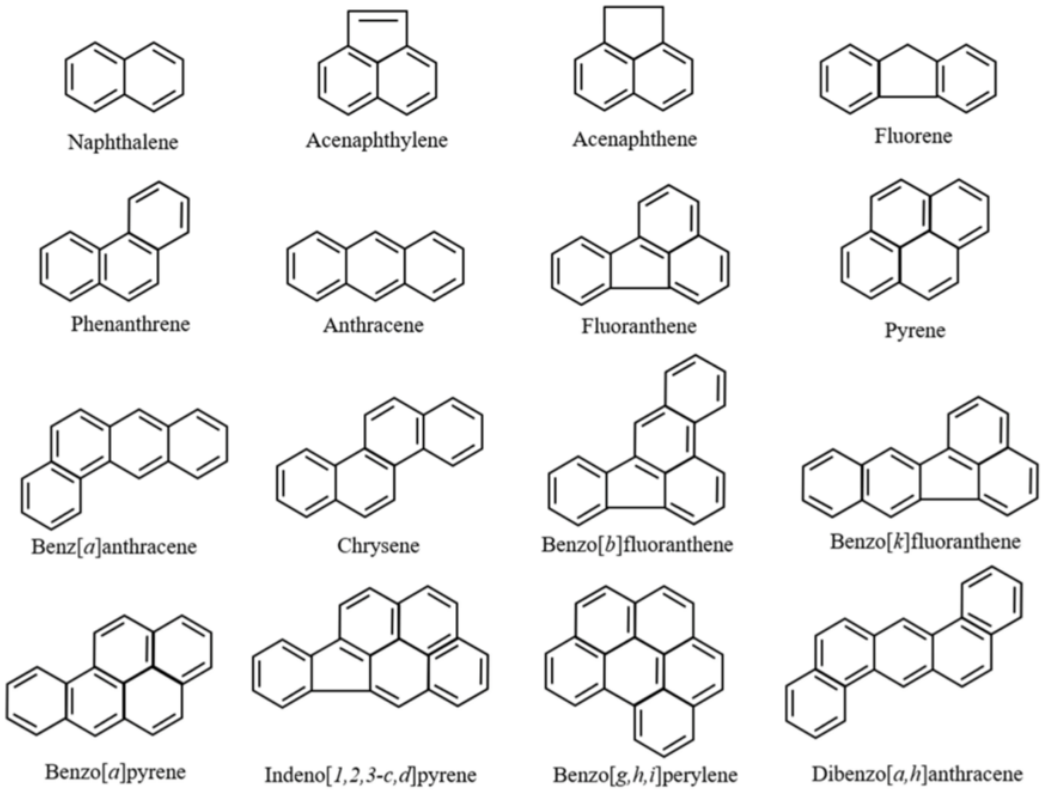

Figure 1.1. The 16 polycyclic aromatic hydrocarbons (PAHs) considered to be priority pollutants under the USEPA. (Honda and Suzuki, 2020).

The physiochemical properties of PAHs are related to their ring size. In general, PAHs are solid at room temperature due to their relatively high melting and boiling points (Abdel-Shafy and Mansour, 2016). Boiling points increase proportionately with ring size, with the lower range spanning between 200 to 400 °C for bicyclic and tricyclic PAHs and 500 to 600 °C for PAHs containing 6 or more rings (Achten and Andersson, 2015). PAHs possessing 4 to 5 rings exhibit boiling points in between this range from 300 to 500 °C. Similarly, melting point is positively correlated to ring size (e.g., 2-ringed naphthalene mp: 81 °C and 6-ringed benz*[ghi]*perylene: 278.3 °C) (Kielhorn et al., 2003). Comparatively, vapor pressure is inversely related to PAH ring size and becomes exponentially smaller for larger PAHs (e.g., naphthalene: 3.2×10^{-2} and benz*[ghi]*perylene: 1.4×10^{-8} Pa at 25 °C) (Kielhorn et al., 2003). A 13-fold increase in vapor pressure is observed as PAH size decreases from 10 to 2 rings (Achten and Andersson, 2015). Likewise, PAH water solubility is inversely proportional to ring size (Abdel-Shafey and Mansour, 2016) (e.g., naphthalene 9.18 and benz*[ghi]*perylene 0.00026 mg/L). A 5-fold reduction in water

solubility is seen with a size increase from a 2-ringed PAH to 10 rings (Achten and Andersson, 2015).

1.1.3. PAH Log K_{OW} Values and Chemical Partitioning

The concept of partitioning is used to understand the behavior of chemicals in organic and aqueous matrices. The octanol-water partition coefficient (K_{OW}) is a measurement used to predict how organic chemicals move between lipid-water systems (Alsaadi et al., 2018). This term represents the ratio of chemical dissolved in octanol v. water. The log K_{OW} value is inversely related to water solubility. Hydrophobicity describes a chemical's preference for an organic, non-polar environment over an aqueous, polar one. Hydrophobic chemicals tend to exhibit high log K_{OW} values while having low water solubility (Abdel-Shafy and Mansour, 2016). In general, HMW PAHs have higher log K_{OW} values, meaning their high lipid-water partitioning ratios enable them to more easily partition into lipids over water (Achten and Andersson, 2015; Alsaadi et al., 2018). By comparison, LMW PAHs are more water-soluble as represented by their lower log K_{OW} values, meaning low lipid-water partitioning ratios (Achten and Andersson, 2015; Abdel-Shafy and Mansour, 2016). A general trend among PAHs is that an increase in ring size (2 – 10) corresponds to an increase in log K_{OW} values (3 – 10) and hydrophobicity (Achten and Andersson, 2015). PAH alkyl functional groups are hydrophobic, therefore PAHs with these functional groups consequently exhibit higher log K_{OW} values. Comparatively, PAHs with polar functional groups tend to be more hydrophilic and exhibit lower log K_{OW} values. Log K_{OW} values are useful in understanding the movement of PAHs in aquatic systems and enable the prediction of environmental fate and bioavailability.

1.1.4. Environmental Fate

PAH distribution and fate in aquatic ecosystems is influenced by their physical-chemical properties including vapor pressure, volatility and water solubility. These properties collectively effect how PAHs move through the environment and ultimately their fate. In general, LMW PAHs have higher vapor pressure than HMW PAHs (Choi et al., 2010). This higher vapor pressure leads to LMW PAHs being more volatile and partitioning to the atmosphere at levels above HMW PAHs (Montuori et al., 2022). Comparatively, the low volatility of HMW PAHs make them less likely to evaporate into the atmosphere but rather remain in liquid or solid medias (Choi et al., 2010). Specifically, HMW PAHs are attracted

to hydrophobic medias as they have low water solubility so cannot readily dissolve in water (Abdel-Shafy and Mansour, 2016). Comparatively, LMW PAHs are generally more water-soluble than HMW PAHs and can be more easily entrapped in water.

PAHs are prone to adsorb onto solid particulate when they encounter them (Sabbah et al., 2004). Soil, sediment and dissolved organic matter (DOM) are common materials that adsorb PAHs. When PAHs adsorb and concentrate in the particulate phase as opposed to dissolving in water, PAH sinks can form. Sediment is a primary sink for PAHs and acts as a reservoir (Grmasha et al., 2023). Generally, HMW PAHs tend to be in greater quantities in solid media like sediment due to their increased tendency to adsorb in soil or sediment (Choi et al., 2010). Additionally, sediment type can impact PAH mobility as PAHs have reduced mobility in porous sands compared to sediment (Grmasha et al., 2023).

The binding of PAHs to DOM in water is influenced by characteristics of both the PAHs and DOM, as well as environmental conditions. The chemical composition of DOM, largely its functional groups, influence its ability to interact and bind with PAHs. Hydroxyl, carboxyl or phenolic groups in DOM can be triggered under light to make reactive oxygen species (ROS) which in turn interact with PAHs to potentially degrade them (Zhao et al., 2020). The properties of PAHs, such as their molecular weight, hydrophobicity, and chemical structure, affect their affinity for binding to DOM. PAHs are inherently hydrophobic, meaning they repel water and tend to associate with organic matter and lipids (Abdel-Shafy and Mansour, 2016). PAHs with higher molecular weights and greater hydrophobicity tend to exhibit stronger binding capacity to DOM. Interestingly, DOM-PAH complexes that form can reduce their overall adsorptive behavior, lending to increased solubility of PAHs (Sabbah et al., 2004). PAH-DOM complexes may also increase the persistence of PAHs in water (Sabbah et al., 2004). In particular, colloids, amphiphilic molecules containing a hydrophobic center surrounded by a hydrophilic region, may entrap PAHs in their hydrophobic region, protecting them from degradation processes or sequestering it in dissolved form (Nagpal, 1993).

A key aspect of environmental fate is bioavailability, which refers to the amount or dose of compound that has the potential to be absorbed by an organism (Vallero, 2016). PAHs can exist in two primary forms: freely dissolved in the water (water-soluble) and bound to organic matter or sediment particles (non-water-soluble). Only the water-soluble fraction of PAHs is bioavailable to aquatic organisms. The bound or non-water-soluble PAHs are

effectively sequestered and less accessible to organisms (Haftka et al., 2010). Generally, LMW PAHs tend to be freely dissolved while HMW PAHs are often bound and less bioavailable (Jung et al., 2013). The bound fraction often constitutes a significant portion of the total PAHs in aquatic ecosystems but does not pose an immediate threat to aquatic life unless it becomes resuspended or undergoes desorption processes. However, under certain conditions, the binding interactions can also facilitate the transfer of PAHs across biological membranes. Low DOM concentrations have been found to increase PAH bioconcentration in some cases (Haftka et al., 2010). As well, variation in the organic matter comprising DOM can increase DOM lipophilicity, leading to increased affinity for compounds to adsorb to DOM. Under these conditions, PAH-DOM binding can increase PAH bioavailability. Therefore, PAH bioavailability varies based on the conditions surrounding PAH-DOM binding interactions.

DOM and microbiota have been shown to aid the transport of PAHs from surface water to deeper waters (Li et al., 2020). DOM can form large aggregates known as marine snow whose masses of inorganic matter, detritus and live organisms can entrap PAHs (Koudryashova et al., 2022). Marine snow is particularly known as a sink for HMW PAHs and often leads to PAH-contaminated sea floors and sediment. PAHs can further spread into the water column by scavenging microorganisms that eat DOM and later expel PAHs in fecal pellets (Koudryashova et al., 2022). Environmental conditions including temperature, pH, and ionic strength, also play a role in PAH-DOM binding. Higher temperatures and lower pH levels generally enhance the binding interactions, while elevated ionic strength may reduce binding due to increased competition for binding sites (Haftka et al., 2010).

Abiotic factors such as water temperature and salinity influence PAH bioavailability (Lee et al., 2015). Firstly, PAHs dissolve more readily in warmer water. PAH solubility in water increases 3 to 4 x when water temperature is increased from 5 to 30 °C (Nagpal, 1993). While PAH solubility decreases in cold water, PAH degradation is slowed, adding to increased persistence. Secondly, PAHs dissolve more readily in low salinity conditions (Tremblay et al., 2005). In high salinity conditions PAHs more easily adsorb to solids due to a “salting out’ effect which is the tendency for PAHs to precipitate out due to decreased solubility (Oh et al., 2013). High salinity also favors the tendency for PAH particulate to distribute into organic media over aqueous media, further increasing sorption behavior (Oh et al., 2013).

The ability for PAHs to move through biological membranes is influenced by their physiochemical properties, including molecular size and lipophilicity. Smaller, more water-soluble PAHs (LMW PAHs) can pass through biological membranes more easily than larger, less-soluble ones. All PAHs have a degree of lipophilicity, or inherent tendency to associate with hydrophobic materials (Abdel-Shafy and Mansour, 2016). Generally, an increase in PAH molecular size increases lipophilicity, enabling PAHs to more easily pass through hydrophobic membranes or regions. Once PAHs penetrate an organism's membrane their mode of toxicity is often elicited through interactions with cellular components or enzyme systems related to the membrane that potentially disrupt essential biological processes (Abdel-Shafy and Mansour, 2016). Additionally, toxicity can occur through bioaccumulation, or the gradual buildup of PAHs in an organism. The ability to penetrate biological membranes is a key factor in the bioavailability of PAHs to aquatic organisms.

1.1.5. PAH Toxicity

Acute Toxicity

PAH exposure may pose significant challenges to aquatic organisms like fish, including lethal and sublethal effects. Lethal toxicity is usually acute and represents the more immediate and severe consequences of PAH exposure. Sublethal toxicity occurs at lower concentrations resulting in a wide range of effects which may not be immediately apparent, but can have long-term consequences affecting overall fitness. Understanding both lethal and sublethal toxicity is essential for comprehending the full scope of PAH-related effects in aquatic ecosystems and for developing effective strategies for mitigating their impact on fish populations.

In general, LMW PAHs tend to be more acutely toxic and have lower LC50 values compared to HMW PAHs (Salvo et al., 2016). This trend is attributed to several factors. LMW PAHs are typically more water-soluble, lending to higher amounts being present in the water and available for diffusion (Lin, 2020). Therefore, freely dissolved LMW PAHs are readily bioavailable to organisms. As HMW PAHs are more lipophilic than LMW PAHs, the poor water solubility lends to insufficient amounts being present in the water to cause acute toxicity (Salvo et al., 2016).

PAH concentrations that cause acute lethality vary for different PAH compounds and between fish species. Beginning with the smallest PAH, naphthalene, 96-h LC50 values range between 1200 and 5300 µg/L for pink salmon (*Oncorhynchus gorbuscha*) and mummichog (*Fundulus heteroclitus*), respectively (Moles & Rice, 1983; CCME, 1999). Tricyclic PAHs have been cited as some of the most toxic to fish (CCME, 1999). Among those with similar toxicity are acenaphthene and phenanthrene. Reported 96-h LC50 values for acenaphthene range between 580 and 3100 for brown trout (*Salmo trutta*) and sheepshead minnow (*Cyprinodon variegatus*) (Ward et al., 1981; Geiger et al., 1985). Similarly, phenanthrene reports 96-h LC50 values between 234 and 1400 for bluegill sunfish (*Lepomis macrochirus*) and Japanese rice fish (*Oryzias latipes*), respectively (CCME, 1999; Ministry of the Environment Japan, 2019). The tricyclic PAH fluorene shows slightly increased toxicity with 96-h LC50 values ranging between 473 and 910 µg/L for rainbow trout (*Oncorhynchus mykiss*) and bluegill sunfish (*Lepomis macrochirus*), respectively (Finger et al., 1985). Interestingly, some of the lowest acute toxicity values have been reported for anthracene, with 96-h LC50 values ranging between 1.6 and 46 µg/L for zebrafish (*Danio rerio*) and bluegill sunfish (Willis and Oris, 2014; Nagpal, 1993).

Highly acute toxicity ranges have been found to be common for 4-ringed PAHs. A literature search revealed pyrene to be one of the most toxic PAHs as acute toxicity ranged between 2.6 (96-h LC50) and 26 µg/L (120-h LC50) for zebrafish and fathead minnow (*Pimephales promelas*), respectively (Willis and Oris, 2014; Oris and Geisy, 1987). Benz[a]anthracene is only slightly less toxic with LC50 values ranging between 5.6 (40-h) and 48 µg/L(120-h) in fathead minnow (Oris & Giesy, 1987). Comparatively, fluoranthene has a larger range of sensitivity with 96-h LC50 values ranging between 12.3 and 620 µg/L for bluegill sunfish and Inland silverside (*Menidia beryllina*), respectively (Spehar et al., 1999). Both LMW and intermediate (4-ring) PAHs show similar acute toxicity across fish species.

A trend of decreasing acute toxicity appears among HMW PAHs for five or six-ringed PAHs. This is largely due to the highly insoluble nature of these HMW PAHs which limits their concentrations in water (Nagpal, 1993). Their insolubility also makes acute exposure testing difficult, which may explain the lack of toxicity data available in the literature. The acute toxicity data for HMW PAHs mainly reports on benzo[a]pyrene (BaP). BaP exhibits a wide range in toxicity, reporting 96-h LC50 values between 14 and 9600 µg/L for milkfish (*Chanos chanos*) and African sharptooth (*Clarias gariepinus*), respectively (Palanikumar et al., 2012; Ezike et al., 2019). Notably, environmental regulatory bodies such as the BC

Ministry of Environment have pointed out that low acute toxicity values derived in lab studies for HMW PAHs are not realistic; low acute toxicity conditions for HMW PAHs are often not achievable in the natural environment due to their low water solubility (Nagpal, 1993). Therefore, while Bap acute toxicity has also been reported in invertebrates (*Daphnia pulex*) at very low ranges (5 – 10 µg/L), the environmental significance of these toxicity values is debatable. While other HMW PAHs (eg., dibenz[a,h]anthracene, benzo[ghi]perylene, dibenz[a,h]anthracene…etc) have literature chronic toxicity values, the aforementioned BaP values sufficiently relay the broad acute toxicity of HMW PAHs (CCME, 1999).

Sublethal Toxicity

PAHs are known to induce a wide range of sublethal toxic effects in fish that encompass changes on a molecular to whole organism level. Some of the areas of sublethal toxicity include the following: genotoxicity, phototoxicity, teratogenesis, cardiotoxicity, endocrine disruption, impaired reproduction, tissue damage, homeostatic imbalances, immune system dysfunction and behavioral toxicity (Kennedy, 2015; Incardona et al., 2004).

PAH genotoxicity commonly causes chromosomal and DNA damage (Lam et al., 2018; Jung et al., 2011). Evidence for chromosomal damage was recorded in Atlantic killifish (*Fundulus heteroclitus*) sourced from a contaminated wood treatment facility in Portsmouth VA (sediment levels contained 200-400 g/g TPAH concentrations) (Jung et al., 2011). Fish exhibited elevated DNA adducts which showed increased covalent binding of benzo[*a*]pyrene (Jung et al., 2011). Similar genotoxic effects were observed in striped beak perch (*Oplegnathus fasciatus*) affected by the Hebei oil spill in South Korea (2007) (Lee et al., 2011). Additionally, PAHs can damage chromosomes by disrupting cell division or causing pre-mature DNA strand breakage often through inducing nucleotide mutations (Goanvec et al., 2008). As such, chromosomal damage may by reversible or irreversible based on how quickly PAHs may be metabolized and the organism's DNA repair potential. Chromosomal and DNA damage can lead to impairment at both the cellular and organ level, posing potential risk for genetic-induced mutations or diseases.

Photooxidation can increase the toxicity of PAHs (Kennedy, 2015). PAH-induced phototoxicity is dependent on several variables: 1) PAH tissue concentration, 2) the rate of formation of excited triplet state molecules from their former ground-state, 3) exposure

duration and absorption of SUVR (solar ultraviolet radiation), and 4) the probability of a reaction between the excited intermediate and the target molecule (Kennedy, 2015). An example of phototoxicity in fish was reported by Bowling et al. (1983); mortalities were only observed among bluegill sunfish (*Lepomis macrochirus*) co-exposed to anthracene (12.7 µg/L) and SUVR for 48 h compared to fish in shaded areas. However, introduction of sunlight into the shaded area after 4 d caused mortalities despite water-levels showing no traces of anthracene. Hence, mortalities were attributed to phototoxicity which may be exerted through oxidative stress (Bowling et al., 1983; Kennedy, 2015).

Chemical teratogenesis describes a host of structural abnormalities or developmental defects in early-life stage organisms resulting from exposure to chemicals like PAHs. Teratogenic deformities can be classified based on the affected body structure, the underlying mechanism, or other (Jarque et al., 2020). The mechanisms behind these PAH-induced teratogenic effects are broad and may include PAH interference with normal cellular processes or signaling pathways, leading to developmental disruptions. It is vital to note that the specific deformities and mechanisms can vary depending on the fish species, the timing and duration of PAH exposure, as well as the concentration and composition of the PAH mixture.

Some of the most prominent teratogenic deformities related to PAH exposures include edemas and spinal or tail deformities, both common symptoms of “blue sac syndrome” in fish (Billard et al., 2008). PAH-induced edemas have been documented in teleosts like zebrafish (Jung et al., 2013; Perrichon et al., 2016; Philibert et al., 2016), Pacific herring (*Clupea pallasi*) (Carls et al., 1999, 2009); yellowfin tuna (*Thunnus albacares*), bluefin tuna (*Thunnus thynnus*) (Brette et al., 2014) and pink salmon (*Oncorhynchus gorbuscha*) (Carls and Thedinga, 2010). Pericardial edema is associated with impaired blood flow, reduced angiogenesis and potential cardiac failure while yolk edema is related to disrupted nutrient cycling (Billard et al., 2008; Cypher et al., 2017). Both PAH mixtures or single PAHs may cause edemas at low concentrations. For eg., Alaska North Slope crude oil (TPAH = 0.6 - 0.7 µg/L) and *Erika heavy oil* (TPAH = 0.0084 – 119 µg/L) caused edemas in Pacific herring embryos and zebrafish, respectively (Carls et al., 1999; Perrichon et al., 2016). Likewise, single PAH exposures of dibenzothiophene, fluorene and phenanthrene (> 9000 µg/L) caused edemas in zebrafish (Incardona et al., 2004). PAH teratogenesis can also target the tail and spinal region of fish. PAHs disrupt somitogenesis, the mesoderm developmental process responsible for skeletal muscle, tendon, and cartilage formation

critical to spine and tail development (Descalso, 2019). Tail and spinal deformities have been associated with alterations to swimming behavior in fish (de Soysa et al., 2012; Li et al., 2019). Both PAH mixtures or single PAHs have been reported to induce tail and spine deformities. For eg., PAH mixtures (TPAH = 1840 µg/L) induced tail malformations in zebrafish after 5 d (Li et al., 2019). As well, tail curvature was recorded in 96-h zebrafish larvae exposed to phenanthrene, dibenzothiophene, and fluorene (> 9000 µg/L) (Incardona et al., 2004).

PAH cardiotoxicity pertains to a host of symptoms targeting the heart (Incardona et al., 2004). Common PAH-induced cardiotoxic symptoms include bradycardia, cardiac arrhythmias and alterations to electrical conduction, ion channels, and heart structure (Perrichon et al., 2016; Brette et al., 2014). For example, Pacific herring (*Clupea pallasi*) embryos exposed to oil effluents (TPAH: 620 – 8100 ng/g wet weight) exhibited dose-dependent cardiac arrythmias (Incardona et al., 2009). PAHs induce heart defects mainly by interfering with cardiac ion channels (Brette et al., 2014). These interferences often effect a critical step in the heart excitation process known as action potential duration (APD) period in which ion channels are regulated (Brette et al., 2014). PAHs (TPAH = 4 – 61 µg/L) have been shown to prolong APD cycles in juvenile cardiomyocytes of yellowfin (*Thunnus albacares*) and bluefin tuna (*Thunnus thynnus*) (Brette et al., 2014). Furthermore, PAHs can induce morphological cardiac effects. Zebrafish exposed to LMW PAHs (phenanthrene, fluorene, and dibenzothiophene) had abnormal hearts with thin dilated walls that exhibited a collapse and stretching cycle symptomatic of cardiac looping impairment (Incardona et al., 2004).

Many studies substantiate the occurrence of PAH-induced endocrine disruption (ED) in fish which cover many effects. Increased feminization in males has been associated with PAH-induced upregulation of estrogen receptor (ER) and subsequent elevation of vitellogenin levels (Tollefsen et al., 2011). Fish species like Atlantic cod (*Gadus morhua*) (Tollefsen et al., 2011), Yucatan gambusia (*Gambusia yucatan*) (Aguilar et al., 2021), and common roach (*Rutilus rutilus*) (Liney et al., 2006) have reported male feminization following PAH exposure. Male feminization can harm fish populations by causing developmental delays or morphological abnormalities. For instance, PAH-exposed mosquito fish (*Gambusia affinis*) exhibited delayed development of modified anal fins and hemal spines in males (Huang et al., 2019). Conversely, PAH-induced ER upregulation

led to masculinization of females, with their anal fins resembling gonopodium-like structures seen in males (Huang et al., 2019). PAHs also disrupt hormones, enzymes, and steroids through various mechanisms, including interference with hormone synthesis, receptor binding, and signaling pathways. For example, the PAH fluoranthene disrupts the thyroid hormone system, affecting thyroid hormone production and metamorphosis (Fernandes et al., 2010). PAHs can inhibit aromatase, an enzyme responsible for converting androgens to estrogens, causing imbalances in sex hormones (Santos et al., 2017). Furthermore, PAHs can alter steroids which may interfere with sex-steroid binding proteins (SBPs) responsible for transporting and regulating steroids (Tollefsen et al., 2011).

PAHs can significantly impact populations by effecting reproduction. Two main ways PAHs have been shown to do this is through decreasing fecundity or altering hatching (Perrichon et al., 2016; Sogbanmu et al., 2016). Several examples are found in the literature. Reduced fecundity has been reported in both single PAH exposures, in African sharptooth catfish (*Clarias gariepinus*) (Sogbanmu et al., 2016), as well as PAH mixtures, in Atlantic cod (*Gadus morhua*) (Khan, 2013). Reduced hatching success and delayed hatching have also been observed in species such as zebrafish (Perrichon et al., 2016; Butler et al., 2013), Japanese medaka (*Oryzias latipes*) (Rhodes et al., 2005; Bihanic et al., 2016) and pink salmon (*Oncorhynchus gorbuscha*) (Carls and Thedinga, 2010). Collectively, hatching alterations not only lead to a potential increased risk of predation among unhatched eggs, but also increased susceptibility to developmental delays (Carls and Thedinga, 2010). These ED effects significantly impact populations by reducing offspring sizes and overall numbers. Moreover, diminished offspring viability can lead to population losses before hatching, underscoring the critical role of both fecundity and hatching success as key endocrine functions affected by PAHs.

PAHs are associated with causing tissue damage, homeostatic imbalances and immune system dysfunction. PAHs inflict tissue damage by inducing histopathological abnormalities across various organs in fish (Kennedy, 2015). Abnormalities observed in pink salmon fry (*Oncorhynchus gorbuscha*) exposed to crude oil (TPAH = 178 – 384 µg/L) impacted the gills (eg., hyperplasia of mucosa, epithelial lifting and vasoconstriction), liver (eg., macrocytosis, necrosis, steatosis and pleomorphism), and head kidney (eg., enlarged inner cell diameter) (Kennedy, 2015). Hepatic necrosis, evident through patchy lesions in fish liver, has also been associated with PAH exposure (Carls et al., 1998).

Homeostatic imbalances serve as biochemical indicators for stress response and have been reported in fish exposed to PAHs. Increases in plasma ions (potassium, chloride and sodium), cortisol, glucose and lactate were observed in Pacific herring (*Clupea pallasii*) following acute PAH exposure (100 µg/L) and were maintained over a chronic exposure period (9 weeks) as well (Kennedy and Farrell, 2008). Similar increases were observed in flounder (*Pleuronectes flesus*) exposed to PAHs (6 mg/L total AHs) (Alkindi et al., 1996). PAHs can disrupt immune response in various ways. Respiratory burst (RB) activity is the elevation of ROS due to microbial phagocytosis and is an indicator of immune system function. Crude oil exposure (TPAH = 111 – 131 µg/L) increased RB in Pacific herring under acute conditions but decreased RB under chronic conditions (Kennedy and Farrell, 2008). As well, a reduced pathogenic response was also observed as herring exhibited an increase in mortality following chronic pathogenic exposure (*Listonella anguillarum*) (Kennedy and Farrell, 2008).

PAHs induce various behavioral changes in fish that broadly target swimming ability. Studies have documented behavioral changes such as alterations to predation, avoidance, swim performance, stress and exercise recovery (Folmar et al., 1981; Moles et al., 1994; Kennedy and Farrell, 2006). A crude oil exposure (TPAH = 230 – 530 µg/L) in Coho salmon (*Oncorhynchus kisutch*) was associated with lethargy and decreased predation as fish displayed less interest in prey (rainbow trout) after 10 d of exposure (Folmar et al., 1981). Avoidance of PAH-contaminated sediment is another behavioral change. A study on Alaskan fish species (Pacific halibut, rock sole, yellowfin sole) exposed to crude oil reported all species showed avoidance of heavily oiled sediments (TPAHs = 1420 µg/L) while only some (yellowfin sole and Pacific halibut) showed no avoidance to lightly oiled sediments (TPAHS = 495 µg/L) (Moles et al., 1994). This finding suggests fish may only be capable of detecting PAH-contaminated sediment and changing their behavior at higher PAH doses. PAH exposure has been shown to be detrimental to swimming performance as well (Kennedy and Farrell, 2006). Pacific herring (*Clupea pallasii*) exhibited decreased sustained swimming performance after being exposed to crude oil (TPAHs = 9.6 – 120 µg/L) (Kennedy and Farrell, 2006). Alterations to swimming performance were also associated with increasing stress as reflected by elevated plasma cortisol and decreased muscle glycogen levels following burst swimming behavior (Kennedy and Farrell, 2006). These findings suggest PAHs effect fish behavior by reducing swim performance and recovery following exhaustive exercise.

In general, PAH mechanisms of toxicity have been defined to be either aryl-hydrocarbon receptor (AhR)- dependent or independent (Incardona et al., 2017). The AhR-dependent pathway plays a vital role in the toxicity of PAHs. As a transcription factor, AhR regulates the expression of enzymes that function in drug metabolism (Pohjanvirta, 2012). Upon entrance into the cell, PAHs bind to the AhR in the cytoplasm, leading to its translocation into the nucleus. This translocation activates the AhR, facilitating its binding to AhR nuclear translocator (ARNT). The AhR-ARNT complex then binds to xenobiotic response elements (XREs) in the promoter regions of target genes, such as cytochrome P450 (CYP) enzymes (a Phase I enzyme) (Pohjanvirta, 2012). Phase 1 reactions involve the biotransformation of hydrophobic compounds into functionalized substrates for Phase 2 reactions which conjugate the metabolites to facilitate elimination (Honda and Suzuki, 2020; Incardona et al., 2017). AhR-dependent toxicity is seen when PAHs decouple phase 1 and 2 reactions, preventing the removal of toxic metabolites. During the natural process of biotransformation various toxic metabolites are produced. Electrophiles can trigger cytotoxicity by alkylating or acylating various macromolecules like DNA or proteins (Dekant, 2009). Reactive intermediates are formed such as quinones, acyl halides or epoxides as well as free radicals which lead to lipid peroxidation (Dekant, 2009). PAH bioactive metabolites also form DNA adducts which can be responsible for mutations that cause cancer (Idowu et al., 2019). Additionally, the AhR pathway can lead to the generation of reactive oxygen species (ROS) and pro-inflammatory cytokines, contributing to PAH-induced toxicity. This mode of toxicity is often elicited by HMW PAHs which are better ligands for AhR than LMW PAHs (Incardona et al., 2017). This has led toxicologists to associate HMW PAHs with chronic toxicity (Salvo et al., 2016).

Many AhR-independent mechanisms exist but are relatively unknown and require more research. In general, AhR-independent PAH mechanisms are supported through AhR knockdown studies. Generally, LMW PAHs are known to be poor agonists for the AHR and may elicit weak-to-no AHR binding (Incardona et al., 2017). Narcosis has been proposed as an AhR-independent mechanism behind LMW PAH toxicity (Barron et al., 2004; McGrath and Di Toro, 2009). The mechanism behind narcosis can be broadly understood as impairment to the central nervous system through non-specific membrane effects (Barron et al., 2004; Incardona et al., 2004). Here, hydrophobic chemicals partitioning across membranes and nervous tissue elicit an anesthetic effect (Barron et al., 2004). Chemicals exhibiting narcosis-mediated toxicity are generally less toxic than

receptor-mediated toxicants which typically have lower critical body residues and need less chemical to induce a toxic effect (Barron et al., 2004). Touch tests are often used to test drug narcosis as they observe a basic mechanosensory-nerve response between the spine and hindbrain (Incardona et al., 2004). Evidence for AhR-independent toxicity has been observed in knockdown studies (Incardona et al., 2005). For eg., knockdown of the AhR2 ligand blocked CYP1A induction in zebrafish exposed to the tricyclic PAHs dibenzothiophene and phenanthrene; however, fish still exhibited cardiac arrythmias, edemas and intracranial hemorrhaging (Incardona et al., 2005). Defects were exacerbated in oil-exposed morphants with inactivated AhR pathways. While tricyclic PAHs show AhR independence, some studies suggest that phenanthrene and other tricyclic PAHs may selectively bind to AhR2 in zebrafish (Incardona et al., 2005). Chrysene, dibenzothiophene and phenanthrene induced CYP1A induction in vascular endothelium in zebrafish; however, the tricyclic PAHs were only able to mediate induction through AhR2 whereas chrysene also utilized AhR1. This greater number of AhR pathways in chrysene is attributed to its greater hydrophobicity and ability to accumulate and bind in epidermal cells whereas tricyclic PAHs do not accumulate or express AhR1 (Incardona et al., 2005). Overall, AhR-independent pathways are primarily associated with tricyclic PAH toxicity.

1.2. Phenanthrene

1.2.1. Sources

Phenanthrene, a PAH consisting of three fused benzene rings, has pyrogenic, petrogenic, and biogenic origins (Abdel-Shafy and Mansour, 2016). Phenanthrene-containing products include resins, paints, dyestuffs, and explosives (CDC, 2023; Abdel-Shafy and Mansour, 2016). Additionally, it is commonly present in commercial PAH mixtures utilized in various products (GOC, 2023). One of the primary sources of phenanthrene is coal-tar, extensively used in aluminum smelting, roofing sealants, and as fuel for the steel industry (GOC, 2023). Creosote, another product containing phenanthrene, serves as an industrial sealant for marine pilings, telephone poles, and wooden structures (GOC, 2023). Furthermore, phenanthrene can be found in asphalt and bitumen, widely used in road development, pipe sealants, and water-proofing (GOC, 2023). As a petrogenic source, phenanthrene is a major component of crude oil, of which approximately 75 % composition is attributed to tricyclic PAHs (Perrichon et al., 2016). Moreover, it plays a role in the

agricultural industry as it is used in pesticide manufacturing (Abdel-Shafy and Mansour, 2016). Phenanthrene also has biogenic origins, released from organic material by microbes, algae or plants (Rocha and Palma, 2019) as well as by diagenesis (Lourenço et al., 2023).

1.2.2. Environmental fate

Phenanthrene's environmental fate is influenced by its chemical and structural properties (Liu et al., 2017). LMW PAHs like phenanthrene are relatively unstable and not persistent due to their high volatility and capability of being degraded (Lawal, 2017). Phenanthrene is an angular PAH (Fig 1.1.) which take longer to degrade than linear, 2-ring compounds (Abdel-Shafy and Mansour, 2016). Phenanthrene's high vapor pressure (1.21×10^{-4} mm Hg at 25 °C) and volatility lend to its ability to move easily into the atmosphere.

Phenanthrene's water solubility and partitioning behavior are crucial factors of environmental fate. Phenanthrene has a relatively low water solubility (1.1 ± 0.1 mg/L at 22 °C) (NCBI, 2024). However, as phenanthrene is more water-soluble than HMW PAHs, organismal membranes encounter phenanthrene in the water since it is readily dissolvable and abundant. This increases phenanthrene's bioavailability to aquatic organisms (Jung et al., 2013). In terms of partitioning behavior, phenanthrene has a log K_{OW} value of 4.46, indicating its likelihood to dissolve into organic hydrophobic phases. Therefore, phenanthrene can easily partition across biological membranes (Jung et al., 2013). Compounds with high K_{OW} values (4 - 6) often exhibit high bioconcentration factors (BCF), resulting in concentrations in tissues being higher than concentrations in the environmental media (Wang, 2016). Phenanthrene's bioconcentration potential is predicted to fall between 70 – 2630, showing a medium potential to concentrate in fish tissues (NCBI, 2024).

Phenanthrene's relationship between adsorption behavior particulate and volatilization from water is important to its fate. Phenanthrene's relatively high volatility places its volatilization half-lives around 1.3 and 13.7 d for a river or lake, respectively (NCBI, 2024). Despite its tendency to volatilize, phenanthrene has a strong ability to rapidly adsorb to sediment particles which allows it to remain longer in aquatic ecosystems (Yang and Zheng, 2010). Volatilization is weakened by adsorption to sediment or organic material in

water. Phenanthrene's fast sorption rates in marine sediment can counter losses to volatilization and allow phenanthrene to persist in aquatic habitats.

1.2.3. Phenanthrene Toxicity

As an LMW PAH, phenanthrene is acutely toxic to aquatic organisms (Salvo et al., 2016). Acute LC50 values for phenanthrene have been reported for many aquatic species in both early and late life stages (Table 1.1). ELS sensitivity varies greatly across species with 96-h LC50 values ranging from 271 to 1400 µg/L in zebrafish (*Danio* rerio) and Japanese rice fish (*Oryzias latipes*), respectively (Willis and Oris, 2014; Ministry of the Environment Japan, 2019). Acute toxicity increases, with the 120-h LC50 range reporting lethality between 310 – 510 µg/L in zebrafish (Vergauwen et al., 2015; McGrath and Di Toro, 2009).

Acute toxicity trends for phenanthrene show large variability across fish species at the juvenile stage as well (Table 1.1). Reported 96-h LC50 values showed phenanthrene toxicity ranged from 220 to 1410 µg/L for sablefish (*Anoplopoma fimbria*) and African sharptooth catfish (*Clarias gariepinus*) juveniles, respectively (McConville et al., 2018; Sogbanmu et al., 2018). Interestingly, a study on carp (*Cyprinus cario*) revealed the species to have an extremely high tolerance to phenanthrene with an acute toxicity range of 5 – 25 mg/L (Kang et al., 2022). These data show that phenanthrene acute toxicity is similar between juvenile fish and embryos (with the exception of carp), with the former showing only slightly increased sensitivity.

Table 1.1. Summary of acute phenanthrene lethal toxicity data for early and late life stages across fish species.

Species	Life stage	Effect level	Exposure time	Concentration (µg/L)	Reference
Red sea bream (*Pagrosomus major*)	Embryo	LC50	48 h	1970	Zhao et al., 2017
Japanese rice fish (*Oryzias latipes*)	Embryo	LC50	96 h	1400	Ministry of the Environment Japan, 2019
Sheepshead minnow (*Cyprinodon variegatus*)	Embryo	LC50	96 h	671	Moreau et al., 1999
Zebrafish (*Brachydanio rerio*)	Embryo	LC50	96 h	920	Kim et al., 2018
	Embryo	LC50	96 h	271	Willis and Oris, 2014
	Embryo	LC50	120 h	310	(Vergauwen et al., 2015)
	Embryo	LC50	120 h	510	McGrath and Di Toro, 2009
	Embryo	LC50	120 h	> 423	Butler et al., 2013
	Embryo	LC50	144 h	160	Butler et al., 2013
Carp (*Cyprinus cario*)	Juvenile	LC50	24 h	15.926 [a]	Kang et al., 2022
	Juvenile	LC50	96 h	11.198 [a]	Kang et al., 2022
African sharptooth catfish (*Clarias gariepinus*)	Juvenile	LC50	96 h	1410	Sogbanmu et al., 2018
Sablefish (*Anoplopoma fimbria*)	Juvenile	LC50	96 h	220	McConville et al., 2018
Pufferfish (*Takifugu obscurus*)	Juvenile	LC50	96 h	432	Lee et al., 2004
Bluegill (*Lepomis macrochirus*)	Juvenile	LC50	96 h	234	Call et al., 1986
Rainbow trout (*Oncorhynchus mykiss*)	Juvenile	LC50	96 h	375	Call et al., 1986

[a] units are mg/L

Like most chemicals, phenanthrene exhibits sublethal toxicity across various levels. Phenanthrene is a genotoxic, teratogenic, cardiotoxic, and a reproductive toxicant (Frapiccini et al., 2021; Butler et al., 2013; Zheng et al., 2020; Brette et al., 2017; Peng et al., 2019). Therefore, it can disrupt cellular processes, leading to impaired development and physiological function at the organismal level. As well, it can disrupt larger physiological processes leading to wide-spread reproductive and behavioral effects on entire populations.

Phenanthrene exposure can induce genotoxic effects in fish, leading to DNA damage (Lee et al., 2011). Damage can occur directly through breakage of DNA helices or adducts, as well as indirectly through the production of ROS that damage DNA (Lee et al., 2011). This can lead to mutations and genetic alterations that may have long-term consequences for fish populations. Studies have reported increased levels of DNA damage in fish exposed to phenanthrene at both early and late life stages, indicating its potential genotoxicity. Acute exposure (16 h) to relatively low phenanthrene concentrations (18 – 160 µg/L) caused a significant decline in liver DNA integrity in golden grey mullet (*Liza aurata*) (Oliveira et al., 2006). Presence of erythrocytic nuclear abnormalities (ENA) was also a key indicator of genotoxicity in the blood. A similar study observed a significant increase in ENA in estuarine guppy (*Poecilia vivipara*) following a 4 d exposure to phenanthrene (10 – 20 µg/L) (Machado et al., 2014). A significant correlation between phenanthrene and DNA tail damage (Comet assay) was observed in juvenile striped beakperch following an 18-month crude oil exposure (Lee et al., 2011). However, another study assessing gilt-headed seabreams (*Sparus aurata*) found phenanthrene caused increases in CYP1A mRNA levels and DNA damage only when co-exposed with B[a]P and did not cause genotoxicity on its own (Bramatti et al., 2023). It should also be noted that phenanthrene is not considered carcinogenic by US or Canadian regulators. (Incardona et al., 2017; Baan et al., 2019; CAREX Canada, 2023). As phenanthrene is considered unclassifiable as a human carcinogen, the extent of its genotoxicity is debatable and requires more research.

Phenanthrene can also induce oxidative stress, leading to the accumulation of ROS (Frapiccini et al., 2021). ROS have been shown to harm cellular components like lipids, proteins, and DNA (Mai et al., 2019). Antioxidant gene levels (e.g., CAT, GST, SOD) are often studied to determine if ROS are being produced faster than they are being detoxified and eliminated and resultantly causing oxidative stress (Frapiccini et al., 2021). PAH

accumulation in red mullet (*M. barbatus*) was shown to suppress antioxidant gene levels, with phenanthrene specifically being associated with both CAT and GST suppression (Frapiccini et al., 2021). Phenanthrene induced a decrease in the antioxidative defense system, leading to increased vulnerability of oxidative damage. Additionally, as GSTs play a role in detoxification and excretion during Phase II biotransformation, their suppression raises the potential for further oxidative damage (Bramatti et al., 2023). Oxidative stress and antioxidant gene responses appear to be species-specific as other studies have shown PAH-induced increases in GST gene expression in sea ruffe (*Sebastiscus marmoratus*) and common goby (*Pomatoschistus microps*) (Wang et al., 2006; Vieira et al., 2008) following exposure.

Another primary biochemical process phenanthrene impacts is CYP1A activity. While phenanthrene is generally a weak AhR ligand, it still acts as a substrate for CYP1A (Incardona et al., 2004). Evidence for both inductive and inhibitory effects on CYP1A have been reported across fish species exposed to phenanthrene and appear to be influenced by phenanthrene concentration, co-exposure and exposure duration (Correia et al., 2007; Bramatti et al., 2023; Xu et al., 2009). Phenanthrene exposure caused CYP1A induction in both golden grey mullet and zebrafish at concentrations < 500 µg/L (Oliveira et al., 2007; Mai et al., 2019). Hyperactivation of CYP1A induction was associated with liver damage in zebrafish (Mai et al., 2019). In gilt-headed seabreams, CYP1A induction was only observed when phenanthrene (18 – 1782 µg/L) was co-exposed with benzo[a]pyrene (B[a]P), suggesting it potentiates CYP1A activity (Bramatti et al., 2023). Other studies show phenanthrene exposure concentration and duration influences CYP1A activity (Correia et al., 2007; Xu et al., 2009). Low phenanthrene concentrations (20 µg/L) induced CYP1A activity in gilt-headed seabreams while high concentrations (100 µg/L) inhibited CYP1A activity (Correia et al., 2007). This same CYP1A phenomena was reported in Nile tilapia (*Oreochromis niloticus*) where prolonged exposure duration caused CYP1A inhibition at higher concentrations (100 and 400 µg/L) whereas CYP1A induction was reported at all concentrations (50 – 400 µg/L) under shorter exposure duration (Xu et al., 2009). Therefore, CYP1A activity plays a dual role in phenanthrene toxicity through both induction and inhibitory effects.

Phenanthrene can also act as a teratogen and induce a host of morphological defects in fish (Incardona et al., 2009). In individual PAH exposures, phenanthrene was the only PAH to induce dose-dependent teratogenesis in zebrafish embryos (Sogbanmu et al.

2016). Evidence for phenanthrene-induced edemas have been observed in both marine medaka (*Oryzias melastigma*) and zebrafish (*Danio rerio*) embryos at concentrations ranging between 2 – 423 µg/L (Zheng et al., 2020; Butler et al., 2013). Pericardial edema appears to be one of the most common teratogenic effects in fish and can deleteriously impact heart functionality by reducing blood circulation and cardiac cycling (Incardona et al., 2004; Vergauwen et al., 2015). Yolk edema can also impede development by leading to nutrient cycling deficiencies (Billard et al., 2008). Swim bladder impairment, observed in zebrafish embryos exposed to phenanthrene (98 – 402 µg/L), was associated with reduced swimming behavior, showing the potential for teratogenic effects to impact behavior (Vergauwen et al., 2015). Additionally, phenanthrene exposure has been associated with other teratogenic effects in fish such as tail deformities and reductions in jaw size, cranial area, eye size and finfolds (Incardona et al., 2004; Carls et al., 2010; Zheng et al., 2020).

Phenanthrene is also a cardiotoxic chemical and plays a major role in inducing both morphological and functional heart defects in fish (Incardona, 2017; Brette et al., 2014). Morphological heart defects observed in zebrafish include pericardial edema, enlarged hearts and thin, dilated ventricle walls (Incardona et al., 2004; Zhang et al.,2013). Broadly, acute exposure to phenanthrene is believed to cause bradycardia which has been reported in several fish species like zebrafish (McGruer et al., 2021), yellowfin and bluefin tuna (Brette et al., 2014; 2017) and Atlantic cod (Sørhus et al., 2023). Additionally, acute phenanthrene exposure to isolated fish myocytes revealed prolonged action potential durations (APD) and reduced calcium transient levels (CT), both of which can lead to cardiac arrhythmias (Lin et al., 2020; Brette et al., 2017).

Phenanthrene's role as an endocrine disruptor (ED) impacts sexual development individually and on a population scale. Phenanthrene alters hormone and steroid levels which can impact gonad development and function (de Campos et al., 2018; Peng et al., 2019). These changes can lead to delayed sexual maturity or in some cases, induced sex changes across populations (de Campos et al., 2018). For example, an acute 96-h exposure of Dusky grouper juveniles (*Epinephelus marginatus*) to phenanthrene significantly decreased 11-ketotestosterone (11- KT) levels in plasma in both sexes (de Campos et al., 2018). As 11-KT aids in ovary maturation, decreased levels were associated with potential impairment of gonads and sex change dysfunction (de Campos et al., 2018). Steroidal alterations were also observed in zebrafish juveniles exposed to

low levels of phenanthrene (< 5 µg/L) over 4 months (Peng et al., 2019). Both testosterone (T) and estradiol (E2) were significantly reduced in females while males showed reductions in just the latter hormone. These steroidal changes strongly infer phenanthrene's potential to impair sexual development in fish which can lead to reduced reproductive potential (Peng et al., 2019).

Phenanthrene impacts reproduction in fish which can have deleterious long-term effects on fish populations (Peng et al., 2019). 96-h embryological exposures to phenanthrene concentrations (< 10 µg/L) impacted reproductivity of adult zebrafish (*Danio rerio*) which exhibited declines in male spermatozoa and female mature oocytes (Chen et al., 2021). Additionally, adults exposed during early life spawned lower numbers of eggs and had a lower fertilization rate compared to untreated individuals. Chronic adult exposures (4 months) have also been reported to cause decreased egg production in zebrafish (Peng et al., 2019). Reproductive effects following phenanthrene exposure have also been reported in other fish species. Marine medaka (*Oryzias melastigma*) exhibited reduced vitellogenic oocytes following exposure (80 d) to phenanthrene (0.06 and 60 µg/L) (Sun et al., 2015). The same effect was observed in fathead minnows (*Pimephales promelas*) exposed for 7 weeks to phenanthrene (202 µg/L) (Loughery et al., 2018). Declines in mature oocytes, spermatozoa, fecundity and fertilization directly indicate phenanthrene-exposed fish divert their energy from reproduction, and consequently experience reproductive declines (Sun et al., 2015; Loughery et al., 2018).

Phenanthrene exposure can also influence fish behavior, affecting swimming performance, predator avoidance and prey capture (Torreiro-Melo et al., 2015; Carvalho et al., 2008; Sugahara et al., 2014). These physiological effects have been observed following phenanthrene exposure in several fish species. Phenanthrene concentrations between 50 – 200 µg/L caused increased swim speed in Estuarine guppies (*Poecilia vivipara*) whereas high concentrations (500 µg/L) decreased swim speed (Torreiro-Melo et al., 2015). Additionally, altered swimming patterns exhibiting repetitive circular swimming motions were observed. Phenanthrene was also found to induce abnormal swimming in fish when co-administered with other PAHs. Pufferfish (*Takifugu rubripes*) larvae exposed to a 2:1 phenanthrene: pyrene mixture (200: 100 µg/L) exhibited abnormal swimming patterns (Sugahara et al., 2014). Altered swimming behavior is believed to be associated with reduced prey capture rate (Torreiro-Melo et al., 2015). Following exposure to phenanthrene (10 – 100 µg/L), Dourado (*Salminus Brasiliensis*) predatory efficiency

declined between 33-40 % and vision acuity worsened (Carvalho et al., 2008). Furthermore, these modified prey interactions reduced foraging activities (Carvalho et al., 2008; Torreiro-Melo et al., 2015). As swimming performance and predator-prey interactions are measures of fitness, phenanthrene exposure may reduce overall fitness and survivability.

1.3. Zebrafish as a model organism

Zebrafish (*Danio rerio*) are a tropical freshwater species that have become a foundational model organism across scientific fields (Zakaria et al., 2018). As members of the minnow family (*Cyprinidae)*, zebrafish are small, with a maximal body length roughly between 2.5 to 4 cm (Zakaria et al., 2018; Hill et al., 2005). Zebrafish development was documented in detail by Kimmel et al. in 1995 who established zebrafish staging periods from fertilization to early larval period (72 h). This work was foundational in understanding the normal development of zebrafish, providing a reference point to assess abnormal development patterns. Having zebrafish development mapped out was pivotal in establishing zebrafish as a model organism.

Zebrafish have a fast developmental timeline, completing embryogenesis in only 5 d (Zakaria et al., 2018). During this time, their transparency allows for easy manipulation and viewing (McCollum et al., 2011). Both early and late life stages can be tracked in a relatively short period of time, as zebrafish reach the adult stage at 90 d post-fertilization (dpf) (ZFIN, 2024). Zebrafish are economical to use, as their small size translates to less chemical use and waste (Hill et al., 2005). Zebrafish can be cultured and maintained with relative ease as high-density aquariums can be utilized (Veldman and Lin, 2008). Zebrafish are robust breeders and can be bred every two weeks. Additionally, zebrafish are highly fecund as females have the ability to lay hundreds of eggs in a single clutch (Veldman and Lin, 2008).

Zebrafish are a standardized model organism in the field of teratogenesis, featured in assessment tools throughout the literature (Jarque et al., 2020). As a whole-body organism, zebrafish conserve developmental processes, anatomy, genetics and physiology, unlike *in vitro* methods (eg., cell lines or tissue culture) that lack these due to their reductionist nature (Jarque et al., 2020). The OECD recommends the use of zebrafish in early-life stage toxicity testing. Standard protocols include the OECD's Fish

Embryo Acute Toxicity (FET) test 236 (2013) and Fish Early-life Stage Toxicity Test 210 (2013).

1.4. Passive dosing: a novel acute exposure system

One of the largest challenges in PAH exposure studies is their inherent hydrophobic physical profile of most of these compounds: hydrophobic organic compounds (HOCs) are often difficult to dissolve in aqueous solution due to low water solubility (Smith et al., 2010). In addition to chemical dissolution challenges, exposure studies face the challenge of maintaining accurate exposure concentrations. Traditionally, toxicity studies using static-exposure designs rely on chemical re-applications to maintain chemical concentrations (Hedgpeth et al., 2019). Maintaining appropriate exposure concentrations are exacerbated by sorption, degradation, or volatilization which can lead to chemical loss (Renegar et al., 2017). Prior PAH studies show significant losses in total PAH water concentrations over time (Renegar et al., 2017). For example, a conventionally spiked phenanthrene treatment reported losses > 50 % within 24 h (Vergauwen et al., 2015). The advancement of flow-through system technology has ameliorated chemical losses and provide a constant concentration in various exposure systems used in toxicology (Smith et al., 2010).

To aid in introducing PAH into aqueous solution, carrier solvents have classically been used. Since direct application to water does not allow for adequate speedy dissolution, these solvents first solubilize PAH. Commonly-used carrier solvents are methanol, dimethyl-sulfoxide, acetone, ethanol and triethylene glycol (Hutchinson et al., 2006). While carrier solvents may in part resolve the complications of insolubility, they also present a number of disadvantages. A carrier may have limited capabilities of keeping a PAH dissolved and in solution over a long period of time. This presents challenges when controlling concentrations in a water exposure system. Carrier solvents may also be toxic and may interfere with assessing a test chemical's toxicity (Smith et al., 2010). To overcome these issues, passive dosing (PD) has been introduced as a novel exposure technique (Smith et al., 2010).

PD employs a continuous-exposure system that allows for constant and consistent exposure concentrations to be achieved. Unlike traditional methods that may result in chemical concentrations exceeding solubility limits, PD yields concentrations that are

equal or less than true water solubility (Hedgpeth et el., 2019; Butler et al., 2016). A chemical is loaded onto an inert polymer such as silicone or polydimethylsiloxane (PDMS), which is placed into aqueous media, allowing the chemical to partition from the polymer into the aqueous medium. The inert polymer acts as a reservoir from which the chemical is consistently transferred into the aqueous media (Butler et al., 2013). Since partitioning behavior is based on chemical equilibrium between the polymer and water, oversaturation is avoided. PD has become a standard method for exposure systems using hydrophobic organic compounds. PD exposures have been conducted using various sized silicone O-rings from multi-well plates (Smith et al., 2010; Vergauwen et al., 2015) to glass scintillation vials, to larger glass vessels (Butler et al., 2013; 2016). The present study employed the PD exposure model system described in Butler et al. (2013).

1.5. Research objectives

The purpose of this study was to further knowledge on phenanthrene toxicity to both the early and late life stage of *Danio rerio.* Specifically, the toxic endpoints examined were teratogenesis (in embryos) and cardiotoxicity (in adults).

The specific research objectives of this study were:

1. To assess the teratogenic potential of phenanthrene in *Danio rerio* embryos in a sublethal acute exposure;
2. To determine if teratogenic effects are potentially reversible;
3. To determine the toxic effects of phenanthrene in adult *Danio rerio* hearts; and
4. To determine if cardiotoxic effects are potentially reversible.

Chapter 2.

Phenanthrene teratogenicity in zebrafish (*Danio rerio*) exposed to phenanthrene *via* passive dosing

2.1. Introduction

Polycyclic aromatic hydrocarbons (PAHs) are a class of organic contaminants that are a continued toxicity concern due to their ubiquity and persistence in the environment (Honda and Suzuki, 2020). In general, low molecular weight (LMW) PAHs (2 – 3 benzene rings) are acutely toxic, and high molecular weight (HMW) PAHs (> 4 benzene rings) are associated with chronic toxicity and carcinogenicity (CCME, 2010; Idowu et al., 2019). While all PAHs pose a hazard, LMW PAHs are of particular concern in contaminated aquatic ecosystems due to their high bioavailability to aquatic organisms (Jung et al., 2013). Phenanthrene is a tricyclic PAH that is highly abundant and comes from various sources including coal tar, diesel and gasoline fuels, and crude oil (CDC, 2023). Phenanthrene has diverse industrial applications and is present in materials such as paints, pesticides, asphalt, and roofing sealants (CDC, 2023; Abdel-Shafy and Mansour, 2016). Phenanthrene is one of 16 PAHs currently listed among the EPA's 126 priority pollutants and has been categorized as a teratogenic PAH (EPA, 2014). Its relatively high n-octanol/water partition coefficient value (log Kow 4.46) (NCBI, 2024) suggests that phenanthrene can easily move across cell membranes. Although it has relatively low water solubility (1.1 ± 0.1 mg/L at 22 °C), these properties make phenanthrene highly bioavailable compared to many other PAHs (NCBI, 2024; Jung et al., 2013). Phenanthrene displays a moderate potential to bioconcentrate in organisms, with bioconcentration factors (BCFs) ranging from 70 to 2630 (WHO, 2003).

Phenanthrene is acutely lethal to fish and exhibits a large variation in sensitivity across fish species. Literature LC50 values for phenanthrene in early-life stage (ELS) fish report 96-h LC50 values between 271 and 1400 µg/L (zebrafish, *Danio rerio*, and Japanese rice fish, *Oryzias latipes*, respectively) (Willis and Oris, 2014; Ministry of the Environment Japan, 2019). A similar wide range in acute toxicity can be seen in juvenile fish: 96-h LC50 values ranging from 220 to 1410 µg/L (sablefish, *Anoplopoma fimbria*, and African sharptooth catfish, *Clarias gariepinus*, respectively) have been reported (McConville et al.,

2018; Sogbanmu et al., 2018). Therefore, while concentrations causing lethal toxicity appear to be species specific, both early and later life stages present similar susceptibility to phenanthrene-induced mortality.

In addition to acute lethal toxicity, phenanthrene exposure can cause a variety of sublethal effects in fish, impacting their genetics (e.g., DNA strand breakage and adduction formation [Lee et al., 2011]) , biochemistry (e.g., inhibition of antioxidant defense systems and the production of reactive oxygen species [Bramatti et al., 2023]), physiology (e.g., reduced swimming speed [Carvalho et al., 2008]), behavior (e.g., abnormal swimming patterns and impaired predator avoidance behavior [Carvalho et al., 2008; Torreiro-Melo et al., 2015], and reproduction (e.g., reduced fecundity, hatching success and sexual development [Carls and Thedinga, 2010; Sun et al., 2015], feminization and masculinization [Tollefsen et al., 2011; Huang et al., 2019]).

Phenanthrene-induced teratogenesis is a hallmark of its sublethal toxicity. Various studies have reported an array of teratogenic effects in fish. ELS exposures of marine medaka (*Oryzias melastigma*) embryos indicate that concentrations as low as 2 µg/L can induce yolk edema (YE) and pericardial (PE) (Zheng et al., 2020). Swim bladder impairment in zebrafish was also observed at low phenanthrene concentrations (49 µg/L) (Vergauwen et al., 2015). Other teratogenic effects such as reduced fins, cranium and jaws and malformed tails have been observed in zebrafish embryos exposed to 105 – 423 µg/L of phenanthrene (Butler et al., 2013; Vergauwen et al., 2015). While most teratogenic effects appear to worsen in severity over time, there is some evidence for potential edema reversal (Butler et al., 2013). For example, an acute phenanthrene exposure in zebrafish showed that YE and PE reversed by 5 d of exposure, suggesting recovery from teratogenic effects may be possible with time (Butler et al., 2013).

Passive dosing (PD) is a unique exposure method that can achieve consistent exposure concentrations of hydrophobic substances and overcome the challenges of low water solubility and high chemical volatility (e.g., phenanthrene) (Butler et al., 2016; Hedgpeth et al., 2019). Using an inert polymer that behaves as a chemical reservoir, PD maintains concentrations in exposure water as the chemical continually partitions from the polymer into the water (Butler et al., 2013). PD allows for the maintenance of the chemical in solution, replenishing losses occurring by volatilization, avoids the use of potentially toxic

carrier solvents, and allows for exposures at concentrations equal to or less than true water solubility (Hedgpeth et al., 2019; Butler et al., 2016).

The objective of this study was to determine the lethal and sublethal teratogenic effects of phenanthrene in *Danio rerio* embryos using a PD exposure system. In addition, the potential for the reversal of teratogenic effects was also assessed.

2.2. Methodology

2.2.1. Chemical

Silicone O-rings (2.5 mm ID; 1 mm CS) were purchased from O-rings West (Lynnwood, WA). Ethyl acetate, methanol (both HPLC grade), and phenanthrene (purity >98%), penicillin-streptomycin (10,000 units penicillin and streptomycin 10 m /mL, 0.1 µm filtered) and amphotericin B (250 µg/L in deionized water, 0.1 µm filtered) were purchased from Sigma Aldrich (Oakville, ON). NaCl, KCl, Na_2HPO_4, KH_2PO_4, $CaCl_2$, $MgSO_4 \cdot 7H_2O$, $NaHCO_3$ and tricaine methanesulfonate (MS-222) were purchased from Fisher Scientific (Edmonton, AB).

2.2.2. Fish

An outbred strain of *Danio rerio* (AB strain) (Kwantlen Polytechnic University, BC) was reared and crossbred according to standard breeding protocols (Westerfield, 2000). Adult fish were held at 27 ±1 °C, pH 7.5 in ZebTEC recirculating fish racks (Techniplast, Toronto, ON) under a 10:14 h light: dark photoperiod. The system received 10 % water changes daily and weekly water quality monitoring. Fish were fed twice daily with fresh brine shrimp or frozen daphnia *ab libitum.* Fish were held at a 2:1 female: male breeding ratio in 240 mL breeding tanks with tray inserts to inhibit embryo cannibalization by adults. During embryo collection, rapid removal of trays agitated the water to allow dead embryos to rise to the surface and be poured off for disposal. Embryos were then washed consecutively with distilled water and then twice with zebrafish embryo media (ZEM). Collected eggs were pooled in a polystyrene petri dish (150 x 15 mm) containing ZEM media. Using a stereoscope (Stemi 305, Zeiss, Oberkochen, Germany) embryos were selected within a development window between the 2 – 8 cell stage to reduce the potential for collecting embryos arrested in the 1-cell stage (Kimmel et al., 1995). Embryos were transferred into

petri dishes containing exposure media: ZEM media containing 2 % penicillin-streptomycin (20 mL) and 250 ng/L amphotericin B. Temporary holding vessels were used to ensure exposure start times were within the OECD guideline of 90 minutes-post-fertilization (OECD 2013).

2.2.3. Passive dosing system

A static PD exposure system was employed that utilized silicone O-rings loaded with phenanthrene; these delivered appropriate dissolved concentrations to the aqueous media in exposure vials (Butler et al., 2013). For optimal chemical loading, O-rings were prepared through a series of 24-h washes in the following order: ethyl acetate (1x), methanol (3x), and distilled water (3x). For each wash, rings were immersed in a 1 L Erlenmeyer flask containing 500 mL of the respective wash solvent and placed on a continuous stir plate. In between each wash, O-rings were blotted dry with Kimwipes before immediately being transferred to the next wash. Following washes, O-rings were dried in a 110 °C oven for 1 h and then stored at room temperature until needed (Butler et al., 2013).

Partitioning calculations provided in Renegar et al. (2017) shown in Equation 2.1 were used to prepare a phenanthrene stock solution. The volume of water (V_{water}, 20 mL), MeOH (V_{MeOH}, 200 mL) and polydimethylsiloxane (PDMS) O-rings (V_{PDMS}, 12 O-rings) were used in this calculation. Volumes were determined based on a loading capacity of 12 O-rings per 250 mL Erlenmeyer flask used for dosing. Both K terms are partitioning coefficients where $K_{MeOH\text{-}PDMS}$ is the partitioning coefficient of phenanthrene between MeOH and PDMS (log $K_{MeOH\text{-}PDMS}$ = 0.43) and $K_{PDMS\text{-}Water}$ is the partitioning coefficient of phenanthrene between PDMS and water (log $K_{PDMS\text{-}Water}$ = 3.84). Here, water refers to the exposure media which is ZEM (2 % penicillin-streptomycin and 250 ng/L amphotericin B). C_{Target} is the desired target concentration of phenanthrene in the exposure media (mg/L).

$$C_{MeOH} = \left(K_{MeOH\text{-}PDMS} + \frac{[V_{PDMS}]}{[V_{MeOH}]}\right) \times \left(K_{PDMS\text{-}Water} + \frac{[V_{Water}]}{[V_{PDMS}]}\right) \times C_{Target}$$

(Equation 2.1 [Renegar et al., 2017]).

Phenanthrene was dissolved in 700 mL methanol to achieve a nominal stock concentration of 350 µg/L. The stock was placed under continuous stirring for 24 h in an

Erlenmeyer flask and wrapped in aluminum foil to protect the solution from potential light degradation. The stock concentration was diluted with methanol to make up the remaining treatment concentrations: 50, 110, 150, 200 and 275 µg/L. The 350 µg/L stock solution was included as the highest treatment concentration. Twelve O-rings were placed in a 250 mL Erlenmeyer flask containing the appropriate volume of the serial dilution for each concentration for chemical loading. O-rings remained in the phenanthrene/methanol solutions for 72 h protected from light and under continuous stirring at 22 °C (Vergauwen et al., 2015). Following the loading period, O-rings were transferred to 250 mL Erlenmeyer flasks containing 200 mL of distilled water. Flasks were allowed to continuously stir over 24 h to remove any MeOH.

For exposures, individual O-rings were placed in 22 mL glass scintillation vials containing ZEM (with 2 % pen-strep and 250 ng/L amphotericin B). No headspace remained in vials to reduce chemical loss by volatilization. Previous studies have shown chemical loss by volatilization to be an issue with exposure vessels containing a headspace >10 % (Negri et al., 2016). Vials were then capped and shaken for a partitioning period of 24 h (150 rpm) to allow phenanthrene to partition into the media from the O-rings (Butler et al., 2013).

Phenanthrene concentrations were verified by spectrophotometric analysis. Representative water samples were taken on d 1 and d 5 of exposures. Each scintillation vial was inverted 3 x to ensure adequate mixing prior to transferring via pipette to quartz cuvettes (Spectrosil, 12.5 x 12.5 x 45 mm, 3 mL). Water samples were analyzed for phenanthrene concentration on a Cary Eclipse Spectrophotometer (Varian, model Eclipse, East Lyme, CT) set to the following parameters: exit and emission wavelength ranges of 247 and 364 nm, respectively. Exit and emission slit lengths were 5 nm, excitation and emission filters set to automatic and open, PMT voltage at a medium level and the average run time of each reading was set at 3 s. Standard curves by spectrophotometric analysis were validated with water samples analyzed by gas chromatography–mass spectrometry analysis by SGS Axys Analytical Services Ltd. (Sidney, BC).

2.2.4. Exposures

The PD exposure protocol followed Butler et al. (2013) while control acceptance standards and observation protocol were based on the OECD's FET test 210 (OECD, 2013).

Exposure of zebrafish embryos were carried out over 5 d in 22 mL glass vials that contained one O-ring that generated the appropriate phenanthrene concentration in the exposure media (ZEM x1 with 2 % pen-strep and 250 ng/L amphotericin B). A preliminary embryo viability study determined that the survivability of embryos over 5 d in these vials limited embryo test numbers to one embryo/vial. Selected embryos were pipetted into a collection petri dish containing exposure media. Embryo selection criteria excluded 1-cell embryos to eliminate collecting embryos with potential developmental delays. In accordance with OECD (2013) guidelines, exposures were started within 90 min post-fertilization (maximum 16-cell stage) (OECD, 2013). To ensure minimal delays for exposures to meet this criterion, exposures were carried out in 5 separate runs. For each run, all 6 treatments and control had 10 replicates each (n = 10) in separate scintillation vials. This yielded a total sample size of 350 embryos (n = 50 per treatment/control). Embryos were individually pipetted into each vial containing 1 O-ring in dosed media. Vials were capped to avoid potential chemical loss through volatilization and placed upright in an incubator at 27.5 ±1 °C (Butler et al., 2013).

The following exposure concentrations were used: 0, 50, 110, 150, 200, 275 and 350 µg/L. A methanol-loaded O-ring in exposure media was used as the solvent control. (A negative control containing an O-ring in exposure media was used to affirm the silicone material had no effect). Literature values for phenanthrene 120-h LC50 values ranged from 310 to 510 µg/L (Vergauwen et al., 2015; Butler et al., 2013); therefore, concentrations were chosen that were potentially high enough to cause teratogenesis with the understanding that some mortality would occur at the higher concentrations. All other selected test concentrations were scaled below the literature LC50 range with the goal of maintaining embryo viability to examine the potential reversibility of teratogenic abnormalities.

2.2.5. Mortality assessment

Mortality was measured continuously over the 5-d exposure period. Individual zebrafish embryos were monitored every 24 h for lethality based on the OECD's FET 236 guidelines (2013). Lethal endpoints included the coagulation of fertilized eggs and lack of heartbeat (OECD, 2013). For each run, every treatment vial was observed individually to allow for the tracking of each replicate embryo. Daily observations were done using a stereomicroscope (Stemi 305, Zeiss, Oberkochen, Germany). The contents of each vial were poured into a polystyrene petri dish (150 x 15 mm) to allow for observation of the

embryos. The time embryos spent outside of the vials during observation was < 1 min, and embryos were immediately transferred back to their respective vials following observation.

2.2.6. Teratogenic assessment

Teratogenic deformities were assessed over the 5-d exposure period at the same time as lethality for each individual embryo. Teratogenic deformities were recorded only for viable embryos and included pericardial edema (PE), yolk edema (YE) and tail kinking (TK). Teratogenic deformities were recorded as either present or absent. The zebrafish developmental toxicity assay (Panzica-Kelley et al., 2015) was used as a guide when assessing the presence of teratogenic deformities. Delayed hatching (DH) was also recorded and considered as embryos remaining unhatched after 3 dpf. This is in accordance with the literature's established hatching stage as hatching can naturally occur sporadically up to 72 hpf (Westerfield, 2000; Kimmel et al., 1995).

2.2.7. Calculations and statistical analysis

Since each embryo was exposed individually, data were binary for both mortality (1= alive, 0 = dead) and teratogenic effects (1= present, 0 =absent). Lethal and teratogenic effects were normalized to the methanol control for each run (Ali and Legler, 2011). Normalization was also done to account for batch-to-batch variation among the runs due to the potential influence of time and breeding differences. For each run, percent mortality was recorded every exposure d by taking the average of the replicates for each treatment (n = 10). Percent mortalities were then normalized to the MeOH control. As well, the percent of fish exhibiting each teratogenic effect (PE, YE, TK) and DH was recorded for each treatment in the same way. A total of 5 runs were performed, yielding a sample size of 50 embryos per treatment concentration (n = 50). Across all treatments this yielded a total experimental sample size of 350 embryos. Mortality-log concentration curves were generated for each d of exposure using GraphPad Prism version 10.0.1 (GraphPad Software, 2023). Mean percent mortality did not reach the 50 % effect level so LC50 values could not be calculated. The data was fitted with nonlinear regression curves and their LC10 values calculated.

SAS on Demand statistical software was used for all statistical analyses using Proc Glimmix and Proc Logistic (Firth Bias approximation). For lethal and sublethal effects, a generalized mixed effects model using binomial logistic regression was used to test for differences in mean response outcomes. A binomial logistic regression was suitable since there were two possible outcomes for both lethal (dead or alive) and sublethal (present or absent) effects. Mean response outcomes were differences across percent mortality and percent affected between d of exposure and concentrations. Time and concentration effects were measured by establishing both d of exposure (1 – 5) and treatment concentration (50, 110, 150, 200, 275 and 350 µg/L) as fixed effect categorical factors in the models. As well, the two-way interaction between day and concentration also had to be considered a fixed factor. Each run (n= 5), or batch, was considered a random effect since variability in embryo health could not be controlled across runs due to obtaining embryos from different breeding cycles. Post hoc Tukey-Kramer tests were used to detect statistical significance between days or concentrations for each lethal and sublethal effect. A Firth Bias approximation using Proc Logistic was needed when some of response percentages were 0% and 100%. A Firth Bias approximation was used to limit small sample size bias and is suitable for binary response models (Wang, 2014).

2.3. Results

2.3.1. O-ring Spectrophotometry Analysis

To assess the efficiency of the PD methodology, water samples were taken from the scintillation vials on d 1 and 5 and analyzed by gas chromatography–mass spectrometry analysis by SGS Axys Analytical Services Ltd. (Sidney, BC). Predicted concentrations based on the initial Cary Eclipse Spectrophotometer readings (Varian, model Eclipse, East Lyme, CT) were graphed against measured concentrations (gas chromatography–mass spectrometry analysis) and are presented in Figure 2.1. The data demonstrated a linear correlation between predicted and measured values on both d 1 and 5. Actual concentrations were reported to be between 92 – 95 % of the nominal concentrations. The PD system was shown to be effective at maintaining exposure concentrations over the 5 d.

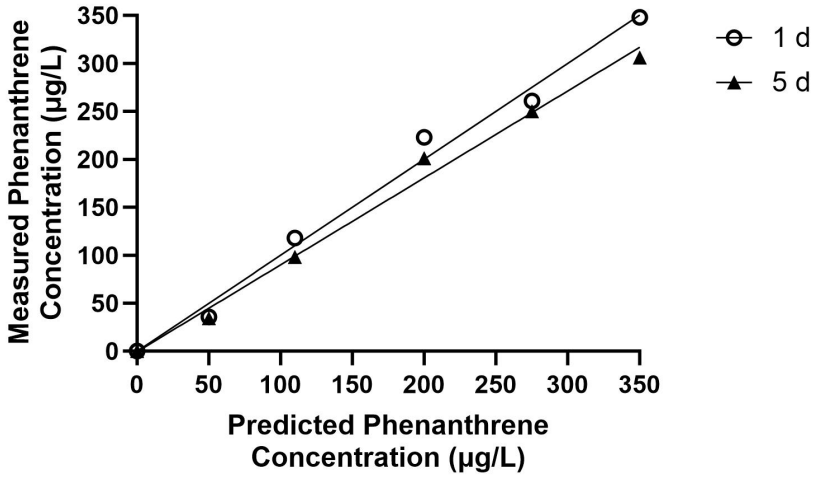

Figure 2.1. Comparison between predicted and measured phenanthrene exposure concentrations in ZEM media using passive dosing with silicone O-rings in glass scintillation vials. Both lines represent measured phenanthrene concentrations at two time points over the exposure: 1 d and 5 d. Each point represents the mean concentration of two replicates.

2.3.2. Mortality

Zebrafish embryos were exposed to ZEM containing various phenanthrene concentrations (0, 50, 110, 150, 200, 275 and 350 µg/L) for 5 d. The methanol control met OECD guidelines (2013) (< 10 % mortality) exhibiting a % mortality of 10 ± 5.7 % on d 5. Percent mortality values were recorded each day for every treatment concentration and are shown in Table 2.1.

Percent mortality over time for each treatment concentration is shown in Figure 2.2. This scatterplot allows direct observation of daily changes in mortality among embryos between phenanthrene treatments. Time did not cause a significant increase in mortality over d 1 to 5 in any treatment concentration ($p = 0.2920$). Because there were no mortalities on D0, D0 could not be used in the assessment of time on mortality. The highest increase in mortality for all treatments occurred before d 1; therefore, significant mortality was predicted to be occurring during the first 24 h of exposure. Mortality stabilized between d 1 and 2 for most treatment concentrations with small and gradual increases past d 1 indicating that mortality was not stage-specific past this developmental stage.

Phenanthrene concentration had a significant effect on mortality across all days of the exposure ($p < 0.0001$). Mortalities were significantly different from the control at phenanthrene concentrations ≥ 110 µg/L. No significant mortalities occurred in the lowest treatment concentration (50 µg/L). Mean percent mortality was significantly higher in both the highest concentrations (275 and 350 µg/L) relative to all other concentrations across all exposure days. A concentration-dependent mortality response was seen at phenanthrene concentrations ≥ 110 µg/L. Overall, % mortality on d 5 ranged from 3.8 ± 5.4 to 52.1 ± 17.2 % (50 and 350 µg/L treatments, respectively).

Concentration-mortality curves for each d of exposure are presented in Figure 2.3. These curves show % mortality based on logarithmic treatment concentrations and provide understanding behind the causality between the xenobiotic, phenanthrene, and the response outcome, mortality. As mortality did not approach 50 % lethality LC50 values could not be calculated. LC10 values were computed for each d of exposure. LC10 values ranged between 106.6 (CI 10.8 – 207.2 µg/L) and 87.4 µg/L (CI 18.8 – 157.4 µg/L) at 24 and 120 h, respectively. LC10 values for each d of exposure are reported in Table 2.2. Lethal toxicity increased with longer exposure times.

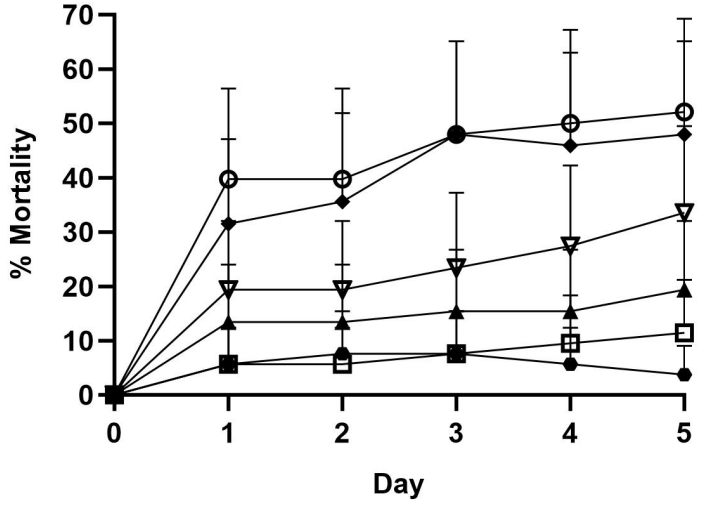

Figure 2.2. Percent mortality in *Danio rerio* embryos exposed to phenanthrene; (⬣) 50, (□) 110, (▲) 150, (▽) 200, (◆) 275, and (○) 350 µg/L over 5 d. Values were normalized to the methanol control. Error bars represent standard error values at the 95% confidence level. Total sample size over the 5 runs yielded 350 embryos (50 per treatment).

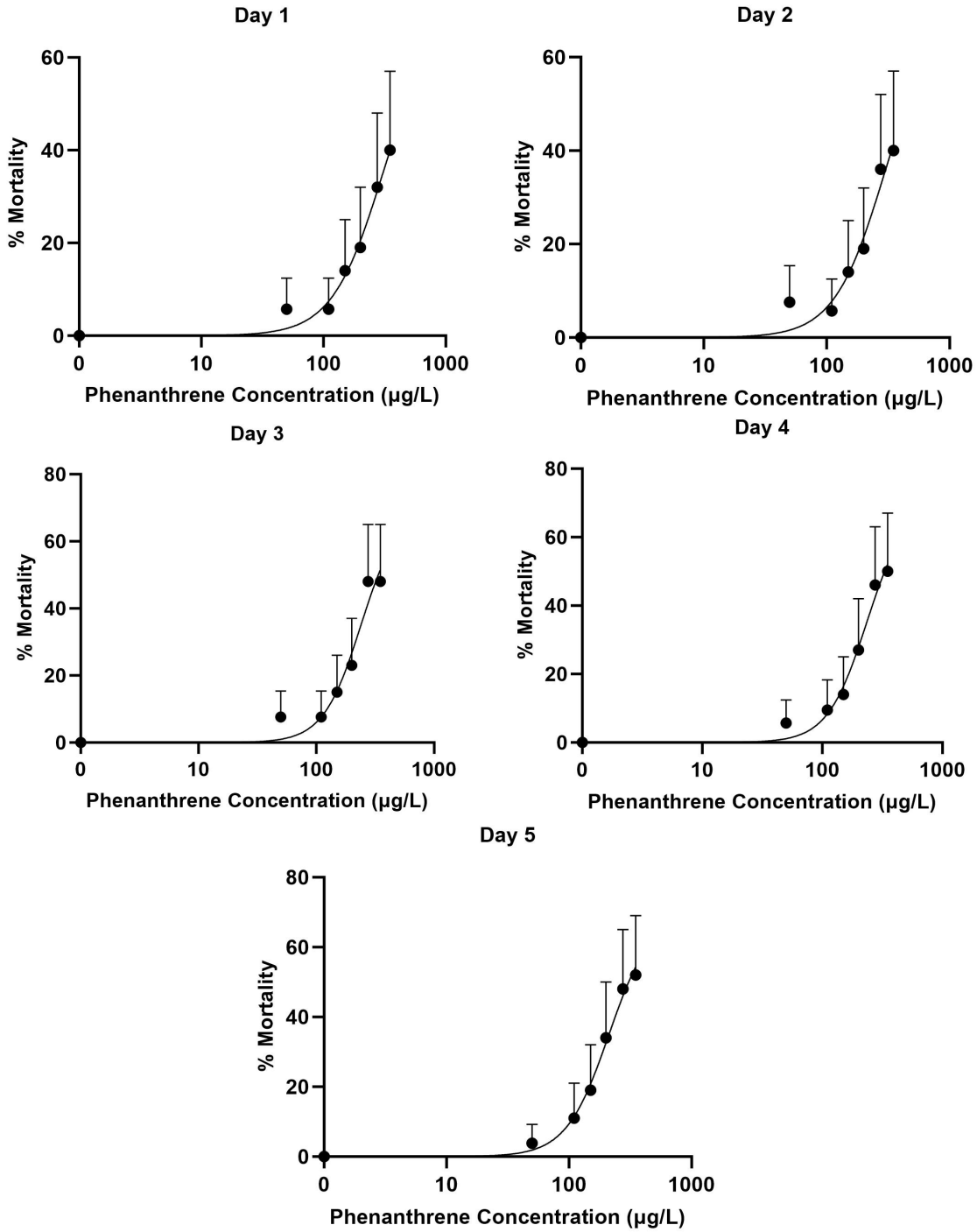

Figure 2.3. **Phenanthrene concentration-mortality curves for *Danio rerio* embryos for 1-5 d exposures. Each point represents the normalized mean % mortality for a respective treatment concentration. Values were normalized to the methanol control. Error bars represent standard error values at the 95% confidence level. Total sample size over the 5 runs yielded 350 embryos (50 per treatment).**

2.3.3. Teratogenesis

Photographic examples of teratogenic deformities recorded for the teratogenic assessment are shown in Figure 2.4. The percent of embryos with teratogenic effects in each measured category in the methanol control are shown in Figure 2.5. Less than 10 % of the methanol control embryos had deformities in any category. At d 5, % affected by yolk edema (YE) and pericardial edema (PE) in controls were 0 %. The % affected by delayed hatching (DH) and tail kinking (TK) at d 5 in controls were 6.0 ± 4.6 % and 2.0 ± 4.4 %, respectively.

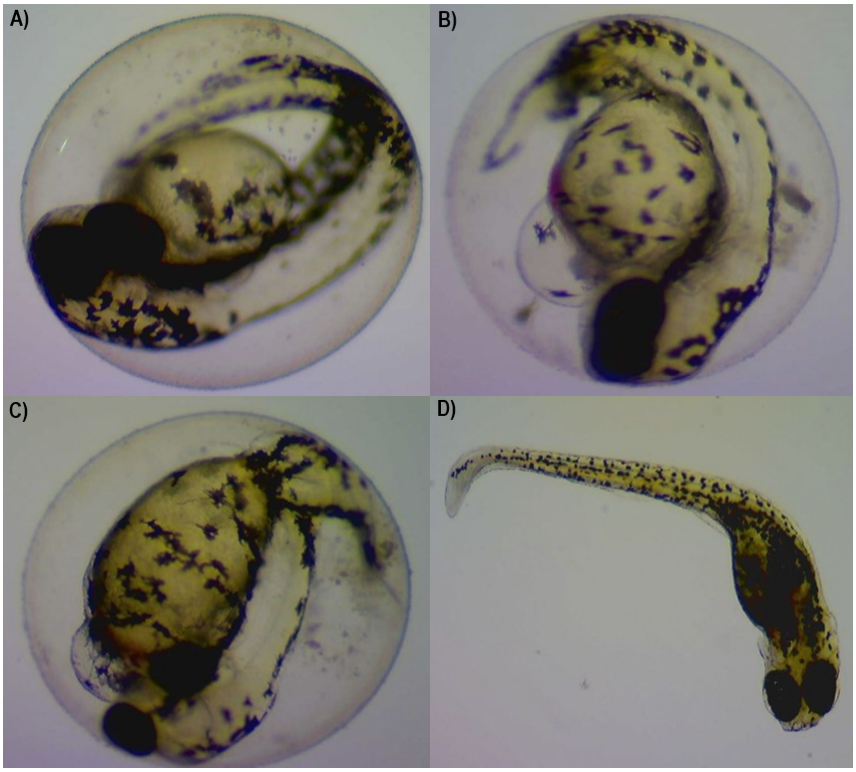

Figure 2.4. Photographs of teratogenic deformities in *Danio rerio* embryos showing a) 48 h normal embryo, b) 48 h embryo with pericardial edema, c) 48 h embryo with yolk edema and d) 72 h embryo with tail kinking.

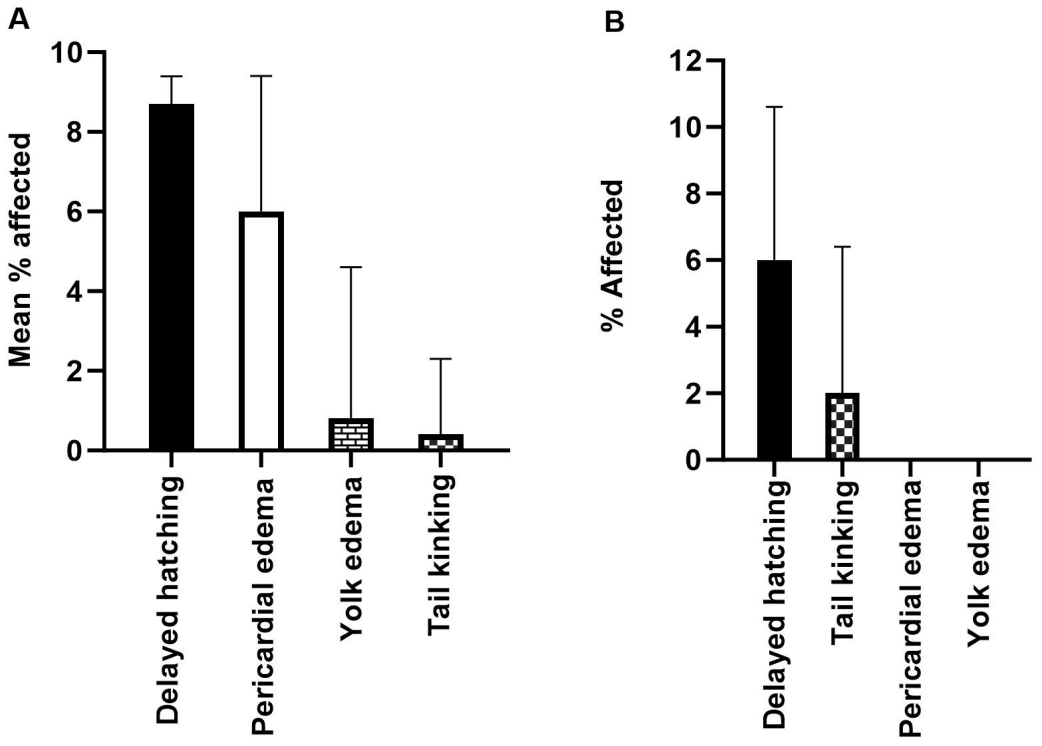

Figure 2.5. Mean % affected (A) and % affected (B) by teratogenic effects in *Danio rerio* embryos in the methanol control at 5 d. Error bars represent standard error of the means at the 95% confidence level. Note: mean percent effected by delayed hatching was calculated over days 3 to 5 to account for the hatching period. Total sample size over the 5 runs yielded 350 embryos (50 per treatment).

Pericardial Edema

Treatment concentration had a significant effect on the proportion of embryos with PE (p= 0.0366). All treatments were normalized to controls, therefore any treatment that was not 0 % PE was significantly different from the control. All treatments except the 150 and 350 µg/L treatment groups, were significantly different from the control. Figure 2.6A shows the % PE among embryos on d 5 for all phenanthrene concentrations.

Although treatment concentration had a significant effect on PE, a clear concentration-dependent response was lacking. % PE at d 5 ranged from 7.1 ± 7.9 to 16.7 ± 13.0 % (350 and 200 µg/L, respectively). To depict the incidence of PE across all exposed fish, % PE was calculated and modeled over the original number of fishes exposed (*n* = 10 per treatment across 5 runs). The % of embryos exhibiting PE was also calculated over the survivors and is included in the appendix (Fig C.1). The low % PE observed at the highest

concentration and lack of a concentration-dependent effect was shown not to be due to mortality in the higher treatment group and the death of embryos that exhibited PE. Daily values for mean percent of embryos affected by PE across all treatment concentrations are shown in Table 2.3.

For all treatment concentrations, PE significantly changed over time ($p < 0.0001$). To capture the change in % PE over the 5 d exposure period, the progression of PE in relation to mortality with time is presented in Figure 2.7. For all treatments, there were two general trends among the % of embryos with PE over time: first, % PE either remained constant or increased from d 1 to 2 for all concentrations. Second, % PE decreased from d 2 to 5 in treatment groups below 200 µg/L. Specifically, a significantly lower proportion of embryos were affected by PE later in the exposure period (d 4 and 5).

The data show that PE reversal was occurring; in some treatments, the relative decreases in % PE exceeded those explained by increases in % mortality. This potential reversal only occurred in treatment groups below 200 µg/L. These treatments revealed PE incidence declines between 14 – 29 % alongside mortality increases between 2 – 15 %.

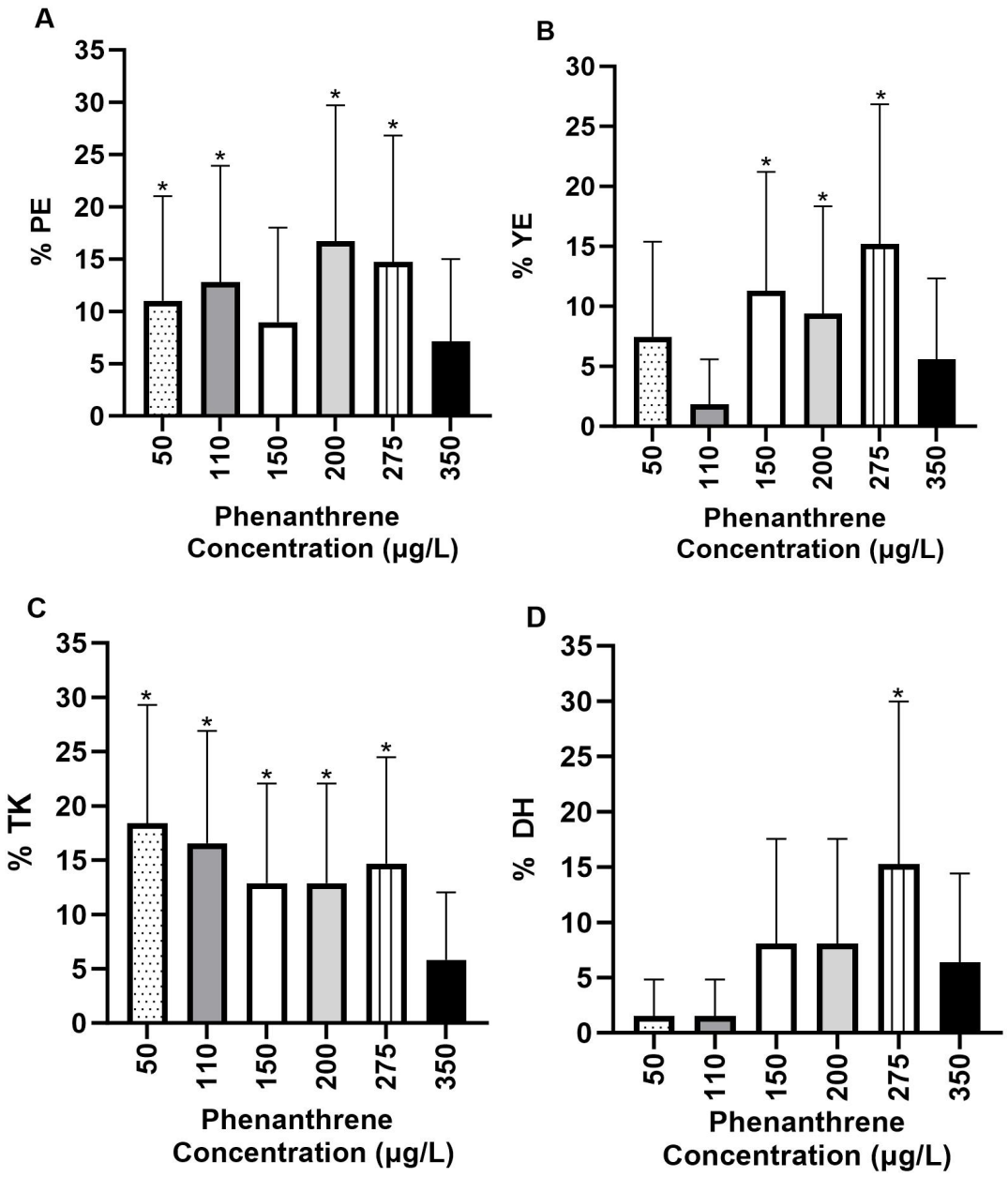

Figure 2.6. **Day 5 % effects for PE (A), YE (B), TK (C) and DH (D) in *Danio rerio* across all phenanthrene treatment concentrations. Each column represents the normalized mean % for the respective effect. Values were normalized to the methanol control. Error bars represent standard error values at the 95 % confidence level. Asterix denote significant difference between treatments ($p < 0.05$). Total sample size over the 5 runs yielded 350 embryos (50 per treatment).**

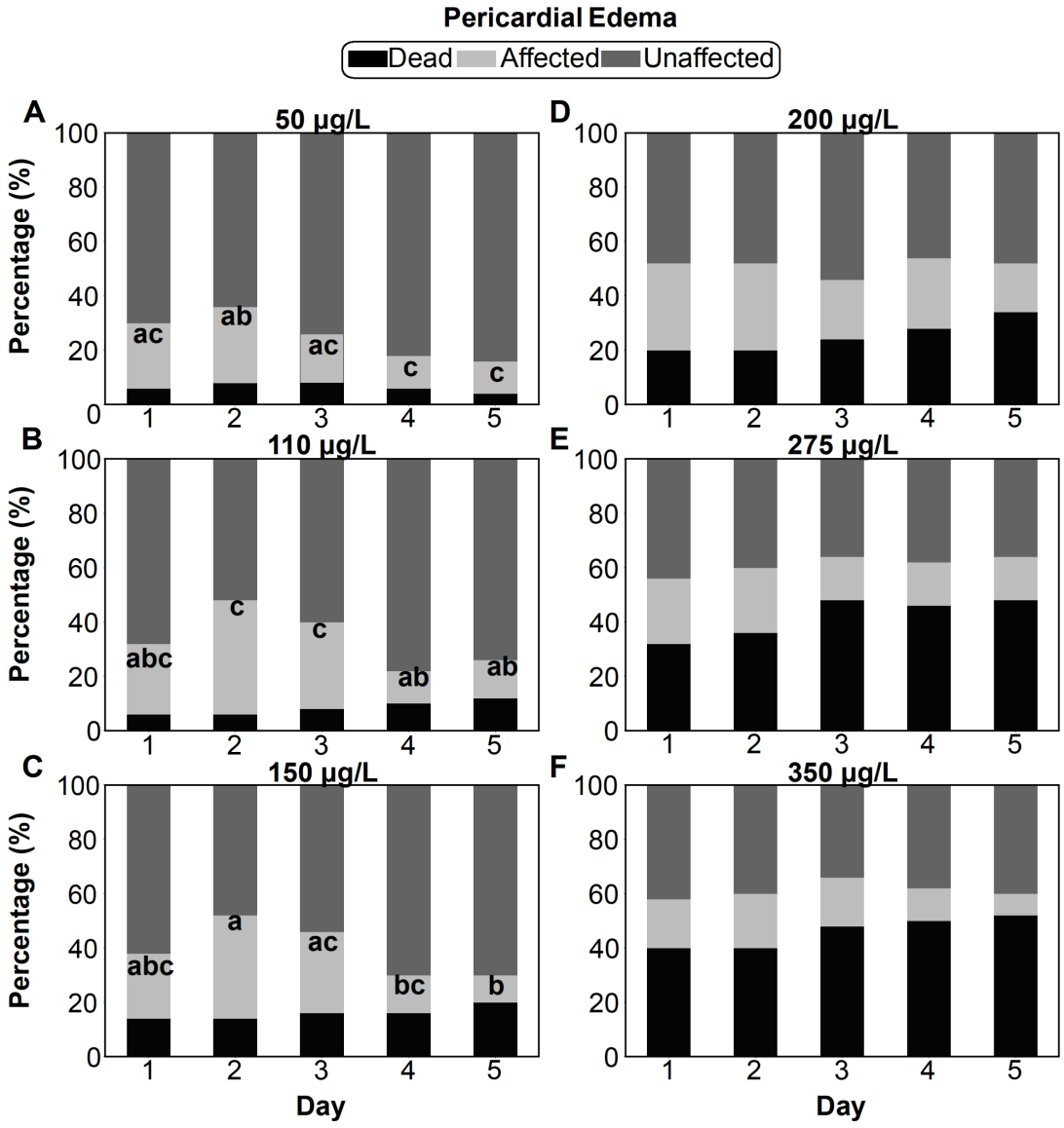

Figure 2.7. **Percent of *Danio rerio* embryos that were dead, affected and unaffected by pericardial edema following exposure to varying concentrations of phenanthrene up to 5 d. Letters denote significant difference across days ($p < 0.05$). Total sample size over the 5 runs yielded 350 embryos (50 per treatment).**

Yolk Edema

Phenanthrene treatment concentration had a significant effect on the proportion of embryos with YE (p= 0.0018). Figure 2.6B shows the % YE at d 5 for all phenanthrene concentrations. All treatments were normalized to controls, therefore any treatment that was not 0 % YE was significantly different from the control. Only the 150, 200 and 275 µg/L treatments were significantly different from the control.

Although treatment concentration had a significant effect on YE, it appeared to exhibit a random pattern as no clear concentration-dependent response was observed. % YE at d 5 ranged from 1.8 ± 3.8 % to 15.2 ± 11.6 % (110 and 275 µg/L treatments, respectively). To depict the incidence of YE across all exposed fish, % YE was calculated and modeled over the original number of fishes exposed (n = 10 per treatment across 5 runs). The % of embryos exhibiting YE was also calculated over the survivors and is included in the appendix (Fig C.1). The low % YE observed at the highest concentration was shown not to be due to mortality in the higher treatment group and the death of embryos that exhibited YE. Daily values for mean percent of embryos affected by YE across all treatment concentrations are shown in Table 2.3.

For all treatment concentrations, YE significantly changed over time (p= 0.0007). To capture the change in % YE over the 5 d exposure period, the progression of YE in relation to mortality with time is presented in Figure 2.8. In general, embryos in treatment groups ≤ 200 µg/L showed an initial increase in YE, followed by a decline after d 2. Comparatively, embryos in the highest groups (≥ 275 µg/L) appeared to decline in YE for all exposure days. A statistically significant decline in YE incidence was reported in the 110, 200 and 350 µg/L treatments. Treatments where the relative decreases in % YE exceed those explained by increases in % mortality were attributed to YE reversal. Treatment groups below 200 µg/L exhibited YE incidence declines between 13 – 27 % while mortalities ranged between 2 – 15 %.

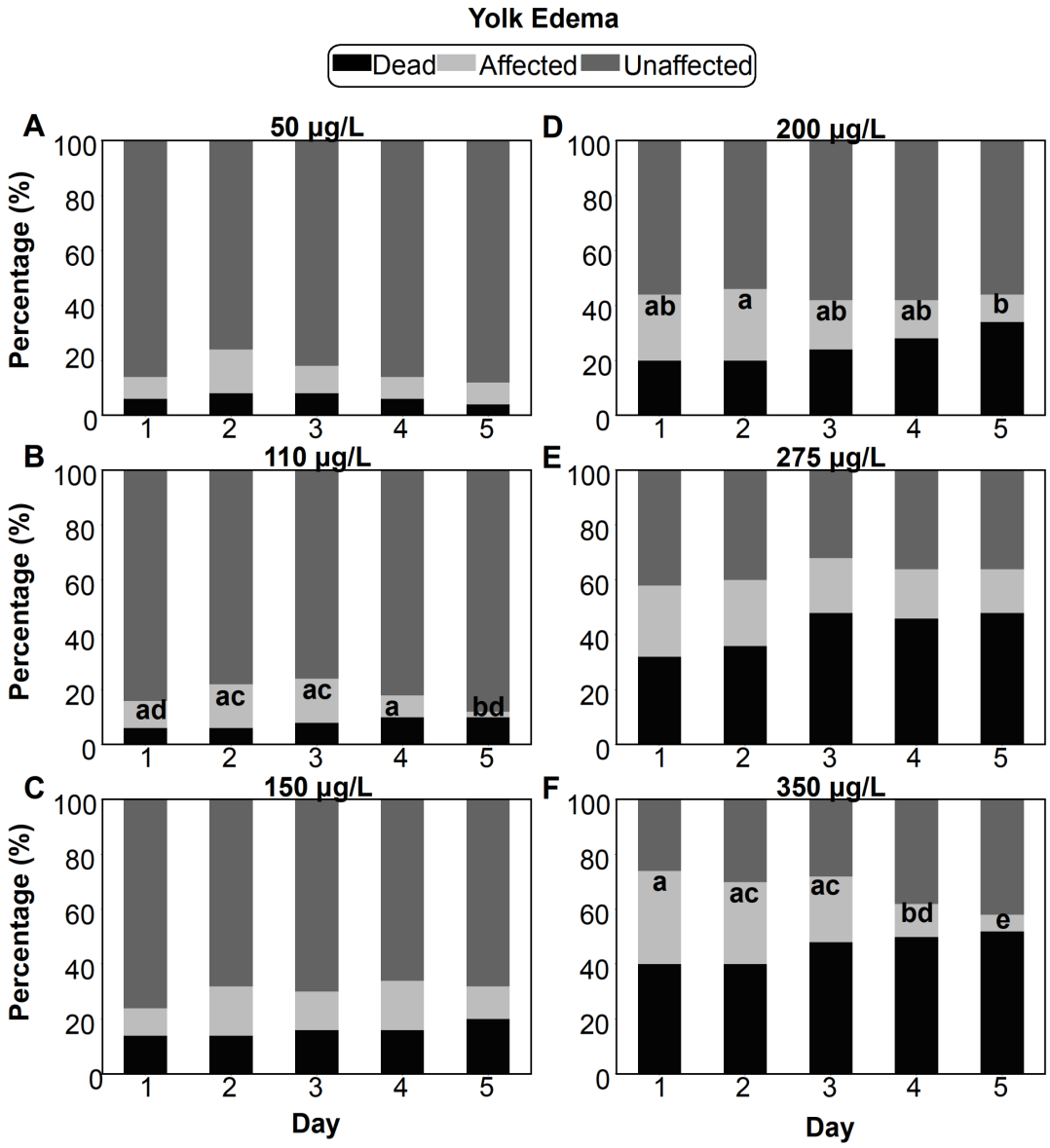

Figure 2.8. **Percent of *Danio rerio* embryos that were dead, affected and unaffected by yolk edema following exposure to varying concentrations of phenanthrene up to 5 d. Letters denote significant difference across days ($p < 0.05$). Total sample size over the 5 runs yielded 350 embryos (50 per treatment).**

Tail Kinking

In the TK statistical analysis, batch variation was treated as a fixed factor under the Logistic regression model and Firth approximation bias. TK incidence was significantly affected by batch variation ($p < 0.0001$). TK was not significantly affected by treatment concentration across all days of exposure ($p = 0.0815$). However, significant differences in TK were observed across treatment concentrations specifically on d 5 ($p < 0.0001$). Figure 2.6C shows the % TK among embryos at d 5 for all phenanthrene concentrations. All treatments were normalized to controls, therefore any treatment that was not 0 % TK was significantly different from the controls. All treatments except 350 µg/L were significantly different. % TK at d 5 ranged between 5.8 ± 6.2 – 18.4 ± 10.9 % (350 and 50 µg/L, respectively). To depict the incidence of TK across all exposed fish, % TK was calculated and modeled over the original number of fishes exposed (*n* = 10 per treatment across 5 runs). The % of embryos exhibiting TK was also calculated over the survivors and is included in the appendix (Fig C.1). The low % TK observed at the highest concentration was shown not to be due to mortality in the higher treatment group and the death of embryos that exhibited TK.

For all treatment concentrations, TK significantly changed over time ($p = 0.0003$). To capture the change in % TK over the 5 d exposure, the progression of TK in relation to mortality with time for each treatment concentration is presented in Figure 2.9. The general trend across most treatments revealed TK incidence increased over time. This increase appeared to occur after d 1 (50 µg/L) or d 2 (110 µg/L) as these days revealed significantly lower TK incidences relative to d 5.

Assessing TK changes alongside mortality revealed the apparent decreases in TK were mainly due to increases in mortality. For example, in the 150 µg/L treatment group, a 2 % decrease in TK was noted from d 4 to d 5, that coincided with a simultaneous 5 % increase in mortality. Therefore, apparent declines in TK were associated with increasing mortality and not TK reversibility. Daily values for mean percent of embryos affected by TK across all treatment concentrations are shown in Table 2.3.

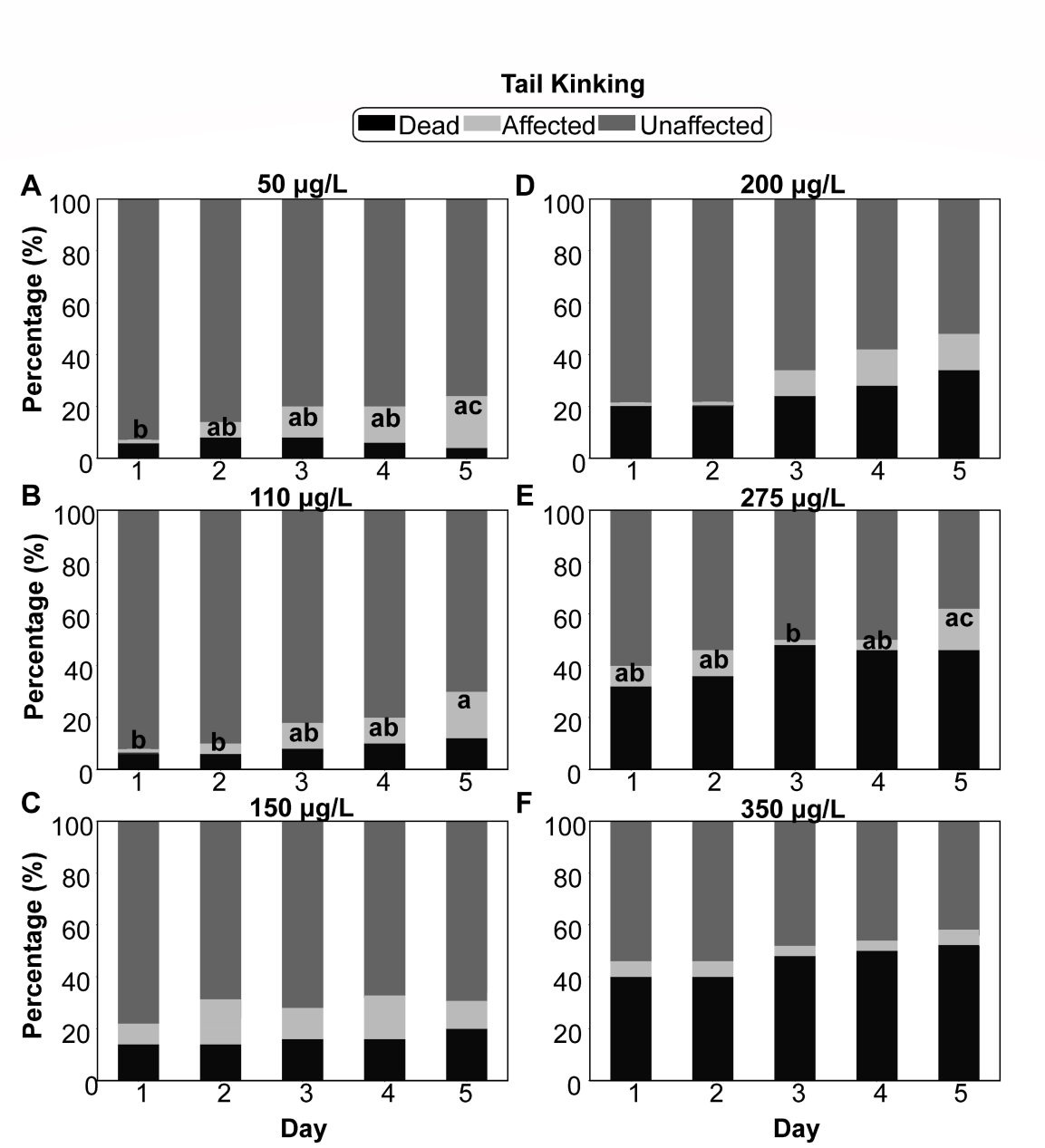

Figure 2.9. **Percent of *Danio rerio* embryos that were dead, affected and unaffected by tail kinking following exposure to varying concentrations of phenanthrene up to 5 d. Letters denote significant difference across days ($p < 0.05$). Total sample size over the 5 runs yielded 350 embryos (50 per treatment).**

Delayed Hatching

Phenanthrene treatment concentration had a significant effect on delaying hatching (DH) ($p= 0.0205$) although there was no concentration-dependent response. The % DH among embryos at d 5 for all phenanthrene concentrations are shown in Figure 2.6D. All treatments were normalized to controls, therefore any treatment that was not 0 % DH was significantly different from the control. % DH at d 5 ranged between 1.5 ± 3.3 % to 15.3 ± 14.7 % (50 and 275 µg/L treatments, respectively). To depict the incidence of DH across all exposed fish, % DH was calculated and modeled over the original number of fishes exposed (n = 10 per treatment across 5 runs). The % of embryos exhibiting DH was also calculated over the survivors and is included in the appendix (Fig C.1). Embryos were only significantly affected by DH in the 275 µg/L phenanthrene treatment. The low % DH observed in the higher concentrations was shown not to be due to mortality in the higher treatment group and the death of embryos that exhibited DH.

For all treatment concentrations, DH significantly changed over time ($p< 0.0001$). To capture the development of DH over the 5 d exposure, the progression of DH in relation to mortality with time is presented in Figure 2.10. The general trend showed DH incidence significantly declining between 10 and 37 % from d 3 to 5 in all treatment groups (with the exception of the 350 µg/L treatment). DH incidence did not significantly change from d 4 to 5 of exposure. This indicated that the majority of hatching occurred at 4 d, 24 h past the literature reported hatching time. Decreases in % DH were not associated with late hatching. Daily values for mean percent of embryos affected by DH across all treatment concentrations are shown in Table 2.3.

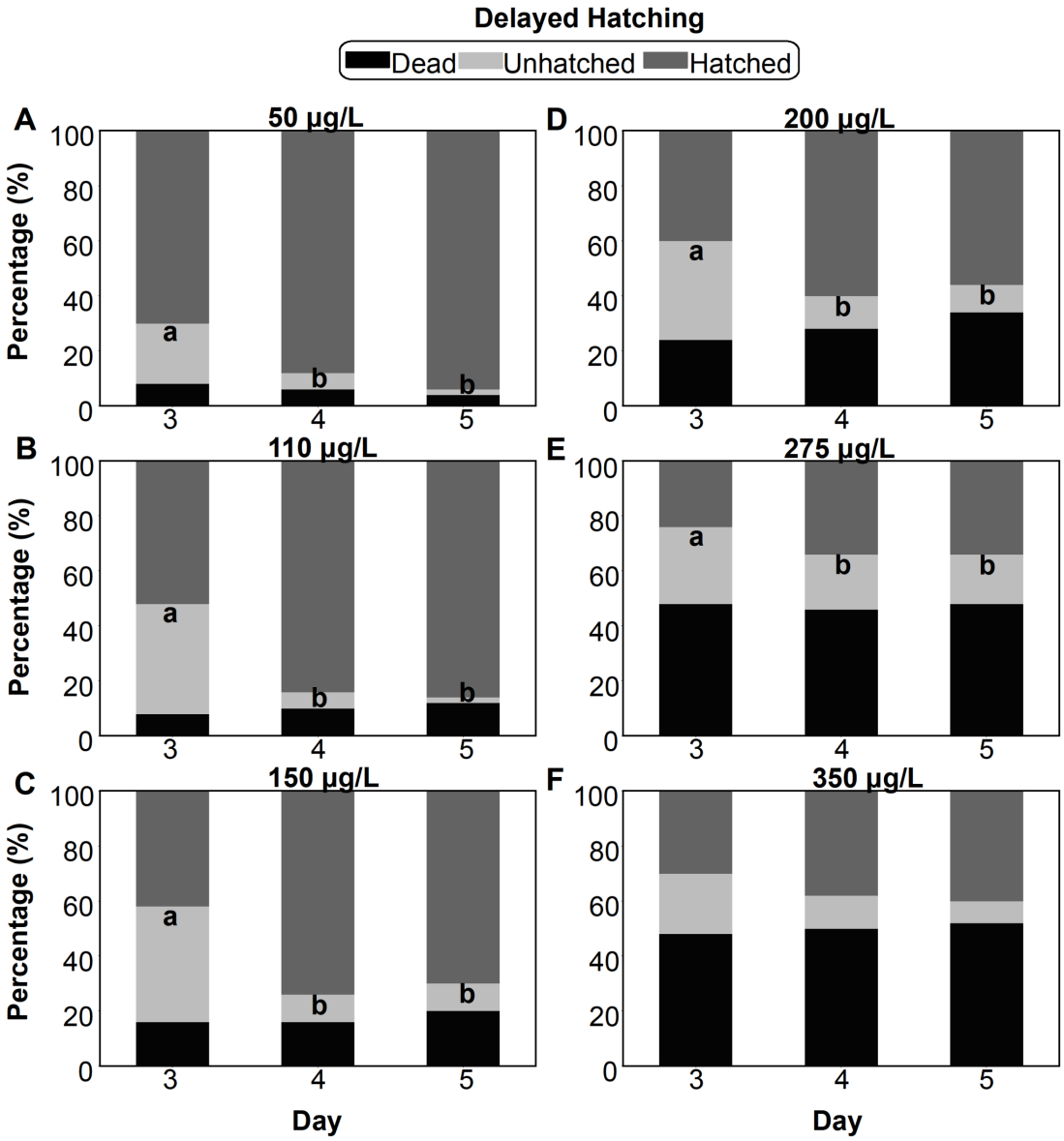

Figure 2.10. **Percent of *Danio rerio* embryos that were dead, affected and unaffected by delayed hatching following exposure to varying concentrations of phenanthrene up to 5 d. Letters denote significant difference across days ($p < 0.05$). Total sample size over the 5 runs yielded 350 embryos (50 per treatment).**

2.4. Tables

Table 2.1. Mean % mortality for *Danio rerio* embryos over a 5 d exposure to phenanthrene. Mortality percentages were normalized to the methanol control and statistical difference measured across treatments. Original methanol control values were reported below. Statistical difference denotes treatments significantly different from the normalized methanol control (null). Values are reported at the 95 % confidence limit with 2 standard error values.

	Phenanthrene concentration (µg/L)							
	Day	MeOH	50	110	150	200	275	350
Mortality (%)	1	6.0 ± 4.4	5.7 ± 6.7	5.7 ± 6.7	*14 ± 11	*19 ± 13	*32 ± 16	*40. ± 17
	2	6.0 ± 4.4	7.6 ± 7.8	5.7 ± 6.7	*14 ± 11	*19 ± 13	*36 ± 16	*40. ± 17
	3	6.0 ± 4.4	7.6 ± 7.8	7.6 ± 7.8	*15 ± 11	*23 ± 14	*48 ± 17	*48 ± 17
	4	8.0 ± 3.6	5.7 ± 6.7	*9.5 ± 8.8	*14 ± 11	*27 ± 15	*46 ± 17	*50. ± 17
	5	10. ± 5.7	3.8 ± 5.4	*11 ± 10.	*19 ± 13	*34 ± 16	*48 ± 17	*52. ± 17

The '*' denotes statistical difference. (n = 50).

Table 2.2. Calculated LC10 values for *Danio rerio* embryos over a 5 d exposure to phenanthrene. Confidence intervals are denoted at the 95 % confidence level.

Time (h)	LC10 (µg/L)	Confidence Interval
24	106.6	10.8 - 207.2
48	104.2	9.6 - 200.8
72	106.2	23.4 - 184.9
96	102.2	23.6 - 178.9
120	87.4	18.8 - 157.4

Table 2.3. Mean % sublethal effects for *Danio rerio* embryos over a 5 d exposure to phenanthrene. Sublethal effect percentages were normalized to the methanol control and statistical difference measured across treatments. Original methanol control values were reported below. Statistical difference denotes treatments significantly different from the normalized methanol control (null). Values are reported at the 95 % confidence limit with 2 standard error values.

Teratogenic deformity	Phenanthrene concentration (µg/L)							
	Day	MeOH	50	110	150	200	275	350
Pericardial edema	1	2.0 ± 3.6	*23 ± 15	*25 ± 16	*23 ± 15	*31 ± 18	*23 ± 15	*17 ± 13
	2	12 ± 10.	*27 ± 17	*42 ± 20.	*37 ± 19	*31 ± 18	*23 ± 15	*19 ± 14
	3	10 ± 5.7	*17 ± 13	*31 ± 18	*29 ± 17	*21 ± 15	*15 ± 12	*17 ± 13
	4	6.0 ± 4.4	*11 ± 10.	*11 ± 10.	*13 ± 11	*25 ± 16	*15 ± 12	*11 ± 10
	5	0.0 ± 0.0	*11 ± 10.	*13 ± 11	9.0 ± 9.0	*17 ± 13	*15 ± 12	*7.1 ± 7.9
Yolk Edema	1	0.0 ± 10.	7.5 ± 7.9	*9.4 ± 9.0	*9.4 ± 9.0	*23 ± 14	*25 ± 15	*33 ± 17
	2	4.0 ± 3.6	*15 ± 12	*15 ± 12	*17 ± 12	*25 ± 15	*23 ± 14	*29 ± 16
	3	0.0 ± 4.4	*9.4 ± 9.0	*15 ± 12	*13 ± 11	*17 ± 12	*19 ± 13	*23 ± 14
	4	0.0 ± 0.0	7.5 ± 7.9	7.5 ± 7.9	*17 ± 12	*13 ± 11	*17 ± 12	*11 ± 9.9
	5	0.0 ± 0.0	7.5 ± 7.9	1.8 ± 3.8	*11 ± 9.9	*9.4 ± 9.0	*15 ± 12	5.6 ± 6.7
Tail Kinking	1	0.0 ± 3.6	0.8 ± 2.3	0.8 ± 2.3	*7.5 ± 7.1	0.8 ± 2.3	*7.5 ± 7.1	5.8 ± 6.2
	2	0.0 ± 3.6	5.8 ± 6.2	4.1 ± 5.2	*9.3 ± 7.8	0.8 ± 2.3	*9.3 ± 7.8	5.8 ± 6.2
	3	0.0 ± 0.0	*11 ± 8.5	*9.3 ± 7.8	*11 ± 8.5	*9.3 ± 7.8	2.5 ± 4.0	4.1 ± 5.2
	4	0.0 ± 0.0	*13 ± 9.2	*9.3 ± 7.8	*15 ± 9.8	*13 ± 9.2	4.1 ± 5.2	4.1 ± 5.2
	5	2.0 ± 4.4	*18 ± 11	*17 ± 10.	*13 ± 9.2	*13 ± 9.2	*15 ± 9.8	5.8 ± 6.2
Delayed Hatching	3	19 ± 4.6	*19 ± 17	*38 ± 25	*41 ± 25	*34 ± 23	*25 ± 20.	*19 ± 17
	4	14 ± 0.0	4.7 ± 6.6	4.7 ± 6.6	8.1 ± 9.5	9.8 ± 11	*17 ± 16	9.8 ± 11
	5	6.0 ± 4.6	1.5 ± 3.3	1.5 ± 3.3	8.1 ± 9.5	8.1 ± 9.5	*15.2 ± 14.7	6.4 ± 8.1

The '*' denotes statistical difference. (n = 50).

2.5. Discussion

The objective of this study was to assess the teratogenicity of phenanthrene. For this, an acute 5-d passive-dosing exposure was carried out in the model organism *Danio rerio* and the following sublethal teratogenic effects monitored daily: pericardial edema (PE), yolk edema (YE), tail kinking (TK) and delayed hatching (DH)]. This study also aimed to determine if phenanthrene induced teratogenicity, and if it was reversible.

2.5.1. Passive Dosing System

Passive dosing (PD) was shown to be an effective exposure methodology, capable of achieving and maintaining phenanthrene test concentrations over the exposure period.

Measured concentrations were close to nominal values (92 – 95 %) through the 5 d of exposure over the phenanthrene concentration range (50 – 350 µg/L). A strong linear correlation between measured and predicted nominal concentrations has been reported using both flow-through PD with O-rings (for chronic exposures) and coated PDMS vials (for acute exposures) using comparable phenanthrene concentrations (32 - 423 µg/L) in a similar study (Butler et al., 2013). In another study, phenanthrene-loaded O-rings in polystyrene well plates reported measured concentrations between 49 – 60 % of the nominal values (Vergauwen et al., 2015). This low similarity between measured and nominal concentrations may be due to phenanthrene adsorbing to plastics (Zuo et al., 2019; Smith et al., 2010). For this reason, this study used inert glass as recommended by the OECD in cases where adsorption to polystyrene may arise (OECD, 2013). Glass was shown to be an effective material for PD. Furthermore, PD was effective at maintaining test concentrations that were environmentally relevant since concentrations were below phenanthrene's water solubility value (1.1 ± 0.1 mg/L at 22 °C) and were maintained at constant values.

2.5.2. Mortality

The acute lethality of phenanthrene to fish has been well documented in the literature (Honda and Suzuki, 2020). Compared to HMW PAHs that are characterized by high chronic toxicity, LMW PAHs like phenanthrene are acutely toxic and more hazardous than other PAHs (Salvo et al., 2016). Acute lethality values for phenanthrene report a range of 96-h LC50 values between 271 and 1400 µg/L for early-life-stage (ELS) fish (Butler et al., 2013; Vergauwen et al., 2015; Mu et al., 2014; Moreau et al., 1999; Ministry of the Environment Japan, 2019; Willis and Oris, 2014).

In this study, calculated lethal toxicity values for phenanthrene were below literature values. While determining acute lethality was not a direct study objective, values were derived for the NOEC, LOEC and LC10. This study reports a NOEC and LOEC of 50 and 110 µg/L, respectively. This NOEC falls within the literature range which reports 120-h NOEC values between 10 and 105 µg/L in Fathead minnow (*Pimephales promelas*) larvae and zebrafish (*Danio* rerio) embryos, respectively (Verbruggen, 2012; Butler et al., 2013). Comparatively, this study's derived LOEC is on magnitude 3 to 4-fold lower than documented values in the literature (between 362 – 423 µg/L) for zebrafish embryos (Vergauwen et al., 2015; Butler et al., 2013). The current study's derived LC10 value is

also approximately 4-fold lower than previously reported. While LC10 values for ELS fish are generally lacking, one study reported a 72-h LC10 of 423 µg/L in zebrafish embryos (Sogbanmu et al., 2016); a value well above the 72-h LC10 value of 106 µg/L derived in this study. Higher acute toxicity reported here is likely attributed to maintaining stable phenanthrene concentrations through PD exposure. Previous phenanthrene exposures have reported chemical losses over 50 % (Vergauwen et al., 2015), suggesting that the current calculated values are likely more accurate.

2.5.3. Teratogenesis

Phenanthrene is an identified teratogen in fish known to elicit teratogenic effects as both a single or multi-PAH exposure (e.g., crude oil) in many fish species including sea ruffe (*Sebastiscus marmoratus*) (Li et al., 2011), marine medaka (*Oryzias melastigma*) (Zheng et al., 2020; Mu et al., 2014), Pacific herring (*Clupea pallasi*) (Carls et al., 1999, 2009; Incardona et al., 2009), pink salmon (*Oncorhynchus gorbuscha*) (Heintz et al., 1999) and zebrafish (*Danio rerio*) (Butler et al., 2013; Vergauwen et al., 2015). These teratogenic effects target a wide range of developing body systems to impede embryological development (Sogbanmu et al., 2016; Li et al., 2020).

Edemas

Phenanthrene caused edemas in zebrafish at concentrations near or below previously reported values. Statistically significant PE and YE were detected at 50 and 150 µg/L, respectively. Likewise, studies with the same exposure duration as this current one report phenanthrene concentrations between 105 – 362 µg/L were capable of inducing edemas in zebrafish (Butler et al., 2013; Vergauwen et al., 2015; Xu et al., 2022). Expectantly, the literature reports lower phenanthrene concentrations with longer exposure times; significant edema was reported in rockfish (*Sebastiscus marmoratus*) larvae exposed to 50 µg/L over 8 d (Li et al., 2011). Furthermore, marine medaka (*Oryzias melastigma*) larvae exhibited edema following exposure to 2 µg/L over 28 d (Zheng et al., 2020; Li et al., 2011). While standard chemical behavior shows increasing sublethal toxicity over time, these studies provide a broad scope of phenanthrene's potency. Based on the acute exposure time of this current study, the findings indicate zebrafish may be more sensitive to phenanthrene than previously reported, as indicated by the low phenanthrene concentrations shown to be effective at inducing edemas.

Edemas are attributed to increasing overall malformation prevalence in fish embryos (Xu et al., 2022; Zheng et al., 2020). Respectively, 12 – 25 % increases in malformations for zebrafish and marine medaka have been reported over phenanthrene exposures (Xu et al., 2022; Zheng et al., 2020). Malformations observed included spinal deformities, PE and YE, of which edemas were noted as the predominant effects (Xu et al., 2022; Zheng et al., 2020). This current study showed similar increases in malformation prevalence with maximal levels between 15 – 18 % above the control (PE and TK, respectively). While both PE and TK were detected at the lowest phenanthrene concentration, TK look longer to develop and was only significant on d 5. Comparatively, significant edema over the exposure duration indicates its predominant nature as a common malformation in fish.

Deleterious health effects that play a role in edemas include both reduced kidney function and cardiac circulation (Burggren and Dubansky, 2018). For eg., hydrodynamic forces produced by a fish's beating heart is pivotal for kidney glomeruli development; therefore, reduced circulation often decreases kidney perfusion which consequently leads to edema (Burggren and Dubansky, 2018). Multiple studies have observed these health effects in fish. Zebrafish embryos exhibiting severe YE following phenanthrene exposure (9624 µg/L) also had impaired kidneys with decreased circulation in pronephric tubule epithelium (Incardona et al., 2004). Reduced circulation was also reported to precede both yolk and pericardial edema formation in marine medaka (*Oryzias melastigma*) embryos exposed to phenanthrene (> 400 µg/L) (Mu et al., 2014). Therefore, the interrelation between circulation and kidney perfusion both effect the occurrence of edemas in fish.

Poor circulation maintained under the influence of edemas often leads to altered cardiac rhythms in fish (Cypher et al., 2017). Phenanthrene-induced edemas have been associated with causing bradycardia in fish embryos under both acute (6 – 96 h) (Incardona et al., 2004; Cypher et al., 2017; McGruer et al., 2021) and chronic (6 – 10 dpf) exposure durations (Zheng et al., 2020). Edemas are believed to play a role in bradycardia by contributing to reduced pericardial perfusion (Cypher et al., 2017). Conversely, one study reported phenanthrene elevated heartrate in zebrafish embryos after 72 h (Xu et al., 2022). Researchers suggest heart rate effects are multifactorial and may vary based on fish species, PAH type and exposure concentration (Mu et al., 2014).

The occurrence of edemas has been associated with osmoregulatory disruption in fish (Li et al., 2011; Zheng et al., 2020). Phenanthrene impairs osmoregulation on both an

enzymatic and physiological level (Li et al., 2011; Sørhus et al., 2023). Both Na^+/K^+-ATPase and Ca^{2+}-ATPase are enzymes that help regulate the ion balance critical for homeostasis (Li et al., 2011). Phenanthrene exposure studies have reported alterations to these enzymes led to subsequent fluid imbalances and edema in fish (Li et al., 2011). For eg., phenanthrene inhibition of both Na^+/K^+-ATPase and Ca^{2+}-ATPase in sea ruffe (*Sebastiscus marmoratus*) was correlated to a significant increase in both PE and YE after 8 d of exposure (Li et al., 2011). A decline in ATPase levels was also reported in marine medaka (*Oryzia melastigma*) larvae exhibiting edema after a 28-d exposure to phenanthrene (Zheng et al., 2020). On a physiological level, phenanthrene is shown to effect marginal finfolds, an anatomical region that plays a role in osmoregulation by functioning as a reservoir for regulating water balance (Sørhus et al., 2023). Phenanthrene-exposed Atlantic cod (*Gadus morhua*) embryos displayed a decrease in marginal finfolds as well as significant edema after 6 d of exposure (Sørhus et al., 2023). While neither enzyme activity nor marginal finfolds were endpoints measured in this current study, their known association with edemas in the literature offers insight into the potential mechanism behind the edemas observed herein.

This study provided evidence for the recovery of edemas. PE reversal occurred at lower phenanthrene concentrations (< 200 µg/L) whereas YE reversal randomly occurred across a range of concentrations. A similar study reported complete reversal of edemas in zebrafish following a 5-d exposure to phenanthrene (Butler et al., 2013). Comparatively, the current study observed only partial edema reversal among embryos. As both studies had the same exposure duration and similar phenanthrene concentrations, it is hard to deduce why differences in edema reversal were observed. These studies reflect the unpredictable nature of edema reversal. Rather, the degree of reversal appears to occur randomly. However, both studies exhibited similar recovery periods where edemas declined after the hatching period on d 3. This recovery timeline coincides with zebrafish circulatory development as the heart is fully developed by 72 h to maintain heart perfusion necessary to mitigate edema (Kimmel et al., 1995; Burggren and Dubansky, 2018).

Tail Kinking

Phenanthrene caused tail kinking (TK) in zebrafish at concentrations below those reported in the literature. This current study found 50 µg/L of phenanthrene was capable of inducing TK in zebrafish after 120 h whereas higher ranges between 362 – 423 µg/L have been

reported for the same exposure period in the literature (Butler et al., 2013; Vergauwen et al., 2015). Dorsal curvature was reported in zebrafish exposed to 891 µg/L of phenanthrene for 96 h (Wolińska et al., 2011). Another study reported stunted tail growth in zebrafish exposed to 524 µg/L for 72 h (Sogbanmu et al., 2016). The higher sublethal toxicity in this study is likely due to the accurate phenanthrene concentrations maintained by PD. Therefore, the 7-fold lower effective concentration reported herein suggests fish are likely more sensitive to phenanthrene-induced tail deformities than previously reported.

In addition to TK, the literature has documented many types of tail deformities in fish related to both PAH and phenanthrene exposures. These deformities include tail curvature, tissue deviation, elbow, or spinal curvature (lordosis, kyphosis and scoliosis) (Vergauwen et al., 2015; Vignet et al., 2019). Therefore, tail deformities encompass multiple morphological effects and can elicit various physiological effects.

Tail deformities have been observed alongside several behavioral effects including abnormal swimming patterns and swim behavior in fish, both of which have been associated with exposure to PAH mixtures and phenanthrene (Carls et al.,1999; de Soysa et al., 2012; Descalso, 2019). Zebrafish embryos exhibiting spinal curvature had decreased movement, lacked forward propulsion, and exhibited abnormal circular swimming patterns after a 3-d exposure to phenanthrene (Descalso, 2019). This association between spinal curvature and decreased swimming ability was also reported in Pacific herring (*Clupea pallasi*) embryos exposed for 16 d to weathered crude oil (containing predominantly tricyclic PAHs including phenanthrene) (Carls et al., 1999). The authors denoted a strong correlation between swimming ability and spinal curvature, with spinal curvature being the strongest predictor among other predicting factors like lower jaw size and yolk sac edema (Carls et al., 1999). Another study noted PAH-induced alterations to swim behavior in zebrafish embryos included impaired escape responses, lower sensitivity to touch tests, and reduced swimming time (de Soysa et al., 2012). Furthermore, significant dorsal tail curvature was observed in embryos displaying impaired escape response (de Soysa et al., 2012). The authors concluded altered swimming behavior is likely associated with morphological tail abnormalities in the musculature. However, as impairment to neural transmission is another potential mechanism to explain this behavior, further research is needed (de Soysa et al., 2012). Overall, the literature

suggests PAH-induced tail deformities likely play a role in altering swim behavior in fish embryos.

In general, tail and spine deformities are believed to arise when skeletal and musculature developmental processes are disrupted (de Soysa et al., 2012; Incardona et al., 2004). A possible mechanism behind tail deformities is phenanthrene's ability to disrupt somitogenesis, the process during which mesoderm is organized into morphologically distinct vertebral segments (de Soysa et al., 2012). Somitogenesis, beginning at the end of the gastrula stage, initiates the formation of the tail bud which marks the boundary between the first and second somite (somatic furrow) (Kimmel et al., 1995). Tail formation is completed during the segmentation stage (10 – 24 hpf) (Kimmel et al., 1995). Studies have assessed how PAHs disrupt somitogenesis in fish and lead to tail deformities. Zebrafish embryos exhibited abnormally shaped somites and disrupted segments following a 72-h exposure to crude oil (TPAH < 12 µg/L) (de Soysa et al., 2012). Fish also showed muscle loss and disorganization, reflecting potential impairment of peripheral nervous system development (de Soysa et al., 2012). Zebrafish embryos exposed to phenanthrene for 72 h failed to develop all 30 somite pairs; rather, the majority developed only 28 somites and also exhibited curved spines and tail truncation (Descalso, 2019).

Other possible mechanisms behind tail deformities include impaired osmoregulation and blood circulation (Li et al., 2011; Vergauwen et al., 2015). As osmoregulation plays a large role in mineral uptake, disruptions can deleteriously impact skeletal formation and lead to tail deformities. Increased dorsal curvature in sea ruffe (*Sebastiscus marmoratus*) was directly correlated with a decrease in Na^+/K^+-ATPase and Ca^{2+}-ATPase activity following 8 d of phenanthrene exposure (Li et al., 2011). In terms of circulation, the literature shows tail deformities have also been associated with reduced blood circulation (Vergauwen et al., 2015). No blood circulation was observed in zebrafish embryos exhibiting tail malformations following 5 d of phenanthrene exposure (Vergauwen et al., 2015). Another study reported zebrafish exhibiting dorsal curvature also had decreased blood circulation in their trunk region (Incardona et al., 2004). As blood flow through the posterior caudal vein and dorsal aorta keep the tail oxygenated during somitogenesis, it is reasonable maintaining tail blood circulation is critical for proper tail formation and avoidance of potential tail deformities (Nakajima et al., 2021).

TK incidence increased over time, with no evidence of reversal. The irreversibility of tail deformities is also corroborated in the literature as Butler et al. (2013) reported tail curvature was the only sublethal effect present in zebrafish embryos after a 120-h exposure to phenanthrene. The irreversibility of tail deformities is likely due to the critical somatogenic processes occurring early on in zebrafish development (Descalso, 2019). Irregularly developed somites or missing somites often induce irreparable damage. As well, the earlier the exposure time, that is, embryos exposed early after fertilization are more susceptible to incomplete somitogenesis (Descalso, 2019). One study found phenanthrene had a more pronounced effect on zebrafish development, specifically incomplete somitogenesis and spinal curvature, when exposed at the earlier blastula stage (2.25 h) opposed to the 6-somite stage (12 h) (Descalso, 2019). As the current study utilized an even earlier exposure (1.5 hpf), it is reasonable phenanthrene would induce irreversible tail effects. Based on the irreversible nature of TK observed in this current study, TK incidence would be expected to further increase under chronic conditions, further compromising organismal health.

Delayed Hatching

DH is considered as the prolonged maintenance of an embryo's intact chorion past an organism's normal hatching period. The hatching period of *danio rerio* is reported to be between 48 - 72 hpf (Kimmel et al., 1995) and so, embryos remaining unhatched after 72 h are considered to exhibit DH.

Multiple studies, including the present one, have reported on phenanthrene's ability to cause DH in fish at similar concentrations (Butler et al., 2013; Li et al., 2020b; Zheng et al., 2020). DH has been observed in zebrafish between a range of LOEC values of 105 – 362 µg/L (Butler et al., 2013; Vergauwen et al., 2015). For marine medaka (*Oryzias melastigma*), a lower LOEC range between 10 – 50 µg/L was reported to cause DH (Zheng et al., 2020; Li et al., 2020b).

Oxygen availability in fish embryos plays a large role in hatching and development. As hatching promotes oxygen uptake, DH can lead to an increased risk of hypoxia among unhatched fish due to the egg shell limiting gas exchange (Candolin, 2022). Hypoxia in fish has been associated with increased deformities and developmental alterations (Candolin, 2022). A study carried out phenanthrene exposures in zebrafish embryos under both normoxic and hypoxic conditions to assess if oxygen deprivation exacerbates

cardiotoxicity and teratogenesis in fish (Cypher et al., 2017). Individuals under both conditions exhibited delayed hatching (72 – 96 hpf), increased edema and decreased heart rates, with symptoms worsened under hypoxic conditions (Cypher et al., 2017). Another study that observed DH in sea ruffe (*Sebastiscus marmoratus*) exposed to phenanthrene reported significant upregulation of Erythropoietin (*epo*), a mediator gene of erythrocyte production under hypoxic conditions (Li et al., 2011). These results suggest phenanthrene exposure can further drive hypoxia through eliciting DH, and can lead to further deleterious health effects. Conversely, a study on the effects of oxygen availability on hatching in rainbow trout (*Oncorhynchus mykiss*) embryos revealed hatching may be triggered when oxygen levels are insufficient to meet aerobic metabolic requirements (Latham and Just, 1989). The authors reported hatching was stimulated in rainbow trout when low oxygen conditions were introduced (Latham and Just, 1989). This suggests fish may have evolved an adaptive internal response to low oxygen availability under normal conditions. However, under the influence of a xenobiotic like phenanthrene, the literature shows DH may persist under hypoxic conditions (Cypher et al., 2017). Therefore, variation in hatching time is most likely influenced by differences in species, oxygen availability, and chemical exposure time or concentration.

Studies have revealed that fish fecundity and hatching is greatly affected by pH (Kwong et al., 2014; Kong et al., 2023; Zahangir et al., 2015). Alterations to pH can cause dysregulation of ion levels critical for homeostatic balance, which can affect reproductive processes. For eg., an acidic pH is often associated with inhibition of the sodium-hydrogen exchanger and ATPases responsible for maintaining sodium, chlorine and sodium bicarbonate, all molecules which regulate metabolic and reproductive function (Kwong et al., 2014). Studies show pH rearing conditions that deviate outside of a neutral pH range exhibit reduced fecundity, delayed hatching and declines in hatching success among fish (Zahangir et al., 2015; Kong et al., 2023). Zebrafish embryos reared in acidic treatments for 15 d (pH 5.0 – 6.0) exhibited mean daily egg declines around 45 % while basic treatments (pH 9.0 – 10.0) revealed losses as high as 90 % (Zahangir et al., 2015). Hatching time was delayed in the pH 10 treatment to 87 hpf relative to the pH 7 control at 68 hpf. Likewise, a hatching delay of 83 hpf was exhibited in the pH 4 treatment (Zahangir et al., 2015). A similar study revealed significant hatching rate declines in obscure pufferfish (*Takifugu obscurus*) in both acidic (pH 5.0 – 6.0) and basic (pH 10.0 – 11.0)

conditions (Kong et al., 2023). Therefore, pH is a critical factor that can further exacerbate deleterious hatching effects of xenobiotics like phenanthrene.

The underlying mechanism behind hatching in zebrafish involves both the regulation of embryonic zinc (Zn^{2+}) levels by transporter genes, and the actions of zebrafish hatching enzyme (ZHE1) (Muraina et al., 2020; Hedgpeth et al., 2019). Zebrafish possess two main hatching enzymes, ZHE1 and ZHE2; however, hatching is mainly driven by ZHE1 whereas the latter is rarely expressed in pre-hatching embryos (Sano et al., 2008). As a metalloprotease, ZHE1 facilitates the digestion of the chorion through zinc (Zn^{2+}) secretions which cause the chorion to swell and soften before embryonic contractile movements cause it to rupture (Okada et al., 2009). Specifically, muscular contractions arising during somitogenesis (at the 20-somite stage approximately 19 hpf) are responsible for this rupturing step (Descalso, 2019). Additionally, ZHE1 aids in the distension of the embryo to prepare it for hatching (Hedgpeth et al., 2019; Sano et al., 2008). Zinc released from ZHE1 is regulated by zinc transporters Zip10 and Znt1a, which control the influx and efflux of Zn^{2+} out of the embryo, respectively (Muraina et al., 2020). A study showed knockdown of genes related to Zip10 and Znt1a transporters effected Zn^{2+} concentrations and hatching ability in zebrafish (Muraina et al., 2020). *Zip10* knockdown decreased Zn^{2+} levels in the hatching gland cells (HGC) and led to the displacement and eventual loss of hatching glands, zebrafish hatching enzymes (eg., *he1a* and *catL1b*) and hatching ability. Knockdown of *Znt1a* had the opposite effect on hatching and resulted in the upregulation of hatching enzymes and Zn^{2+} ions in the HGC (Muraina et al., 2020. Therefore, maintenance of zinc by transporter genes and hatching enzymes appears to be fundamental to hatching and any dysregulation in this mechanism can lead to impaired or delayed hatching (Muraina et al., 2020).

There is a lack in the literature regarding how PAHs mechanistically alter hatching ability in zebrafish. While there are no known studies regarding PAH effects on zinc or zinc transporters involved in hatching, some studies suggest PAHs may affect hatching by impairing ZHE1 in zebrafish (Hedgpeth et al., 2019; Elfawy et al., 2021). For eg., one study observed benzo[a]pyrene (BaP) has a high binding affinity to ZHE1 (Elfawy et al., 2021). Computational analysis revealed BaP altered the structure of ZHE1 by interacting with its functional and integral sites, leading to ZHE1 inhibition (Elfawy et al., 2021). As well, down-regulation of the *Zhe1* gene was indicative of gene suppression effects. These molecular changes translated to physiological hatching effects as BaP-exposed embryos exhibited

delayed hatching beyond 96 h (Elfawy et al., 2021). While no other study has assessed PAH-induced modifications of ZHE1, Hedgpeth et al. (2019) postulated lack of hatch in zebrafish embryos exposed to various petroleum products (eg. Dilbit, crude oils, cracked gas oil, vacuum gas oil, and straight-run gas oil) was due to a lack of ZHE1. As ZHE1 is a critical part of the mechanism behind hatching, it is plausible PAHs target this enzyme. Any alterations to ZHE1 that affect its binding capacity or availability, or the gene expression of *Zhe1,* are probable mechanisms behind PAH-induced delayed hatching. Further research is needed to examine if phenanthrene utilizes these mechanisms.

Hatching success in fish is related to the contents of the embryo's yolk sac (McGruer et al., 2023; Laurel et al., 2019; Hedgpeth et al., 2019). Xenobiotics that alter the fat content of the yolk sac prior to hatching can weaken embryos and reduce their hatching success (McGruer et al., 2023). Acute phenanthrene exposure (72 h) has been reported to decrease lipid and metabolite levels in zebrafish yolks (McGruer et al., 2023). Other PAH-related yolk defects were reported in Polar cod (*Boreogadus saida*) embryos following an acute crude oil exposure (Laurel et al., 2019). In addition to yolk sacs having altered free fatty acids, triglycerides and total lipids, there was an overall decrease in hatching success (Laurel et al., 2019). These studies show that maintenance of fat content in the yolk sac plays a large role in successful hatching. Therefore, phenanthrene-induced alterations to yolk sac content, such as lipid and metabolite declines, may be a key mechanism behind reduced hatching success. Currently there is a gap in the literature regarding how phenanthrene mechanistically alters the content of teleost yolk sacs to impact hatching. The current study attests to phenanthrene's role on promoting delayed hatching in zebrafish; however, future research efforts should assess if yolk sac modifications are driving this effect.

2.6. Conclusion

This study examined the teratogenic effects of phenanthrene in zebrafish (*Danio rerio*) and delayed hatching of embryos. Besides only one known study in the literature, this is the only other study that assesses the reversal of phenanthrene-induced teratogenic effects. The teratogenic effects observed herein are reported below previously reported phenanthrene concentrations and draw concern for the fitness and survival individually and at the population level of all teleost species. The results indicate only edemas (both pericardial and yolk sac) were capable of partial reversal; this reflects the potential ability

of embryos to recover from initial teratogenesis during development. The significant decline in edemas observed after 2 dpf suggests recovery may occur after the pharyngula stage (24 – 48 h). This is likely because the development of a heartbeat during this stage may achieve adequate perfusion to counteract edema through osmoregulatory control. However, the observance of edema reversal only at lower phenanthrene concentrations suggests edema is still a potent sublethal effect and cause for concern if maintained into adulthood. Comparatively, the non-reversibility of tail kinking indicates some forms of teratogenesis are not capable of recovery during development. This further reflects concerns for fish development if tail kinking is maintained or worsened. In terms of hatching, the results indicated phenanthrene delays hatching by 1 d past the literature hatching period. As each d of the embryonic stage is marked by rapid development, this delay raises concerns for proper embryonic development. Further research is needed to determine if delayed hatching affects larval development. Future research efforts should focus on monitoring larval development following acute phenanthrene exposures. Amid the observed teratogenesis, significant mortality observed below previously reported thresholds indicates acute toxicity concerns of phenanthrene. Therefore, low concentrations of phenanthrene are capable of exerting both acute and sublethal toxic effects in fish.

Passive dosing was shown to be an effective exposure system for hydrophobic chemicals with low water solubilities. Maintenance of phenanthrene concentrations through PD indicates accurate effect concentrations were derived. This was attributed to the achieved dissolution of phenanthrene and continual bioavailability to embryos during the acute PD exposure. Exposure was indicative of real-life exposure scenarios as environmentally-relevant concentrations below phenanthrene's water solubility value (1.1 ± 0.1 mg/L at 22 °C) were used. As previous studies report the majority of observed toxicity from phenanthrene takes place during the first 6 d of zebrafish development (Butler et al., 2013), the application of PD during this acute exposure window is critical for accurate assessment. This study recommends the use of PD in chronic exposures as well where chemical loss by volatilization is a large concern.

ELS acute exposures are necessary for accurately assessing phenanthrene toxicity. While teleost embryos are characteristically more robust in nature compared to adults, developmental toxicity of phenanthrene is still cause for concern on the long-term viability of species. As fish undergo a plethora of changes during organogenesis, these results

emphasize the importance of assessing developmental toxicity under acute conditions to safeguard early-life stage organisms undergoing development.

2.7. References

Abdel-Shafy, H. I., & Mansour, M. S. M. (2016). A review on polycyclic aromatic hydrocarbons: Source, environmental impact, effect on human health and remediation. *Egyptian Journal of Petroleum*, *25*(1), 107–123. https://doi.org/10.1016/j.ejpe.2015.03.011

Achten, C., & Andersson, J. T. (2015). Overview of Polycyclic Aromatic Compounds (PAC). *Polycyclic Aromatic Compounds*, *35*(2-4), 177–186. https://doi.org/10.1080/10406638.2014.994071

Ali, T.E. and Legler, J. (2011). Developmental toxicity of nonylphenol in zebrafish (Danio rerio) embryos. *Indian Journal of Marine Sciences, 40*(4), 509-515. https://nopr.niscpr.res.in/bitstream/123456789/12763/1/IJMS%2040%284%29%20509-515.pdf

Alkindi, A. Y. A., Brown, J. A., Waring, C. P., & Collins, J. E. (1996). Endocrine, osmoregulatory, respiratory and haematological parameters in flounder exposed to the water soluble fraction of crude oil. *Journal of Fish Biology*, *49*(6), 1291–1305. https://doi.org/10.1111/j.1095-8649.1996.tb01796.x

Alsaadi, F., Hodson, P. V., & Langlois, V. S. (2018). An Embryonic Field of Study: The Aquatic Fate and Toxicity of Diluted Bitumen. *Bulletin of Environmental Contamination and Toxicology*, *100*(1), 8–13. https://doi.org/10.1007/s00128-017-2239-7

Aguilar, L., Lara-Flores, M., Rendón-von Osten, J., Kurczyn, J. A., Vilela, B., & da Cruz, A. L. (2021). Effects of polycyclic aromatic hydrocarbons on biomarker responses in Gambusia yucatana, an endemic fish from Yucatán Peninsula, Mexico. *Environmental Science and Pollution Research International*, *28*(34), 47262–47274. https://doi.org/10.1007/s11356-021-13952-0

Bandowe, B. A. M., & Meusel, H. (2017). Nitrated polycyclic aromatic hydrocarbons (nitro-PAHs) in the environment – A review. *The Science of the Total Environment*, *581-582*, 237–257. https://doi.org/10.1016/j.scitotenv.2016.12.115

Barron, M. G., Carls, M. G., Heintz, R., & Rice, S. D. (2004). Evaluation of Fish Early Life-Stage Toxicity Models of Chronic Embryonic Exposures to Complex Polycyclic Aromatic Hydrocarbon Mixtures. *Toxicological Sciences*, *78*(1), 60–67. https://doi.org/10.1093/toxsci/kfh051

Billiard, S. M., Meyer, J. N., Wassenberg, D. M., Hodson, P. V., & Di Giulio, R. T. (2008). Nonadditive effects of PAHs on Early Vertebrate Development: mechanisms and implications for risk assessment. *Toxicological Sciences*, *105*(1), 5–23. https://doi.org/10.1093/toxsci/kfm303

Bowling, J. W., Leversee, G. J., Landrum, P. F., & Giesy, J. P. (1983). Acute mortality of anthracene-contaminated fish exposed to sunlight. *Aquatic Toxicology*, *3*(1), 79–90. https://doi.org/10.1016/0166-445X(83)90008-5

Bramatti, I., Matos, B., Figueiredo, N., Pousão-Ferreira, P., Branco, V., & Martins, M. (2023). Interaction of Polycyclic Aromatic Hydrocarbon compounds in fish primary hepatocytes: From molecular mechanisms to genotoxic effects. *The Science of the Total Environment*, *855*, 158783–158783. https://doi.org/10.1016/j.scitotenv.2022.158783

Brette, F., Machado, B., Cros, C., Incardona, J. P., Scholz, N. L., & Block, B. A. (2014). Crude Oil Impairs Cardiac Excitation-Contraction Coupling in Fish. *Science (American Association for the Advancement of Science)*, *343*(6172), 772–776. https://doi.org/10.1126/science.1242747

Brette, F., Shiels, H. A., Galli, G. L. J., Cros, C., Incardona, J. P., Scholz, N. L., & Block, B. A. (2017). A Novel Cardiotoxic Mechanism for a Pervasive Global Pollutant. *Scientific Reports*, *7*(1), 41476. https://doi.org/10.1038/srep41476

Brinkworth, L. C., Hodson, P. V., Tabash, S., & Lee, P. (2003). CYP1A INDUCTION AND BLUE SAC DISEASE IN EARLY DEVELOPMENTAL STAGES OF RAINBOW TROUT (ONCORHYNCHUS MYKISS) EXPOSED TO RETENE. *Journal of Toxicology and Environmental Health, Part A*, *66*(7), 627–646. https://doi.org/10.1080/15287390309353771

Butler, J. D., Parkerton, T. F., Letinski, D. J., Bragin, G. E., Lampi, M. A., & Cooper, K. R. (2013). A novel passive dosing system for determining the toxicity of phenanthrene to early life stages of zebrafish. *The Science of the Total Environment*, *463-464*, 952–958. https://doi.org/10.1016/j.scitotenv.2013.06.079

Burggren, W., & Dubansky, B. (2018). Case Study: The 2010 Deepwater Horizon Oil Spill and Its Environmental Developmental Impacts. In *Development and Environment* (pp. 235–283). Springer International Publishing AG. https://doi.org/10.1007/978-3-319-75935-7_10

Butler, J. D., Parkerton, T. F., Redman, A. D., Letinski, D. J., & Cooper, K. R. (2016). Assessing Aromatic-Hydrocarbon Toxicity to Fish Early Life Stages Using Passive-Dosing Methods and Target-Lipid and Chemical-Activity Models. *Environmental Science & Technology*, *50*(15), 8305–8315. https://doi.org/10.1021/acs.est.6b01758

Call, D.J., Brooke, L.T., Harting, S.L., Poirier, S.H., McCauley, D.J. (1986). Toxicity of Phenanthrene to Freshwater Species. Center for Lake Superior Environmental Studies.

Canadian Council of Ministers of the Environment. (1999). Polycyclic Aromatic Hydrocarbons. (PAHs). Canadian Water Quality Guidelines For the Protection of Aquatic Life. https://ccme.ca/en/res/polycyclic-aromatic-hydrocarbons-pahs-en-canadian-water-quality-guidelines-for-the-protection-of-aquatic-life.pdf

Canadian Council of Ministers of the Environment. (2010). Polycyclic Aromatic Hydrocarbons. Canadian Soil Quality Guidelines CARCINOGENIC AND OTHER POLYCYCLIC AROMATIC HYDROCARBONS (PAHs) (Environmental and Human Health Effects).

Candolin, U., Goncalves, S., & Pant, P. (2022). Delayed early life effects in the threespine stickleback. *Proceedings of the Royal Society. B, Biological Sciences*, *289*(1976), 20220554–20220554. https://doi.org/10.1098/rspb.2022.0554

Carls, M. G., Marty, G. D., Meyers, T. R., Thomas, R. E., & Rice, S. D. (1998). Expression of viral hemorrhagic septicemia virus in prespawning Pacific herring (Clupea pallasi) exposed to weathered crude oil. *Canadian Journal of Fisheries and Aquatic Sciences*, *55*(10), 2300–2309. https://doi.org/10.1139/cjfas-55-10-2300

Carls, M. G., Rice, S. D., & Hose, J. E. (1999). Sensitivity of fish embryos to weathered crude oil: Part I. low-level exposure during incubation causes malformations, genetic damage, and mortality in larval pacific herring (clupea pallasi). *Environmental Toxicology and Chemistry, 18*(3), 481-493. https://doi.org/10.1002/etc.5620180317

Carls, M.G., Hose, J.E. and Thomas, R.E. (2009). Exposure of pacific herring to weathered crude oil: Assessing effects on ova. *Environmental Toxicology and Chemistry, 19*(6), 1649 – 1659. https://doi.org/10.1002/etc.5620190624

Carls, M. G., & Thedinga, J. F. (2010). Exposure of pink salmon embryos to dissolved polynuclear aromatic hydrocarbons delays development, prolonging vulnerability to mechanical damage. *Marine Environmental Research*, *69*(5), 318–325. https://doi.org/10.1016/j.marenvres.2009.12.006

CAREX Canada. 2023. PAHs Profile. https://www.carexcanada.ca/profile/polycyclic_aromatic_hydrocarbons/

Carvalho, P. S. M., Kalil, D. da C. B., Novelli, G. A. A., Bainy, A. C. D., & Fraga, A. P. M. (2008). Effects of naphthalene and phenanthrene on visual and prey capture endpoints during early stages of the dourado Salminus Brasiliensis. *Marine Environmental Research*, *66*(1), 205–207. https://doi.org/10.1016/j.marenvres.2008.02.059

CDC. 2023. Biomonitoring Summary. Polycyclic aromatic hydrocarbons review. https://www.cdc.gov/biomonitoring/Phenanthrene_BiomonitoringSummary.html

Chávez-Veintemilla, C. and Adalberto Val. (2019). Effects of Phenanthrene on the Amazonian Fish Tambaqui Colossoma macropomum: LC50, Growth and Haematology. Environment and Ecology Research 7(5): 293-302, 2019. DOI: 10.13189/eer.2019.070504

Chen, Y., Zhang, Y., Yu, Z., Guan, Y., Chen, R., & Wang, C. (2021). Early-life phenanthrene exposure inhibits reproductive ability in adult zebrafish and the mechanism of action. *Chemosphere (Oxford)*, *272*, 129635. https://doi.org/10.1016/j.chemosphere.2021.129635

Choi, H., Harrison, R., Komulainen, H. and Delgado Saborit, J.M. (2010). Polycyclic aromatic hydrocarbons. In *WHO Guidelines for Indoor Air Quality: Selected Pollutants.* Available from: https://www.ncbi.nlm.nih.gov/books/NBK138709/

Correia, A. D., Gonçalves, R., Scholze, M., Ferreira, M., & Henriques, M. A.-R. (2007). Biochemical and behavioral responses in gilthead seabream (Sparus aurata) to phenanthrene. *Journal of Experimental Marine Biology and Ecology*, *347*(1), 109–122. https://doi.org/10.1016/j.jembe.2007.03.015

Cypher, A. D., Consiglio, J., & Bagatto, B. (2017). Hypoxia exacerbates the cardiotoxic effect of the polycyclic aromatic hydrocarbon, phenanthrene in Danio rerio. *Chemosphere (Oxford)*, *183*, 574–581. https://doi.org/10.1016/j.chemosphere.2017.05.109

de Campos, M. F., Lo Nostro, F. L., Da Cuña, R. H., & Moreira, R. G. (2018). Endocrine disruption of phenanthrene in the protogynous dusky grouper Epinephelus marginatus (Serranidae: Perciformes). *General and Comparative Endocrinology*, *257*, 255–263. https://doi.org/10.1016/j.ygcen.2017.06.020

Dekant, W. (2009). The role of biotransformation and bioactivation in toxicity. *EXS (Basel)*, *99*, 57–86. https://doi.org/10.1007/978-3-7643-8336-7_3

Descalso, K.N. 2019. Morphological Effects of Phenanthrene on Somitogenesis in Zebrafish via Perturbation of the Wnt/β-catenin Signaling Pathway. https://scholarworks.calstate.edu/downloads/gx41mj476

de Soysa, T. Y., Ulrich, A., Friedrich, T., Pite, D., Compton, S. L., Ok, D., Bernardos, R. L., Downes, G. B., Hsieh, S., Stein, R., Lagdameo, M. C., Halvorsen, K., Kesich, L.-R., & Barresi, M. J. F. (2012). Macondo crude oil from the Deepwater Horizon oil spill disrupts specific developmental processes during zebrafish embryogenesis. *BMC Biology*, *10*(1), 40–40. https://doi.org/10.1186/1741-7007-10-40

Di Nunzio, M., Valli, V., Tomás-Cobos, L., Tomás-Chisbert, T., Murgui-Bosch, L., Danesi, F., & Bordoni, A. (2017). Is cytotoxicity a determinant of the different in vitro and in vivo effects of bioactives? *BMC complementary and alternative medicine*, *17*(1), 453. https://doi.org/10.1186/s12906-017-1962-2

Environmental Protection Agency. 2014. Priority Pollutant List. https://www.epa.gov/sites/default/files/2015-09/documents/priority-pollutant-list-epa.pdf

Esbaugh, A. J., Mager, E. M., Stieglitz, J. D., Hoenig, R., Brown, T. L., French, B. L., Linbo, T. L., Lay, C., Forth, H., Scholz, N. L., Incardona, J. P., Morris, J. M., Benetti, D. D., & Grosell, M. (2016). The effects of weathering and chemical dispersion on Deepwater Horizon crude oil toxicity to mahi-mahi (Coryphaena hippurus) early life stages. *The Science of the Total Environment*, *543*(Pt A), 644–651. https://doi.org/10.1016/j.scitotenv.2015.11.068

Ezike, C.O., Echor, F.O., Igugo R., Uwadiegwu, N.C. (2019). Benzo [a] Pyrene-carcinogenic and mutagenic equivalents of Clarias gariepinus (Burchell, 1822) to Nigerian-crude and diesel oils. *International Journal of Fisheries and Aquatic Studies, 7*(5): 62 – 67.

Finger, S.E., Little, E.F., Henry, M.G., Fairchild, J.F., Boyle, T.P. (1985). Comparison of laboratory and field assessment of fluorene - Part I: Effects of fluorene on the survival, growth, reproduction, and behavior of aquatic organisms in laboratory tests. In: Boyle TP, ed. Validation and predictability of laboratory methods for assessing the fate and effects of contaminants in aquatic ecosystems. ASTM STP 865. Philadelphia, PA: American Society for Testing and Materials. pp. 120-133.

Folmar, L. C., Craddock, D. R., Blackwell, J. W., Joyce, G., & Hodgins, H. O. (1981). Effects of petroleum exposure on predatory behavior of coho salmon (Oncorhynchus kisutch) [Alaska]. *Bulletin of Environmental Contamination and Toxicology*, *27*(4), 458–462. https://doi.org/10.1007/BF01611048

Frapiccini, E., Cocci, P., Annibaldi, A., Panfili, M., Santojanni, A., Grilli, F., Marini, M., & Palermo, F. A. (2021). Assessment of seasonal relationship between polycyclic aromatic hydrocarbon accumulation and expression patterns of oxidative stress-related genes in muscle tissues of red mullet (M. barbatus) from the Northern Adriatic Sea. *Environmental Toxicology and Pharmacology*, *88*, 103752–103752. https://doi.org/10.1016/j.etap.2021.103752

Garner, L. V. T., & Di Giulio, R. T. (2012). Glutathione transferase pi class 2 (GSTp2) protects against the cardiac deformities caused by exposure to PAHs but not PCB-126 in zebrafish embryos. *Comparative Biochemistry and Physiology. Toxicology & Pharmacology*, *155*(4), 573–579. https://doi.org/10.1016/j.cbpc.2012.01.007

Geiger, D.L., Northcott, C.E., Call, D.J., Brooke, L.T. eds. 1985. Acute Toxicities of Organic Chemicals to Fathead Minnows (Pimephales Promelas). Superior, WI, USA: Center for Lake Superior Environmental Studies, University of Wisconsin Superior.

Goanvec, C., Theron, M., Lacoue-Labarthe, T., Poirier, E., Guyomarch, J., Le-Floch, S., Laroche, J., Nonnotte, L., & Nonnotte, G. (2008). Flow cytometry for the evaluation of chromosomal damage in turbot Psetta maxima (L.) exposed to the dissolved fraction of heavy fuel oil in sea water: a comparison with classical biomarkers. *Journal of Fish Biology*, *73*(2), 395–413. https://doi.org/10.1111/j.1095-8649.2008.01901.x

Government of Canada. 2023. Fact sheet: Phenanthrene. https://gost.tpsgc-pwgsc.gc.ca/Contfs.aspx?ID=43&lang=eng

Grmasha, R. A., Abdulameer, M. H., Stenger-Kovács, C., Al-sareji Osamah J., Al-Gazali, Z., Al-Juboori, R. A., Meiczinger, M., & Hashim, K. S. (2023). Polycyclic aromatic hydrocarbons in the surface water and sediment along Euphrates River system: Occurrence, sources, ecological and health risk assessment. *Marine Pollution Bulletin*, *187*, 114568. https://doi.org/10.1016/j.marpolbul.2022.114568

Haftka, J. J. H., Govers, H. A. J., & Parsons, J. R. (2010). Influence of temperature and origin of dissolved organic matter on the partitioning behavior of polycyclic aromatic hydrocarbons. *Environmental Science and Pollution Research International*, *17*(5), 1070–1079. https://doi.org/10.1007/s11356-009-0263-9

Hawkins, S. A., Billiard, S. M., Tabash, S. P., Brown, R. S., & Hodson, P. V. (2002). Altering cytochrome P4501A activity affects polycyclic aromatic hydrocarbon metabolism and toxicity in rainbow trout (Oncorhynchus mykiss). *Environmental Toxicology and Chemistry*, *21*(9), 1845–1853. https://doi.org/10.1002/etc.5620210912

Hedgpeth, B. M., Redman, A. D., Alyea, R. A., Letinski, D. J., Connelly, M. J., Butler, J. D., Zhou, H., & Lampi, M. A. (2019). Analysis of Sublethal Toxicity in Developing Zebrafish Embryos Exposed to a Range of Petroleum Substances. *Environmental Toxicology and Chemistry*, *38*(6), 1302–1312. https://doi.org/10.1002/etc.4428

Heintz, R. A., Short, J. W., & Rice, S. D. (1999). Sensitivity of fish embryos to weathered crude oil: Part II. Increased mortality of pink salmon (Oncorhynchus gorbuscha) embryos incubating downstream from weathered Exxon valdez crude oil. *Environmental Toxicology and Chemistry*, *18*(3), 494–503. https://doi.org/10.1002/etc.5620180318

Hill, A. J., Teraoka, H., Heideman, W., & Peterson, R. E. (2005). Zebrafish as a Model Vertebrate for Investigating Chemical Toxicity. *Toxicological Sciences*, *86*(1), 6–19. https://doi.org/10.1093/toxsci/kfi110

Honda, M., & Suzuki, N. (2020). Toxicities of Polycyclic Aromatic Hydrocarbons for Aquatic Animals. *International Journal of Environmental Research and Public Health*, *17*(4), 1363. https://doi.org/10.3390/ijerph17041363

Huang, G.-Y., Liu, Y.-S., Liang, Y.-Q., Shi, W.-J., Yang, Y.-Y., Liu, S.-S., Hu, L.-X., Chen, H.-X., Xie, L., & Ying, G.-G. (2019). Endocrine disrupting effects in western mosquitofish Gambusia affinis in two rivers impacted by untreated rural domestic wastewaters. *The Science of the Total Environment*, *683*, 61–70. https://doi.org/10.1016/j.scitotenv.2019.05.231

Hutchinson, T. H., Shillabeer, N., Winter, M. J., & Pickford, D. B. (2006). Acute and chronic effects of carrier solvents in aquatic organisms: A critical review. *Aquatic Toxicology*, *76*(1), 69–92. https://doi.org/10.1016/j.aquatox.2005.09.008

Idowu, O., Semple, K. T., Ramadass, K., O'Connor, W., Hansbro, P., & Thavamani, P. (2019). Beyond the obvious: Environmental health implications of polar polycyclic aromatic hydrocarbons. *Environment International*, *123*, 543–557. https://doi.org/10.1016/j.envint.2018.12.051

Incardona, J. P., Collier, T. K., & Scholz, N. L. (2004). Defects in cardiac function precede morphological abnormalities in fish embryos exposed to polycyclic aromatic hydrocarbons. *Toxicology and Applied Pharmacology*, *196*(2), 191–205. https://doi.org/10.1016/j.taap.2003.11.026

Incardona, J. P., Carls, M. G., Teraoka, H., Sloan, C. A., Collier, T. K., & Scholz, N. L. (2005). Aryl Hydrocarbon Receptor-Independent Toxicity of Weathered Crude Oil during Fish Development. *Environmental Health Perspectives*, *113*(12), 1755–1762. https://doi.org/10.1289/ehp.8230

Incardona, J. P., Carls, M. G., Day, H. L., Sloan, C. A., Bolton, J. L., Collier, T. K., & Scholz, N. L. (2009). Cardiac Arrhythmia Is the Primary Response of Embryonic Pacific Herring (*Clupea pallasi*) Exposed to Crude Oil during Weathering. *Environmental Science & Technology*, *43*(1), 201–207. https://doi.org/10.1021/es802270t

Incardona, J. P. (2017). Molecular Mechanisms of Crude Oil Developmental Toxicity in Fish. *Archives of Environmental Contamination and Toxicology*, *73*(1), 19–32. https://doi.org/10.1007/s00244-017-0381-1

International Tanker Owners Pollution Federation Limited (2023). Oil Tanker Spill Statistics 2023. https://www.itopf.org/knowledge-resources/data-statistics/statistics/

Ishigaki, M., Yasui, Y., Puangchit, P., Kawasaki, S., & Ozaki, Y. (2016). In Vivo Monitoring of the Growth of Fertilized Eggs of Medaka Fish (Oryzias latipes) by Near-Infrared Spectroscopy and Near-Infrared Imaging-A Marked Change in the Relative Content of Weakly Hydrogen-Bonded Water in Egg Yolk Just before Hatching. *Molecules (Basel, Switzerland)*, *21*(8), 1003. https://doi.org/10.3390/molecules21081003

Jarque, S., Rubio-Brotons, M., Ibarra, J., Ordoñez, V., Dyballa, S., Miñana, R., & Terriente, J. (2020). Morphometric analysis of developing zebrafish embryos allows predicting teratogenicity modes of action in higher vertebrates. *Reproductive Toxicology (Elmsford, N.Y.)*, *96*, 337–348. https://doi.org/10.1016/j.reprotox.2020.08.004

Jung, D., Matson, C. W., Collins, L. B., Laban, G., Stapleton, H. M., Bickham, J. W., Swenberg, J. A., & Di Giulio, R. T. (2011). Genotoxicity in Atlantic killifish (Fundulus heteroclitus) from a PAH-contaminated Superfund site on the Elizabeth River, Virginia. *Ecotoxicology (London)*, *20*(8), 1890–1899. https://doi.org/10.1007/s10646-011-0727-9

Jung, J.-H., Hicken, C. E., Boyd, D., Anulacion, B. F., Carls, M. G., Shim, W. J., & Incardona, J. P. (2013). Geologically distinct crude oils cause a common cardiotoxicity syndrome in developing zebrafish. *Chemosphere (Oxford)*, *91*(8), 1146–1155. https://doi.org/10.1016/j.chemosphere.2013.01.019

Kang, X., Li, D., Zhao, X., Lv, Y., Chen, X., Song, X., Liu, X., Chen, C., & Cao, X. (2022). Long-Term Exposure to Phenanthrene Induced Gene Expressions and Enzyme Activities of Cyprinus carpio below the Safe Concentration. *International Journal of Environmental Research and Public Health*, *19*(4), 2129. https://doi.org/10.3390/ijerph19042129

Kennedy, C.J. (2015). Ch 1: Multiple effects of oil and its components in fish. In J.B. Alford., M.S. Peterson & C.C. Green (Eds.), *Impacts of oil spill disasters on marine habitats and fisheries in North America* (pp. 4 – 28). CRC Press.

Kennedy, C. J., & Farrell, A. P. (2006). Effects of exposure to the water-soluble fraction of crude oil on the swimming performance and the metabolic and ionic recovery postexercise in Pacific herring (Clupea pallasi). *Environmental Toxicology and Chemistry*, *25*(10), 2715–2724. https://doi.org/10.1897/05-504R.1

Kennedy, C. J., & Farrell, A. P. (2008). Immunological alterations in juvenile Pacific herring, Clupea pallasi, exposed to aqueous hydrocarbons derived from crude oil. *Environmental Pollution (1987)*, *153*(3), 638–648. https://doi.org/10.1016/j.envpol.2007.09.003

Khan, R.A. (2013). Effects of polycyclic aromatic hydrocarbons on sexual maturity of Atlantic cod, Gadus morhua, following chronic exposure. *Environment and Pollution, 2*(1): 1 – 10. doi:10.5539/ep.v2n1p1

Kielhorn, J., Wahnschaffe, U. and Mangelsdorf, I. (2003.) Environmental Health Criteria 229: Selected nitro- and nitro- oxy- polycyclic aromatic hydrocarbons. Available from: https://www.inchem.org/documents/ehc/ehc/ehc229.htm

Kim, K., Jeon, H.-J., Choi, S.-D., Tsang, D. C. W., Oleszczuk, P., Ok, Y. S., Lee, H.-S., & Lee, S.-E. (2018). Combined toxicity of endosulfan and phenanthrene mixtures and induced molecular changes in adult Zebrafish (Danio rerio). *Chemosphere (Oxford)*, *194*, 30–41. https://doi.org/10.1016/j.chemosphere.2017.11.128

Kimmel, C. B., Ballard, W. W., Kimmel, S. R., Ullmann, B., & Schilling, T. F. (1995). Stages of embryonic development of the zebrafish. *Developmental Dynamics*, *203*(3), 253–310. https://doi.org/10.1002/aja.1002030302

Koudryashova, Y., Chizhova, T., Inoue, M., Hayakawa, K., Nagao, S., Marina, E., & Mundo, R. (2022). Deep Water PAH Cycling in the Japan Basin (the Sea of Japan). *Journal of Marine Science and Engineering*, *10*(12), 2015. https://doi.org/10.3390/jmse10122015

Kramer, N. I., Krismartina, M., Rico-Rico, A., Blaauboer, B. J., & Hermens, J. L. M. (2012). Quantifying Processes Determining the Free Concentration of Phenanthrene in Basal Cytotoxicity Assays. *Chemical Research in Toxicology*, *25*(2), 436–445. https://doi.org/10.1021/tx200479k

Kong, X., He, F. & Li, H. (2023). The effect of pH value on fertilized eggs, larva fish and juvenile fish of Takifugu obscurus. Preprints, 2023030261. https://doi.org/10.20944/preprints202303.0261.v1

Kwong, R. W. M., Kumai, Y., & Perry, S. F. (2014). The physiology of fish at low pH: the zebrafish as a model system. *Journal of Experimental Biology*, *217*(Pt 5), 651–662. https://doi.org/10.1242/jeb.091603

Lam, M. M., Engwall, M., Denison, M. S., & Larsson, M. (2018). Methylated polycyclic aromatic hydrocarbons and/or their metabolites are important contributors to the overall estrogenic activity of polycyclic aromatic hydrocarbon–contaminated soils. *Environmental Toxicology and Chemistry*, *37*(2), 385–397. https://doi.org/10.1002/etc.3958

Latham, K. E., & Just, J. J. (1989). Oxygen Availability Provides a Signal for Hatching in the Rainbow Trout (Salmo gairdneri) Embryo. *Canadian Journal of Fisheries and Aquatic Sciences*, *46*(1), 55–58. https://doi.org/10.1139/f89-008

Laurel, B. J., Copeman, L. A., Iseri, P., Spencer, M. L., Hutchinson, G., Nordtug, T., Donald, C. E., Meier, S., Allan, S. E., Boyd, D. T., Ylitalo, G. M., Cameron, J. R., French, B. L., Linbo, T. L., Scholz, N. L., & Incardona, J. P. (2019). Embryonic Crude Oil Exposure Impairs Growth and Lipid Allocation in a Keystone Arctic Forage Fish. *iScience*, *19*, 1101–1113. https://doi.org/10.1016/j.isci.2019.08.051

Lawal, A. T. (2017). Polycyclic aromatic hydrocarbons. A review. *Cogent Environmental Science*, *3*(1), 1339841. https://doi.org/10.1080/23311843.2017.1339841

Lee, H. J., Shim, W. J., Lee, J., & Kim, G. B. (2011). Temporal and geographical trends in the genotoxic effects of marine sediments after accidental oil spill on the blood cells of striped beakperch (*Oplegnathus fasciatus*). *Marine Pollution Bulletin*, *62*(10), 2264–2268. https://doi.org/10.1016/j.marpolbul.2011.07.008

Lee, J.S., Lee, K.T., Kim, D.H., Kim, J.H. and Han, N.H. (2004). Acute Toxicity of Dissolved Inorganic Metals, Organotins and Polycyclic Aromatic Hydrocarbons to Puffer Fish, *Takifugu obscurus*. *Journal of Env Tox. 19*(2), 141- 151.

Lee, K., Boufadel, M., & Chen, B. (2015). *The Royal Society of Canada Expert Panel Report: The Behaviour and Environmental Impacts of Crude Oil Released into Aqueous Environments*. Royal Society of Canada.

Li, R., Zuo, Z., Chen, D., He, C., Chen, R., Chen, Y., & Wang, C. (2011). Inhibition by polycyclic aromatic hydrocarbons of ATPase activities in Sebastiscus marmoratus larvae：Relationship with the development of early life stages. *Marine Environmental RIesearch*, *71*(1), 86–90. https://doi.org/10.1016/j.marenvres.2010.11.002

Li, R., Gao, H., Ji, Z., Jin, S., Ge, L., Zong, H., Jiao, L., Zhang, Z., & Na, G. (2020). Distribution and sources of polycyclic aromatic hydrocarbons in the water column of Kongsfjorden, Arctic. *Journal of Environmental Sciences (China)*, *97*, 186–193. https://doi.org/10.1016/j.jes.2020.04.024

Li, X., Xiong, D., Ding, G., Fan, Y., Ma, X., Wang, C., Xiong, Y., & Jiang, X. (2019). Exposure to water-accommodated fractions of two different crude oils alters morphology, cardiac function and swim bladder development in early-life stages of zebrafish. *Chemosphere (Oxford)*, *235*, 423–433. https://doi.org/10.1016/j.chemosphere.2019.06.199

Li, Y., Wang, J., Yang, G., Lu, L., Zheng, Y., Zhang, Q., Zhang, X., Tian, H., Wang, W., & Ru, S. (2020b). Low level of polystyrene microplastics decreases early developmental toxicity of phenanthrene on marine medaka (Oryzias melastigma). *Journal of Hazardous Materials*, *385*, 121586. https://doi.org/10.1016/j.jhazmat.2019.121586

Liney, K. E., Hagger, J. A., Tyler, C. R., Depledge, M. H., Galloway, T. S., & Jobling, S. (2006). Health effects in fish of long-term exposure to effluents from wastewater treatment works. *Environmental Health Perspectives*, *114 Suppl 1*(Suppl 1), 81–89. https://doi.org/10.1289/ehp.8058

Loughery, J. R., Kidd, K. A., Mercer, A., & Martyniuk, C. J. (2018). Part B: Morphometric and transcriptomic responses to sub-chronic exposure to the polycyclic aromatic hydrocarbon phenanthrene in the fathead minnow (Pimephales promelas). *Aquatic Toxicology*, *199*, 77–89. https://doi.org/10.1016/j.aquatox.2018.03.026

Lourenço, R. A., Lube, G. V., Jarcovis, R. D. L. M., da Silva, J., & de Souza, A. C. (2023). Navigating the PAH maze: Bioaccumulation, risks, and review of the quality guidelines in marine ecosystems with a spotlight on the Brazilian coastline. Marine Pollution Bulletin, 197, 115764–115764. https://doi.org/10.1016/j.marpolbul.2023.115764

Machado, A. A. de S., Hoff, M. L. M., Klein, R. D., Cordeiro, G. J., Lencina Avila, J. M., Costa, P. G., & Bianchini, A. (2014). Oxidative stress and DNA damage responses to phenanthrene exposure in the estuarine guppy Poecilia vivipara. *Marine Environmental Research*, *98*, 96–105. https://doi.org/10.1016/j.marenvres.2014.03.013

Mallo, M., Vinagre, T., & Carapuço, M. (2009). The road to the vertebral formula. *The International Journal of Developmental Biology*, *53*(8-10), 1469–1481. https://doi.org/10.1387/ijdb.072276mm

Marr, L. C., Kirchstetter, T. W., Harley, R. A., Miguel, A. H., Hering, S. V., & Hammond, S. K. (1999). Characterization of Polycyclic Aromatic Hydrocarbons in Motor Vehicle Fuels and Exhaust Emissions. *Environmental Science & Technology*, *33*(18), 3091–3099. https://doi.org/10.1021/es981227l

McCollum, C. W., Ducharme, N. A., Bondesson, M., & Gustafsson, J.-A. (2011). Developmental toxicity screening in zebrafish. *Birth Defects Research. Part C. Embryo Today*, *93*(2), 67–114. https://doi.org/10.1002/bdrc.20210

McConville, M. M., Roberts, J. P., Boulais, M., Woodall, B., Butler, J. D., Redman, A. D., Parkerton, T. F., Arnold, W. R., Guyomarch, J., LeFloch, S., Bytingsvik, J., Camus, L., Volety, A., & Brander, S. M. (2018). The sensitivity of a deep-sea fish species (Anoplopoma fimbria) to oil-associated aromatic compounds, dispersant, and Alaskan North Slope crude oil. *Environmental Toxicology and Chemistry*, *37*(8), 2210–2221. https://doi.org/10.1002/etc.4165

McGrath, J. A., & Di Toro, D. M. (2009). Validation of the target lipid model for toxicity assessment of residual petroleum constituents: Monocyclic and polycyclic aromatic hydrocarbons. *Environmental Toxicology and Chemistry*, *28*(6), 1130–1148. https://doi.org/10.1897/08-271.1

McGruer, V., Bhatia, A., Magnuson, J.T. and Schlenk, D. (2023). Lipid profile altered in phenanthrene exposed zebrafish embryos with implications for neurological development and early life nutritional status. *Environmental Health, 1*(1), 32 – 40. https://doi.org/10.1021/envhealth.3c00002

McGruer, V., Tanabe, P., Vliet, S. M. F., Dasgupta, S., Qian, L., Volz, D. C., & Schlenk, D. (2021). Effects of Phenanthrene Exposure on Cholesterol Homeostasis and Cardiotoxicity in Zebrafish Embryos. *Environmental Toxicology and Chemistry*, *40*(6), 1586–1595. https://doi.org/10.1002/etc.5002

McIntosh, S., King, T., Wu, D., & Hodson, P. V. (2010). Toxicity of dispersed weathered crude oil to early life stages of Atlantic herring (Clupea harengus). *Environmental Toxicology and Chemistry*, *29*(5), 1160–1167. https://doi.org/10.1002/etc.134

Mo, J., Au, D. W.-T., Wan, M. T., Shi, J., Zhang, G., Winkler, C., Kong, R. Y.-C., & Seemann, F. (2020). Multigenerational Impacts of Benzo[a]pyrene on Bone Modeling and Remodeling in Medaka (*Oryzias latipes*). *Environmental Science & Technology*, *54*(19), 12271–12284. https://doi.org/10.1021/acs.est.0c02416

Moles A, Rice SD. 1983. Effects of crude oil and naphthalene on growth, caloric content, and fat content of pink salmon juveniles in seawater. *Trans Am Fisher Soc* 112: 205-211.

Moles, A., Rice, S., & Norcross, B. L. (1994). Non-avoidance of hydrocarbon laden sediments by juvenile flatfishes. *Netherlands Journal of Sea Research*, *32*(3), 361–367. https://doi.org/10.1016/0077-7579(94)90013-2

Montuori, P., De Rosa, E., Di Duca, F., De Simone, B., Scippa, S., Russo, I., Sarnacchiaro, P., & Triassi, M. (2022). Polycyclic Aromatic Hydrocarbons (PAHs) in the Dissolved Phase, Particulate Matter, and Sediment of the Sele River, Southern Italy: A Focus on Distribution, Risk Assessment, and Sources. *Toxics (Basel)*, *10*(7), 401. https://doi.org/10.3390/toxics10070401

Moreau, C. J., Klerks, P. L., & Haas, C. N. (1999). Interaction between phenanthrene and zinc in their toxicity to the sheepshead minnow (*Cyprinodon variegatus*). *Archives of Environmental Contamination and Toxicology*, *37*(2), 251–257. https://doi.org/10.1007/s002449900512

Mu, J., Wang, J., Jin, F., Wang, X., & Hong, H. (2014). Comparative embryotoxicity of phenanthrene and alkyl-phenanthrene to marine medaka (Oryzias melastigma). *Marine Pollution Bulletin*, *85*(2), 505–515. https://doi.org/10.1016/j.marpolbul.2014.01.040

Munnelly, R. T., Windecker, C. C., Reeves, D. B., Rieucau, G., Portier, R. J., & Chesney, E. J. (2021). Effects of short-duration oil exposure on bay anchovy (Anchoa mitchilli) embryos and larvae: mortality, malformation, and foraging. *Aquatic Toxicology*, *237*, 105904–105904. https://doi.org/10.1016/j.aquatox.2021.105904

Nagpal, N.K. (1993). Ministry of Environment, Lands and Parks Province of British Columbia. Ambient Water Quality Criteria for Polycyclic Aromatic Hydrocarbons (PAHs). https://www2.gov.bc.ca/assets/gov/environment/air-land-water/water/waterquality/water-quality-guidelines/approved-wqgs/bc_env_pah_waterqualityguideline_technical.pdf

Nakajima, H., Chiba, A., Fukumoto, M., Morooka, N., & Mochizuki, N. (2021). Zebrafish Vascular Development: General and Tissue-Specific Regulation. *Journal of Lipid and Atherosclerosis*, *10*(2), 145–159. https://doi.org/10.12997/jla.2021.10.2.145

National Center for Biotechnology Information (2024). PubChem Compound Summary for CID 995, Phenanthrene. Retrieved January 29, 2024 from https://pubchem.ncbi.nlm.nih.gov/compound/Phenanthrene

National Oceanic and Atmospheric Association. (2020). Oil Spills: What are the largest marine oil spills in American History? https://www.noaa.gov/education/resource-collections/ocean-coasts/oil-spills#:~:text=On%20April%2020%2C%202010%2C%20an,200%20Olympic%2Dsized%20swimming%20pools.

Negri, A. P., Brinkman, D. L., Flores, F., Botté, E. S., Jones, R. J., & Webster, N. S. (2016). Acute ecotoxicology of natural oil and gas condensate to coral reef larvae. *Scientific Reports*, *6*(1), 21153. https://doi.org/10.1038/srep21153

OECD, 2013. OECD Guidelines for the testing of chemicals: Fish embryo acute toxicity (FET) test. 236: 1-22.

Oh, S., Wang, Q., Shin, W. S., & Song, D.-I. (2013). Effect of salting out on the desorption-resistance of polycyclic aromatic hydrocarbons (PAHs) in coastal sediment. *Chemical Engineering Journal (Lausanne, Switzerland: 1996)*, *225*, 84–92. https://doi.org/10.1016/j.cej.2013.03.069

Okada, A., Nagata, K., Sano, K., Yasumasu, S., Kubota, K., Ohtsuka, J., Iuchi, I., & Tanokura, M. (2009). Crystallization and preliminary X-ray analysis of ZHE1, a hatching enzyme from the zebrafish Danio rerio. *Acta Crystallographica. Section F, Structural Biology and Crystallization Communications*, *65*(10), 1018–1020. https://doi.org/10.1107/S1744309109033016

Oliveira, M., Pacheco, M., & Santos, M. A. (2007). Cytochrome P4501A, genotoxic and stress responses in golden grey mullet (Liza aurata) following short-term exposure to phenanthrene. *Chemosphere (Oxford)*, *66*(7), 1284–1291. https://doi.org/10.1016/j.chemosphere.2006.07.024

Oris, J. T., & Giesy, J. P. (1985). The photoenhanced toxicity of anthracene to juvenile sunfish (Lepomis spp.). *Aquatic Toxicology*, *6*(2), 133–146. https://doi.org/10.1016/0166-445X(85)90012-8

Palanikumar, L., Kumaraguru, A. K., Ramakritinan, C. M., & Anand, M. (2012). Biochemical response of anthracene and benzo [a] pyrene in milkfish Chanos chanos. *Ecotoxicology and Environmental Safety*, *75*(1), 187–197. https://doi.org/10.1016/j.ecoenv.2011.08.028

Pampanin, D. M. & Sydnes, M.O. (2013). Polycyclic Aromatic Hydrocarbons a Constituent of Petroleum : Presence and influence in The Aquatic Environment. IntechOpen. https://doi.org/10.5772/48176

Panzica-Kelly, J. M., Zhang, C. X., & Augustine-Rauch, K. A. (2015). Optimization and Performance Assessment of the Chorion-Off [Dechorinated] Zebrafish Developmental Toxicity Assay. *Toxicological sciences: an official journal of the Society of Toxicology*, *146*(1), 127–134. https://doi.org/10.1093/toxsci/kfv076

Patel, A. B., Shaikh, S., Jain, K. R., Desai, C., & Madamwar, D. (2020). Polycyclic Aromatic Hydrocarbons: Sources, Toxicity, and Remediation Approaches. *Frontiers in Microbiology*, *11*, 562813–562813. https://doi.org/10.3389/fmicb.2020.562813

Peng, X., Sun, X., Yu, M., Fu, W., Chen, H., & Chen, J. (2019). Chronic exposure to environmental concentrations of phenanthrene impairs zebrafish reproduction. *Ecotoxicology and Environmental Safety*, *182*, 109376–109376. https://doi.org/10.1016/j.ecoenv.2019.109376

Perrichon, P., Le Menach, K., Akcha, F., Cachot, J., Budzinski, H., & Bustamante, P. (2016). Toxicity assessment of water-accommodated fractions from two different oils using a zebrafish (Danio rerio) embryo-larval bioassay with a multilevel approach. *The Science of the Total Environment*, *568*, 952–966. https://doi.org/10.1016/j.scitotenv.2016.04.186

Philibert, D. A., Lyons, D., Philibert, C., & Tierney, K. B. (2019). Field-collected crude oil, weathered oil and dispersants differentially affect the early life stages of freshwater and saltwater fishes. *The Science of the Total Environment*, *647*, 1148–1157. https://doi.org/10.1016/j.scitotenv.2018.08.052

Pohjanvirta, R. (2012). *The AH receptor in biology and toxicology edited by Raimo Pohjanvirta.* (1st ed.). Wiley.

Renegar, D. A., Turner, N. R., Riegl, B. M., Dodge, R. E., Knap, A. H., & Schuler, P. A. (2017). Acute and subacute toxicity of the polycyclic aromatic hydrocarbon 1-methylnaphthalene to the shallow-water coral Porites divaricata: Application of a novel exposure protocol. *Environmental Toxicology and Chemistry*, *36*(1), 212–219. https://doi.org/10.1002/etc.3530

Rhodes, S., Farwell, A., Mark Hewitt, L., MacKinnon, M., & George Dixon, D. (2005). The effects of dimethylated and alkylated polycyclic aromatic hydrocarbons on the embryonic development of the Japanese medaka. *Ecotoxicology and Environmental Safety*, *60*(3), 247–258. https://doi.org/10.1016/j.ecoenv.2004.08.002

Rocha, A. C., & Palma, C. (2019). Source identification of polycyclic aromatic hydrocarbons in soil sediments: Application of different methods. *The Science of the Total Environment*, *652*, 1077–1089. https://doi.org/10.1016/j.scitotenv.2018.10.014

Sabbah, I., Rebhun, M., & Gerstl, Z. (2004). An independent prediction of the effect of dissolved organic matter on the transport of polycyclic aromatic hydrocarbons. *Journal of Contaminant Hydrology*, *75*(1), 55–70. https://doi.org/10.1016/j.jconhyd.2004.04.003

Salvo, L. M., Severino, D., Silva de Assis, H. C., & da Silva, J. R. M. C. (2016). Photochemical degradation increases polycyclic aromatic hydrocarbon (PAH) toxicity to the grouper Epinephelus marginatus as assessed by multiple biomarkers. *Chemosphere (Oxford)*, *144*, 540–547. https://doi.org/10.1016/j.chemosphere.2015.09.013

Schirmer, K., Dixon, D., Greenberg, B., & Bols, N. (1998). Ability of 16 priority PAHs to be directly cytotoxic to a cell line from the rainbow trout gill. *Toxicology (Amsterdam)*, *127*(1), 129–141. https://doi.org/10.1016/S0300-483X(98)00030-4

Smith, S. B., Savino, J. F., & Blouin, M. A. (1988). Acute Toxicity to Daphnia Pulex of Six Classes of Chemical Compounds Potentially Hazardous to Great Lakes Aquatic Biota. *Journal of Great Lakes Research*, *14*(4), 394–404. https://doi.org/10.1016/S0380-1330(88)71572-5

Smith, K. E. C., Dom, N., Blust, R., & Mayer, P. (2010). Controlling and maintaining exposure of hydrophobic organic compounds in aquatic toxicity tests by passive dosing. *Aquatic Toxicology*, *98*(1), 15–24. https://doi.org/10.1016/j.aquatox.2010.01.007

Sogbanmu, T. O., Nagy, E., Phillips, D. H., Arlt, V. M., Otitoloju, A. A., & Bury, N. R. (2016). Lagos lagoon sediment organic extracts and polycyclic aromatic hydrocarbons induce embryotoxic, teratogenic and genotoxic effects in Danio rerio (zebrafish) embryos. *Environmental Science and Pollution Research International*, *23*(14), 14489–14501. https://doi.org/10.1007/s11356-016-6490-y

Sogbanmu, T., Osibona, A., Oguntunde, O., & Otitoloju, A. (2018). Biomarkers of toxicity in *Clarias gariepinus* exposed to sublethal concentrations of polycyclic aromatic hydrocarbons. *African Journal of Aquatic Science*, *43*(3), 281–292. https://doi.org/10.2989/16085914.2018.1491825

Sönnichsen, N. (2024). Annual average number of global oil spills per decade 1970-2021. https://www.statista.com/statistics/671539/average-number-of-oil-spills-per-decade/#:~:text=There%20was%20an%20average%20of,spills%20has%20been%20notably%20reduced.

Sørhus, E., Nakken, C. L., Donald, C. E., Ripley, D. M., Shiels, H. A., & Meier, S. (2023). Cardiac toxicity of phenanthrene depends on developmental stage in Atlantic cod (Gadus morhua). *The Science of the Total Environment*, *881*, 163484–163484. https://doi.org/10.1016/j.scitotenv.2023.163484

Spehar, R. L., Poucher, S., Brooke, L. T., Hansen, D. J., Champlin, D., & Cox, D. A. (1999). Comparative toxicity of fluoranthene to freshwater and saltwater species under fluorescent and ultraviolet light. *Archives of Environmental Contamination and Toxicology*, *37*(4), 496–502. https://doi.org/10.1007/s002449900544

Sugahara, Y., Kawaguchi, M., Itoyama, T., Kurokawa, D., Tosa, Y., Kitamura, S.-I., Handoh, I. C., Nakayama, K., & Murakami, Y. (2014). Pyrene induces a reduction in midbrain size and abnormal swimming behavior in early-hatched pufferfish larvae. *Marine Pollution Bulletin*, *85*(2), 479–486. https://doi.org/10.1016/j.marpolbul.2014.04.022

Sun, L., Zuo, Z., Chen, M., Chen, Y., & Wang, C. (2015). Reproductive and transgenerational toxicities of phenanthrene on female marine medaka (Oryzias melastigma). *Aquatic Toxicology*, *162*, 109–116. https://doi.org/10.1016/j.aquatox.2015.03.013

Tollefsen, K. E., Sundt, R. C., Beyer, J., Meier, S., & Hylland, K. (2011). Endocrine Modulation in Atlantic Cod (Gadus morhua L.) Exposed to Alkylphenols, Polyaromatic Hydrocarbons, Produced Water, and Dispersed Oil. *Journal of Toxicology and Environmental Health, Part A*, *74*(7-9), 529–542. https://doi.org/10.1080/15287394.2011.550562

Torreiro-Melo, A. G. A. G., Silva, J. S., Bianchini, A., Zanardi-Lamardo, E., & Carvalho, P. S. M. de. (2015). Bioconcentration of phenanthrene and metabolites in bile and behavioral alterations in the tropical estuarine guppy Poecilia vivipara. *Chemosphere (Oxford)*, *132*, 17–23. https://doi.org/10.1016/j.chemosphere.2014.12.079

Tremblay, L., Kohl, S. D., Rice, J. A., & Gagné, J.-P. (2005). Effects of temperature, salinity, and dissolved humic substances on the sorption of polycyclic aromatic hydrocarbons to estuarine particles. *Marine Chemistry*, *96*(1), 21–34. https://doi.org/10.1016/j.marchem.2004.10.004

Vallero, D.A. (2016). Chapter 3 - Environmental Biochemodynamic Processes. In *Environmental Biotechnology* (Second Edition, pp. 89–150). Elsevier Inc. https://doi.org/10.1016/B978-0-12-407776-8.00003-7

Veldman, M. B., & Shuo Lin. (2008). Zebrafish as a developmental model organism for pediatric research. *Pediatric Research*, *64*(5), 470–476. https://doi.org/10.1203/PDR.0b013e318186e609

Verbruggen, E.M.J. (2012). Environmental risk limits for polycyclic aromatic hydrocarbons (PAHs): For direct aquatic, benthic, and terrestrial toxicity. National Institute for Public Health and the Environment.

Vergauwen, L., Schmidt, S. N., Stinckens, E., Maho, W., Blust, R., Mayer, P., Covaci, A., & Knapen, D. (2015). A high throughput passive dosing format for the Fish Embryo Acute Toxicity test. *Chemosphere (Oxford)*, *139*, 9–17. https://doi.org/10.1016/j.chemosphere.2015.05.041

Vignet, C., Frank, R. A., Yang, C., Wang, Z., Shires, K., Bree, M., Sullivan, C., Norwood, W. P., Hewitt, L. M., McMaster, M. E., & Parrott, J. L. (2019). Long-term effects of an early-life exposure of fathead minnows to sediments containing bitumen. Part I: Survival, deformities, and growth. *Environmental Pollution (1987)*, *251*, 246–256. https://doi.org/10.1016/j.envpol.2019.05.007

Wang, X. (2014). Firth logistic regression for rare variant association tests. *Frontiers in Genetics*, *5*, 187–187. https://doi.org/10.3389/fgene.2014.00187

Wang, Y., Wang, J., Mu, J., Wang, Z., Yao, Z., & Lin, Z. (2014b). Aquatic predicted no-effect concentration for three polycyclic aromatic hydrocarbons and probabilistic ecological risk assessment in Liaodong Bay of the Bohai Sea, China. *Environmental Science and Pollution Research International*, *21*(1), 148–158. https://doi.org/10.1007/s11356-013-1597-x

Wang, W.X. (2016). Chapter 4 - Bioaccumulation and Biomonitoring. In *Marine Ecotoxicology* (pp. 99–119). Elsevier Inc. https://doi.org/10.1016/B978-0-12-803371-5.00004-7

Ward G.S., Parrish P.R., Rigby and R.A. 1981. Early life stage toxicity test with a saltwater fish: Effects of eight chemicals on survival, growth, and development of sheepshead minnows (Cyprinodon variegatus). *J Toxicol Environ Health* 8: 225-240.

Westerfield, 2000. The Zebrafish Book: A guide for the laboratory use of zebrafish (*Danio Rerio*). *4th edition.* https://zfin.org/zf_info/zfbook/chapt1/1.3.html

WHO, 2003. Polynuclear aromatic hydrocarbons in Drinking-water: Background document for development of WHO Guidelines for Drinking-water Quality. https://www.who.int/docs/default-source/wash-documents/wash-chemicals/polynuclear-aromatic-hydrocarbons-background-document.pdf

Wiegand, J., Cheng, V., Reddam, A., Avila-Barnard, S., & Volz, D. C. (2022). Triphenyl phosphate-induced pericardial edema is associated with elevated epidermal ionocytes within zebrafish embryos. *Environmental Toxicology and Pharmacology*, *89*, 103776–103776. https://doi.org/10.1016/j.etap.2021.103776

Willis, A. M., & Oris, J. T. (2014). Acute photo-induced toxicity and toxicokinetics of single compounds and mixtures of polycyclic aromatic hydrocarbons in zebrafish. *Environmental Toxicology and Chemistry*, *33*(9), 2028–2037. https://doi.org/10.1002/etc.2648

Wolińska, L., Brzuzan, P., Woźny, M., Góra, M., Łuczyński M.K., Podlasz, P., Kolwicz, S., Piasecka, S. (2011). Preliminary study on adverse effects of phenanthrene and its methyl and phenyl derivatives in larval zebrafish, Danio rerio. *Environmental Biotechnology,* 7(1), 26-33. http://www.edu.environmentalbiotechnology.pl/eb_dzialy/eb_online/2011/vol7_1/ms137lwolinska.pdf

Xu, K., Ai, W., Wang, Q., Tian, L., Liu, D., Zhuang, Z., & Wang, J. (2022). Toxicological effects of nanoplastics and phenanthrene to zebrafish (Danio rerio). *Gondwana Research*, *108*, 127–132. https://doi.org/10.1016/j.gr.2021.05.012

Xu, W., Li, Y., Wu, Q., Wang, S., Zheng, H., & Liu, W. (2009). Effects of phenanthrene on hepatic enzymatic activities in tilapia (*Oreochromis niloticus* ♀ × *O. aureus* ♂). *Journal of Environmental Sciences (China)*, *21*(6), 854–857. https://doi.org/10.1016/S1001-0742(08)62352-9

Yang, H.-H., Lai, S.-O., Hsieh, L.-T., Hsueh, H.-J., & Chi, T.-W. (2002). Profiles of PAH emission from steel and iron industries. *Chemosphere (Oxford)*, *48*(10), 1061–1074. https://doi.org/10.1016/S0045-6535(02)00175-3

Yang, G.-P., & Zheng, X. (2010). Studies on the sorption behaviors of phenanthrene on marine sediments. *Environmental Toxicology and Chemistry*, *29*(10), 2169–2176. https://doi.org/10.1002/etc.270

Yazdani, M. (2020). Comparative toxicity of selected PAHs in rainbow trout hepatocytes: genotoxicity, oxidative stress and cytotoxicity. *Drug and Chemical Toxicology (New York, N.Y. 1978)*, *43*(1), 71–78. https://doi.org/10.1080/01480545.2018.1497054

Zahangir, M., Haque, F., Mustakim, G., Khatun, H., & Islam, M. (2015). Effect of water pH on the early developmental responses in zebrafish (danio rerio). *Progressive Agriculture (Mymensingh, Bangladesh)*, *26*(1), 85–89. https://doi.org/10.3329/pa.v26i1.24521

Zakaria, Z. Z., Benslimane, F. M., Nasrallah, G. K., Shurbaji, S., Younes, N. N., Mraiche, F., Da'as, S. I., & Yalcin, H. C. (2018). Using Zebrafish for Investigating the Molecular Mechanisms of Drug-Induced Cardiotoxicity. *BioMed Research International*, *2018*, 1642684–10. https://doi.org/10.1155/2018/1642684

Zhang, Y., Huang, L., Zuo, Z., Chen, Y., Wang, C., 2013. Phenanthrene exposure causes cardiac arrhythmia in embryonic zebrafish via perturbing calcium handling. Aquat. Toxicol. 142e143, 26e32. https://doi.org/10.1016/j.aquatox.2013.07.014

Zhao, S., Xue, S., Zhang, J., Zhang, Z., & Sun, J. (2020). Dissolved organic matter-mediated photodegradation of anthracene and pyrene in water. *Scientific Reports*, *10*(1), 3413–3413. https://doi.org/10.1038/s41598-020-60326-6

Zhao, Y., Wang, X., Lin, X., Zhao, S., Lin, J. 2017. Comparative developmental toxicity of eight typical organic pollutants to red sea bream (*Pagrosomus major*) embryos and larvae. *Environ Sci Pollut Res. 24:* 9067–9078.

Zheng, Y., Li, Y., Yue, Z., Samreen, Li, Z., Li, X., & Wang, J. (2020). Teratogenic effects of environmentally relevant concentrations of phenanthrene on the early development of marine medaka (*x*). *Chemosphere (Oxford)*, *254*, 126900–126900. https://doi.org/10.1016/j.chemosphere.2020.126900

Zuo, L.-Z., Li, H.-X., Lin, L., Sun, Y.-X., Diao, Z.-H., Liu, S., Zhang, Z.-Y., & Xu, X.-R. (2019). Sorption and desorption of phenanthrene on biodegradable poly(butylene adipate co-terephtalate) microplastics. *Chemosphere (Oxford)*, *215*, 25–32. https://doi.org/10.1016/j.chemosphere.2018.09.173

Chapter 3.

Phenanthrene cardiotoxicity in zebrafish (*Danio rerio*)

3.1. Introduction

Polycyclic aromatic hydrocarbons (PAHs) are well-known aquatic pollutants and cardiotoxins (Incardona et al., 2017). Cardiotoxicity collectively refers to cardiovascular musculature damage or electrophysiological impairment as a result of exposure (Zakaria et al., 2018). PAH cardiotoxicity in fish has been directly attributed to exposure to 3-ringed PAHs (Brette et al., 2017). In particular, phenanthrene has garnered interest as a cardiotoxic PAH (Hicken et al., 2011; Incardona et al., 2009, 2015; Brette et al., 2017). While high concentrations of phenanthrene can result in cardiac failure, lower doses can impact cardiac performance (Hicken et al., 2011; Incardona et al., 2015; Brette et al., 2014). Cardiotoxicity can be induced in both early and late life stages of fish. In some cases, previously developed heart defects like arrythmias are thought to precede the development of morphological heart defects (Incardona et al., 2004).

Cardiotoxicity induced by phenanthrene can impair cardiac function, leading to reduced oxygen delivery, compromised metabolism, detrimental effects on several other physiological systems, and reduced survival (Hicken et al., 2011; McGruer et al., 2021). It is believed to affect fish hearts through various mechanisms including interference with cardiac contractility, disruptions in ion channel function and altered calcium homeostasis (Brette et al., 2014; Zhang et al., 2023). These cardiotoxic effects have been reported under phenanthrene exposure concentrations ranging between 1 – 10 mg/L in various fish species including Pacific mackerel (*Scomber japonicus*), zebrafish (*Danio rerio*), yellowfin tuna (*Thunnus albacares*) and bluefin tuna (*Thunnus thynnus*) (Brette et al., 2017; McGruer et al., 2021; Zhang et al., 2023).

Cardiotoxicity is often assessed through studies on isolated hearts which allow for physiological measurements that provide insight into cardiac dynamics and function. Optical mapping (OM) is a novel method for assessing cardiotoxicity and offers the advantage of maintaining heart function over several hours without perfusion (Rayani et

al., 2018). In this technique, cardiomyocyte voltage and calcium (Ca^{2+}) transient activity serve as indicators for chemical-induced cardiotoxicity and are visualized using potentiometric dyes (e.g., RH-237) and calcium indicators (e.g., Rhod-2 AM) (Lin et al., 2020; Rayani et al., 2018). OM rigs often employ zebrafish due to the robust nature of the zebrafish heart. A typical zebrafish has an average heartrate (HR) of 120 bpm, which is slower than in rodents (mouse 600 bpm) enabling easier measurements of its slower voltage and calcium cycling (Rayani et al., 2018). Additionally, zebrafish hearts closely resemble the human heart as both action potential (AP) and HR conduction processes are similar (Rayani et al., 2018).

Cardiac conduction is driven by the simultaneous coordination of APs, Ca^{2+} concentrations, and HR. At the cellular level, cardiomyocytes, the principal contractile cells of the heart, generate APs (Nemtsas et al., 2010). These APs generate electrochemical changes necessary for stimulating muscle contraction. Ca^{2+} ions, pivotal second messengers in excitation-contraction coupling, play a critical role in this process (Clusin, 2008). During an AP, voltage-gated calcium channels open, allowing an influx of Ca^{2+} into the cardiomyocyte's cytoplasm. Elevated cytosolic Ca^{2+} concentration instigates a cascade of events, including the activation of the contractile proteins actin and myosin, ultimately leading to muscle contraction (Rayani et al., 2018). HR directly effects the duration of APs; for instance, a faster HR is associated with a more rapid, shorter AP whereas a slower HR is associated with slower APs. Thus, the intricate crosstalk between APs and Ca^{2+} ion dynamics governs the heart's excitation-contraction cycle. Dysregulation of any of these components can have profound implications for cardiac function, potentially leading to arrhythmias or other cardiovascular disorders.

Passive dosing (PD) is becoming a novel protocol in chemical exposure studies for delivering hydrophobic substances into aqueous solution (Butler et al., 2016). PD exploits the science of solvent-to-solvent partitioning by using an inert material to load and partition chemical (Butler et al., 2013). Unlike carrier solvents, PD is less subject to concentration fluctuations resulting from chemical degradation, volatilization, and binding/adsorption (Butler et al., 2013). While PD is traditionally used in whole-organism exposures, this study is the first to apply PD to an OM isolated heart preparation.

The overall objective of this study was to examine the potential cardiotoxic effects of phenanthrene on the function of whole zebrafish hearts. Isolated hearts were acutely

exposed to phenanthrene using PD and cardiac parameters measured through OM. Specific goals of this study were: 1) to assess phenanthrene's sublethal cardiotoxic effects on heart rate, action potential duration (APD) and calcium transient duration (CaTD), and 2) to assess the potential for altered cardiac parameters to recover following cessation of exposure.

3.2. Methodology

3.2.1. Chemicals

NaCl, KCl, $NaHCO_3$, NaH_2 PO_4, $MgCl_2$, Na-HEPES, glucose, creatine, Na-pyruvic acid, $CaCl_2$, and tricaine methasulfonate (MS-222) were obtained from Fisher Scientific (Edmonton, AB, Canada). Blebbistatin was purchased from Toronto Research Chemicals Inc, (Toronto, ON). Mavacamten (MYK- 461) (99.9 % purity) was purchased from Cedarlane Laboratories (Mississauga, ON). Rhod-2AM (96 % purity) and RH-237 (97 % purity) were purchased from Invitrogen (through ThermoFisher Scientific, Waltham, MA). Silicone O-rings were purchased from O-rings West (Lynnwood, WA). Ethyl acetate (HPLC grade), methanol (HPLC grade), phenanthrene, penicillin-streptomycin, and amphotericin B were purchased from Sigma Aldrich (Oakville, ON).

3.2.2. Fish

An outbred strain of adult *Danio rerio* (AB strain) (University of British Columbia) were maintained in ZebTEC recirculating fish racks (Techniplast, Toronto, ON) at the following conditions: temperature 27 ±1 °C, pH 7.5, and photoperiod 10:14 h light: dark (Simon Fraser University). Fish were fed twice daily with fresh brine shrimp or frozen daphnia *ad libitum.*

3.2.3. Passive Dosing System

A static PD exposure system using phenanthrene-loaded silicone O-rings was used to deliver dissolved phenanthrene to the aqueous exposure media (Butler et al. 2013). O-rings were cleaned and prepped as previously described in Butler et al. (2013). O-ring concentrations were described previously in Chapter 2.2.3. Test concentrations were scaled down for isolated heart exposures since previous concentrations were used for

whole-body exposures. Dilutions were carried out to prep a low, medial and high concentration treatment at 10, 50 and 110 µg/L of phenanthrene. O-ring chemical loading concentrations were based on Renegar et al. (2017) partitioning formula (Equation 2.1) and the following variables: [V_{water} = 20 mL, V_{MeOH} = 200 mL, V_{PDMS} = 12 O-rings, log $K_{MeOH-PDMS}$ = 0.43 and log $K_{PDMS-Water}$ = 3.84. Both K terms are partitioning coefficients where $K_{MeOH-PDMS}$ is the partitioning coefficient of phenanthrene between MeOH and PDMS and $K_{PDMS-Water}$ is the partitioning coefficient of phenanthrene between PDMS and water. Water refers to the exposure media (ZEM with 2 % penicillin-streptomycin and 250 ng/L amphotericin B). C_{Target} is the desired target concentration of phenanthrene in the exposure media (mg/L).

A 700 mL phenanthrene stock solution in methanol was prepared (to achieve a final concentration of 350 µg/L) and kept under continuous stirring for 24 h in a light-protected Erlenmeyer flask (aluminum foil wrapped) to avoid potential light degradation. Serial dilutions of this stock solution using methanol were prepped in 250 mL Erlenmeyer flasks for lower concentrations (50, 110, 150, 200 and 275 µg/L) and allowed to partition for 72 h under continuous stirring in light-protected vessels 22 °C (Vergauwen et al., 2015). Following the loading period, O-rings were transferred to 250 mL Erlenmeyer flasks containing 200 mL of water and continuously stirred for 24 h. O-rings were then placed in 22 mL glass scintillation vials containing ZEM (with 2 % pen-strep and 250 ng/L amphotericin B) with no headspace, capped, and shaken for a partitioning period of 24 h (150 rpm) (Butler et al. 2013).

Exposure concentrations for experiments were 0, 10, 50 and 110 µg/L and were made using serial dilution immediately prior to the experiment. Treatment solutions at these concentrations were put into 2 mL polypropylene microcentrifuge tubes. The methanol control was made at a 1:4 dilution using ZEM as the dilutant.

Phenanthrene concentrations were verified by spectrophotometric analysis on a Cary Eclipse Spectrophotometer (Varian, model Eclipse, East Lyme, CT). Exit and emission wavelength ranges of 247 and 364 nm, respectively. Exit and emission slit lengths were 5 nm, excitation and emission filters set to automatic and open, PMT voltage at a medium level and the average run time of each reading was set at 3 s. Standard curves by spectrophotometric analysis were validated with water samples analyzed by gas

chromatography–mass spectrometry analysis by SGS Axys Analytical Services Ltd. (Sidney, BC) as described previously.

3.2.4. Heart Isolation and Exposure

Adult zebrafish (90 dpf) were euthanized by ice-bath immersion (Wallace et al., 2018) and confirmed dead after the cessation of opercular movements (Strkowski and Schech, 2015). To ensure cessation of brain activity, maceration of the brain was done by blunt force prior to decapitation (CCAC, 2020). Hearts were removed by first excising a triangular tissue section out from between the pectoral fins and the gills to open the pericardial cavity. Hearts were kept viable at room temperature by placing the tissue flab in a Petri dish containing Calcium Tyrode's solution (117 mM NaCl, 5.7 mM KCl, 4.4 mM $NaHCO_3$, 1.5 mM NaH_2PO_4, 1.7 mM $MgCl_2$, 10 mM Na-HEPES ($C_8H_{17}N_2O_4S$), 5 mM glucose, 5 mM creatine, 5 mM Na-pyruvic acid, 1.8 mM $CaCl_2$ mM, pH 7.3). Prior to cannulation, HR was recorded as a check for incidental heart damage. Hearts were viewed under a stereoscope (Nikon, SMZ1000) with a high intensity illuminator (Fiber-Lite M1-150, Dolan-Jenner Industries, Boxborough, MA). Hearts exhibiting inherent arrhythmias, or a HR less than 40 bpm were excluded from the study. 40 bpm was chosen as the exclusion cut-off as it is 2/3 below the average zebrafish HR (~ 120 bpm) (Rayani et al., 2018).

Hearts were cannulated based on methodology described in Rayani et al. (2018). A 34-gauge needle syringe (Harvard Apparatus, Holliston, MA) was inserted through the bulbus arteriosus, and air slowly released to inflate the cardiac chambers. This increased visualization of the beating hearts to ensure hearts were circulating fluid. Pooling fluids or leaks were indicative of damage during excision and any hearts exhibiting these were excluded from the study. Each heart was cannulated at the bulbous using a needle (34 gauge) with surgical twine (USP-designation 4-0, d = 0.2 mm) and the heart then submerged in a series of chemical solutions for the loading of potentiometric dyes. Plastic well plates were filled with 500 µL of the potentiometric dyes and the hearts first placed for a 15 min load in 10 µM RH-237 (voltage indicator dye) and then in a second solution of 10 µM mavacamten (contractile inhibitor) for 30 min to reduce movement for OM measurements. Following this, hearts were placed in 10 µM Rhod-2 AM (Ca^{2+} indicator dye) for 10 min (Rayani et al., 2018).

3.2.5. Optical Mapping Rig Protocol

An OM rig was set up as described in Rayani et al. (2018). Individual hearts were submerged in an imaging chamber which consisted of two coverslips containing a well of mavacamten (approximately 2 mL). Hearts were centered between two electrodes and allowed to beat spontaneously. Hearts previously loaded with RH-237 and Rhod-2 AM were run on the OM to obtain voltage and calcium transient measurements, respectively. To obtain these measurements, the rig was equipped with specialized lasers and cameras to acquire fluorescence during image acquisition.

Image acquisition was done through two GE680 cameras (Allied Vision Technologies, Germany) configured to capture calcium transient (cam 0) and voltage (cam 1) images when both Rhod-2 AM and RH-237 are stimulated to fluoresce, respectively. To trigger fluorescence of the dyes a green DPSS laser light (>200 mW, 532 nm; LCS-0532, Laserglow Technologies, Toronto, ON) was shone on the heart through a 560 nm long-pass dichroic mirror (XF2017, 560DRLP, Omega Optical). Heart images were magnified 1.33x through a 75- and 100-mm objective and camera lens, respectively (Rayani et al., 2018). Images were captured at a rate of 205 frames/sec at a resolution quality of 640 x 840 pixels (Rayani et al., 2018). Each image capture was set to 2000 frames which equated approximately to a 10 sec recording for each heart exposure. Frames yielded intensity (I) readings that represented the change in fluorescence over each image capture (10 s). Images and recordings were visualized using IDL 8.6 software. Rig data yielded both clean intensity and average cycle data which were graphically analyzed as waveforms depicting voltage and calcium changes. The waveforms represented the depolarization (upswing) and repolarization (downswing) of each cardiac cycle and were assessed to calculate cardiac parameters.

After loading was complete, hearts were observed for movement artefact by capturing an image on the rig. Movement artefact was exhibited on the software images as an unrestrained baseline where either transient baseline drifted. Any heart exhibiting unrestrained atria was incubated in the imaging chamber in 10 μM of mavacamten until quiescent (up to 30 min). Any heart exhibiting a HR below 40 bpm or arrythmia was excluded.

Preliminary tests showed adult hearts had increased sensitivity (tachycardic) to the methanol control so the control was diluted (1 methanol: 4 ZEM). For phenanthrene exposures, hearts were placed in the imaging chamber over 10-min intervals using the following order of treatments: dilute methanol control (25 %), 10, 50 and 110 µg/L phenanthrene followed by a methanol control washout. 2 mL of each treatment was pipetted into the chamber containing the heart for each exposure then pipetted out for removal between treatments. The effect of time outside of solution was deemed negligible on each heart since hearts were replaced in the next solution within 30 s. Treatments were replaced with minimal movement to the heart to prevent potential excitation. Rig orientation was also maintained for subsequent image capture to limit variability in data acquisition due to electrode position.

To quantify effects, both clean intensity and average cycles for each treatment were analyzed. For voltage, clean intensity cycles were generated which showed all waveforms captured over the image capture (10 s). Voltage intensity was normalized to the maximum intensity value so intensity was represented as a percent (0 – 100 %). Two parameters were calculated for voltage. First, HR was calculated by summing the number of waveform peaks in each reading (each peak signified the conduction of a new heartbeat). HR was then calculated to represent beats per minute (bpm). Second, APD was calculated at both 50 and 75 % where APD50 and APD75 represent the time for which the cell membrane reaches 50 and 75 % of its repolarization during its AP, respectively. This was calculated by summing the upstroke time with the APD50, where APD50 equates to 50 % of the difference between the max and the min (APD50 = [max-min] *0.5). For calcium transient, average cycles were generated over the image capture (10 s). Calcium transient duration (CaTD) was calculated at both 50 and 75 % where CaTD50 and CaTD75 represent the calcium cycle duration for which the cell membrane reaches 50 and 75 % of its repolarization during its AP, respectively. CaTD measurements were calculated the same way as the APD measurements. From these calculations, HR could be directly compared to APD or CaTD.

3.2.6. Statistical analysis

Measurements of HR, APD50, APD75, CaTD50 and CaTD75 were collectively pooled and respective averages found for each treatment. Analysis was done with a sample size of n= 14 – 15 hearts. Two hearts yielded outlier measurements where neither exhibited a HR

after exposure to the 110 µg/L treatment and methanol washout. Since both hearts met the inclusion criteria prior to testing, all measurements were included except for their respective exposures to the 110 µg/L and the methanol control where no HR was exhibited. To control for heart-to-heart variation all parameters were calculated as percentages of the normative methanol control value (100 %). Statistical tests were run using JMP (JMP, 2023). Treatment (methanol washout, 10, 50, and 110 µg/L phenanthrene exposure) and cardiac parameters (% HR, APD50 and APD75, CaTD50 and CaTD75) were considered to be fixed effects. Heart was deemed a random effect in the model since there was intra-variability across hearts. A one-way analysis of variance (ANOVA) was run for each of the 5 cardiac parameters across treatments. Post hoc tests to locate statistically significant differences between treatments were carried out using a Tukey Kramer adjustment ($p < 0.05$).

3.3. Results

Isolated adult *Danio rerio* hearts were run on an OM rig for the measurement of various cardiac parameters (HR, APD50 and APD75, CaTD50, and CaTD75) with and without phenanthrene exposure. For each parameter, measurements were normalized to a methanol control (100 %) to control for heart-to-heart variation and values were represented as a percentage of the normative value.

3.3.1. Heart rate

Phenanthrene treatment had a significant effect on HR ($p< 0.0001$) and exhibited a concentration-dependent response. Figure 3.1 shows HR expressed as a % of the control across all treatments. HR during exposure to 110 µg/L phenanthrene was significantly higher than all other phenanthrene concentrations ($p< 0.0001$) whereas low (10 µg/L) and medium (50 µg/L) concentrations had no significant effect on HR. The high concentration induced a tachycardic effect on the heart shown by the rapid increase in HR. Mean HR % (± 2SE) ranged between 80.8 ± 19.3 and 169.7 % ± 19.3 following exposure to the methanol washout and the 110 µg/L treatment, respectively. After exposure to the methanol washout, HR was significantly lowered by 88.9 %, indicating a drug ‘washout effect’ of the chemical. Therefore phenanthrene-induced HR effects were reversible.

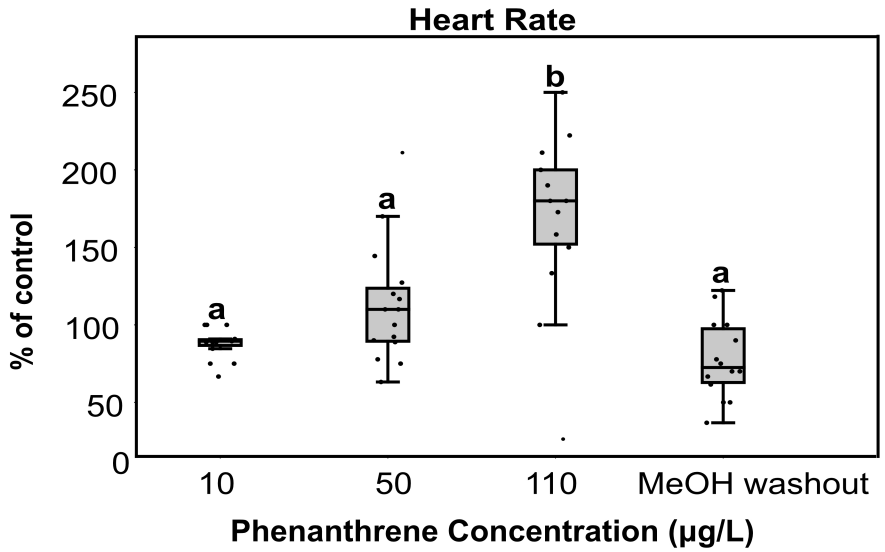

Figure 3.1. Mean % heart rate measured in isolated adult zebrafish hearts exposed to phenanthrene (10, 50, 110 µg/L). All values are normalized to a control heart exposed to methanol (100 %). Box plots show median values (centre horizontal lines), lower 25th and upper 75th percentiles, the minimum and maximum values (whiskers), and individual values (points). *n* = 14 -15. Significant differences (p< 0.05) between treatments are denoted by letters.

3.3.2. APD50 and APD75

APD50 and APD75 represent the time it takes for 50 and 75 % of an APD cycle to be completed. APD50 was significantly decreased by phenanthrene exposure (p< 0.0001) in a concentration-dependent manner (Figure 3.2A). Both the 50 and 110 µg/L treatments yielded significantly shorter APD50s relative to the methanol control (p < 0.0001). As well, a difference was seen between treatments with the 110 µg/L treatment yielding a shorter APD50 relative to the 10 µg/L treatment. Mean APD50 values (± 2SE) ranged between 73.7 ± 19.1 % to 133.7 ± 19.1 % following exposure to 110 µg/L phenanthrene and the methanol washout, respectively. A drug washout effect was shown as APD50 was significantly increased when hearts were transferred from the high concentration into the methanol washout.

Phenanthrene treatment concentration had a significant effect on APD75 (p= 0.0017). The general trend revealed a decreasing APD75 value with increasing phenanthrene concentration (Figure 3.2B). APD75 was significantly shorter following exposure to 110 µg/L phenanthrene compared to both the methanol washout and 10 µg/L phenanthrene (p= 0.0017). Mean APD75 values ranged between 76.1 ± 18.9 – 117.3 ± 18.9 % following

exposure to 110 µg/L phenanthrene and the methanol washout, respectively. APD75 was 41.2 and 40.5 % longer following exposure to the methanol washout and 10 µg/L phenanthrene compared to the 110 µg/L treatment. As expected, the methanol washout showed a drug washout effect as APD75 was significantly increased when hearts were transferred from high phenanthrene concentration into the methanol washout. These findings indicated APD effects were reversible.

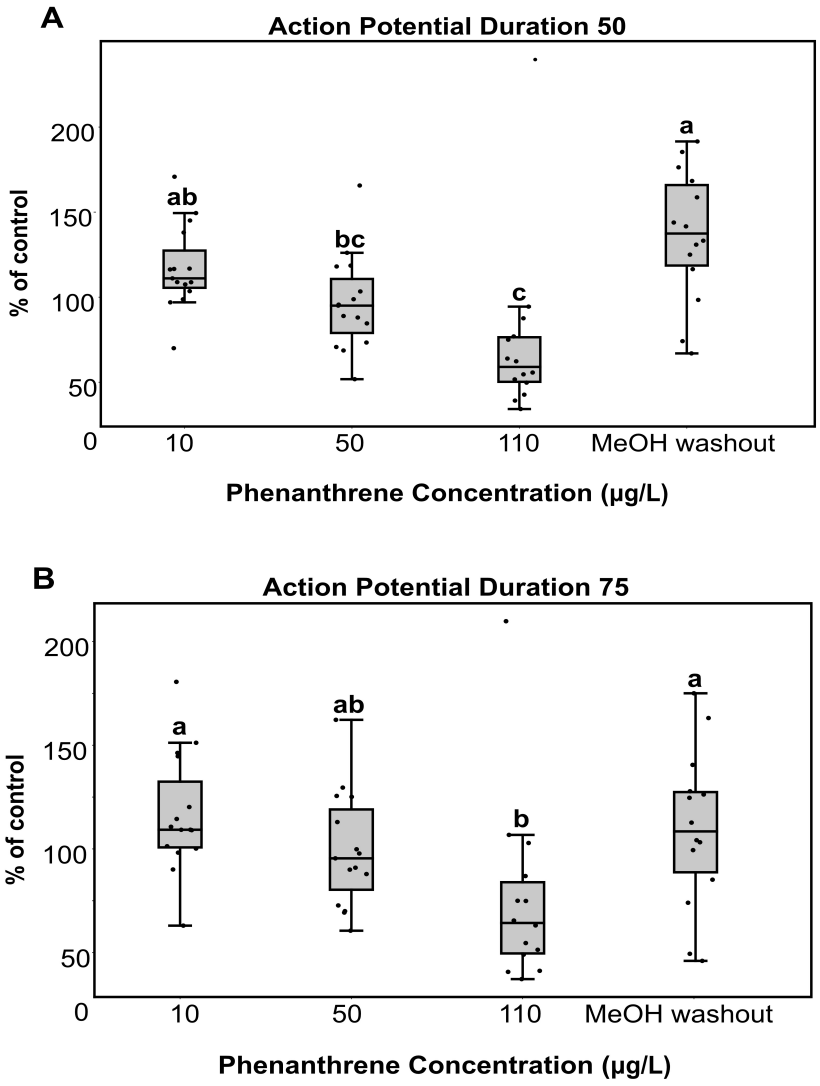

Figure 3.2. Mean APD50 (A) and APD75 (B) measured in isolated adult zebrafish hearts exposed to phenanthrene (10, 50, 110 µg/L). All values are normalized to a control heart exposed to methanol (100 %). Box plots show median values (centre horizontal lines), lower 25th and upper 75th percentiles, the minimum and maximum values (whiskers), and individual values (points). *n* = 14 -15. Significant differences (p< 0.05) between treatments are denoted by letters.

3.3.3. CaTD50 and CaTD75

CaTD50 and CaTD75 represent the time it takes for 50 and 75 % of a CaTD cycle to be completed. CaTD50 was shown be significantly affected by phenanthrene treatment concentration as all treatments were significantly different from the methanol washout ($p= 0.0001$). However, no significant differences were found between treatments indicating no clear dose-dependent response. Rather, the general trend showed all phenanthrene treatments resulted in significantly shorter CaTD50 cycles compared to the methanol washout (Figure 3.3A). Mean CaTD50 values ranged between 89.2 ± 30.0 to 176.2 ± 30.0 % following exposure to 110 µg/L phenanthrene and the methanol washout, respectively. Exposure to 10 and 50 µg/L decreased CaTD50's by 64 and 74.6 % compared to the methanol washout. The methanol washout showed a drug washout effect as CaTD50 significantly increased when hearts were transferred from high phenanthrene concentration into the methanol washout. Therefore, changes to CaTD were reversible.

CaTD75 was shown to be significantly affected by phenanthrene treatment concentration ($p= 0.0005$). CaTD75 was significantly shorter following exposure to all phenanthrene treatments relative to the methanol washout (Figure 3.3B). As previously reported for CaTD response, no differences between individual treatments were found to indicate a dose-dependent response. Rather, all treatments behaved in the same manner of reducing CaTD75. Mean CaTD75 values ranged between 94.8 ± 31.1 to 175.2 % ± 31.1 following exposure to 110 µg/L phenanthrene and the methanol washout, respectively. As expected, a high phenanthrene concentration resulted in the greatest reduction to calcium transient. Comparatively, 10 and 50 µg/L saw CaTD75 reductions of 58.6 and 72.3 % compared to the methanol washout. Hearts transferred from phenanthrene to the methanol washout exhibited significantly increased CaTD75s. This increase was indicative of the drug washout effect and further revealed the heart's ability to recover.

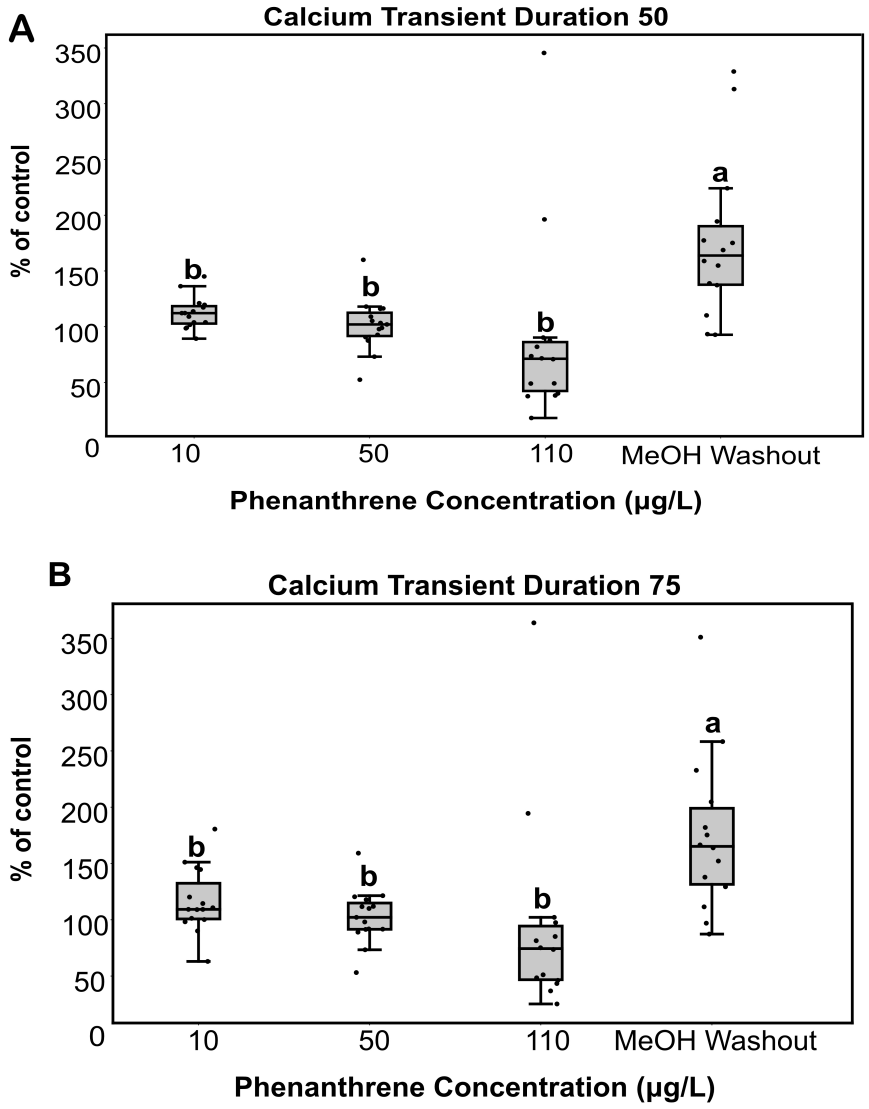

Figure 3.3. **Mean CaTD50 (A) and CaTD75 (B) measured in isolated adult zebrafish hearts exposed to phenanthrene (10, 50, 110 µg/L). All values are normalized to a control heart exposed to methanol (100 %). Box plots show median values (centre horizontal lines), lower 25th and upper 75th percentiles, the minimum and maximum values (whiskers), and individual values (points). *n* = 14 -15. Significant differences ($p < 0.05$) between treatments are denoted by letters.**

3.4. Discussion

Optimal mapping (OM) was utilized to assess cardiotoxicity through the measurements of several cardiac parameters in cannulated hearts from adult *Danio rerio*. The key cardiac indicators, voltage and calcium transients, were analyzed to gain insight into phenanthrene's effect on heart rate (HR), actional potential duration (APD) and calcium transient duration (CaTD) (Brette et al., 2017). These parameters are inter-related as changes in the electrochemical gradient affecting HR subsequently affect the APs maintaining cardiac conduction (Panakova et al., 2010). As the initial release of Ca^{2+} from the sarcomeres trigger cardiomyocytes to open Ca^{2+} channels, APs rely on Ca^{2+} levels (Rayani et al., 2018). Therefore, studying these cardiac parameters alongside each other is necessary for understanding the physiological impact on cardiac function.

3.4.1. Heart rate

HR is a battery test measurement used in both early and late life stage studies to detect for trends of bradycardia, tachycardia or arrythmias. HR was assessed in excised and cannulated adult *Danio rerio* hearts during exposure to varying concentrations of phenanthrene.

Here, phenanthrene exposure increased HR in isolated zebrafish hearts and led to tachycardia. The significant increase in HR at the highest exposure concentration (110 µg/L) coincided with a simultaneous decrease in both APD and CaTD. This supports a cardiac phenomenon called restitution where both APD and CaTD will adaptively change in response to HR alterations (Fossa, 2017). In terms of physiological significance, restitution allows for the heart to recover (Fossa, 2017). In the current study, elevated HR was indicative of an increased demand on cardiac output following phenanthrene exposure. While phenanthrene's mode of action was not a focus of this study, it can be inferred that phenanthrene may have impacted HR by disrupting ion channels in the SA node or reducing contractility and stroke volume. To compensate for these effects, HR increased to maintain cardiac output, subsequently lending to reductions in both APD and CaTD. Therefore, these findings show that restitution was occurring during phenanthrene exposure. As well, phenanthrene's compliance with the drug washout effect shows its ability to recover from a tachycardic state and avoid potential cardiac damage.

The literature corroborates this study's findings on phenanthrene's impact on increasing HR. A recent study observed significant HR increases in zebrafish exposed to phenanthrene concentrations as low as 0.9 – 9.0 µg/L (Zhang et al., 2023). Phenanthrene was a potent heart stimulant as HR was significantly altered by phenanthrene concentrations 10 x lower than this current study's effective concentration (110 µg/L) (Zhang et al., 2023). The observed tachycardia was a significant finding as prior studies have reported bradycardic effects following phenanthrene exposure across various fish species (McGruer et al., 2021; Brette et al., 2017; Incardona et al., 2004).

In contrast to this study, multiple studies provide evidence for phenanthrene's ability to induce bradycardia (Incardona et al., 2004; Brette et al., 2017). Phenanthrene concentrations at 891 µg/L significantly reduced HR in Pacific mackerel adults (Brette et al., 2017). Higher phenanthrene concentrations (2673 – 4456 µg/L) were needed to elicit similar results in *Salmo trutta* (Brown trout) where exposure caused significant prolongation of the QT interval, leading to reduced HR (Ainerua et al., 2020). Bradycardia was induced in zebrafish at phenanthrene concentrations up to 9981 µg/L (Incardona et al., 2004). Notably these studies used concentrations close to 10 x higher than this current study's test concentrations. While these studies report phenanthrene as a bradycardic chemical, a more accurate description would denote the underlying factor behind bradycardia is extremely high phenanthrene concentrations. At low, more environmentally-relevant concentrations phenanthrene appears to cause tachycardia.

The tachycardia observed herein suggests phenanthrene may have impacted contractility. While contractility was not directly measured here, several studies suggest phenanthrene impacts cardiac contractility through altering ion channels (Ainerua et al., 2020; Kompella et al., 2021). Phenanthrene has been reported to depress cardiac contractility due to repression of depolarizing Ca^{+2} currents and repolarizing K^{+} currents (Ainerua et al., 2020). Phenanthrene decreased Ca^{+2} by inihibiting I_{CaL} in zebrafish which displayed elevated HRs and shortened APDs (Kompella et al., 2021). This current study also exhibited increased HRs alongside shortened APDs. Kompella et al. (2021) denote hearts with shortened APDs have decreased refractory periods. This further indicates increasing HR is a physiological response necessary to maintain cardiac output demands. Therefore, reduced contractility may be a likely mechanism behind phenanthrene's mode of cardiotoxicity, lending a potential explanation behind the significant changes in HR reported herein.

Alongside HR effects, phenanthrene exposure has been associated with heart arrythmias (Incardona et al., 2004). Heartrates that severely deviate from their intrinsic value are prone to develop arrythmias that can lead to cardiac failure (Brette et al., 2017). Interestingly, studies remark the potential for fish to recover from heart arrythmias. Zebrafish embryos exposed to phenanthrene developed an arrythmia called a 2:1 atrioventricular (AV) conduction block in which the atria produced twice as many contractions as the ventricle (Incardona et al., 2004). HR was effectively recovered following exposure to clean water over several hours. Likewise, this current study showed that phenanthrene's tachycardic effects were capable of reversal following exposure to the methanol washout. Comparatively, the literature shows continual exposure to high phenanthrene doses can lead to cardiac failure. One study reported continued exposure to very high phenanthrene concentrations (> 8911 µg/L) over 3 d led to complete AV blockages and cardiac failure in zebrafish (Incardona et al., 2004). Therefore, HR recovery is highly dependent on phenanthrene concentration and duration of exposure. This current study shows phenanthrene exposures on an acute timeframe (< 2 h) result in sublethal cardiac effects, which are capable of being reversed. Based on the literature it can be ascertained heart arrythmias would likely develop from prolonged exposure to phenanthrene.

While sublethal cardiotoxicity in adults was assessed in this study, the literature shows phenanthrene may also be lethal at early life stages. Potential lethality behind phenanthrene-induced cardiotoxicity has been associated with the time of exposure in relation to heart development (Sørhus et al., 2023). Atlantic cod (*Gadus morhua*) exposed to phenanthrene (200 µg/L) post heartbeat development (72 h) exhibited adverse cardiac effects such as decreased atrial contraction and ventricle size or the complete absence of ventricular contraction (Sørhus et al., 2023). Comparatively, cod exposed pre-heartbeat development did not exhibit impaired hearts and had higher survival rates (Sørhus et al., 2023). Phenanthrene appears to be more lethal post heart development which further establishes it as a potent cardiotoxic drug. By comparison this study showed acute late-life exposure did not elicit lethality but still had a significant effect on HR, APD and CaTD.

3.4.2. Action Potential Duration

APs play a critical role in establishing the membrane environment and generating a heart electrical impulse during contraction (Wei et al., 2023). Zebrafish AP dynamics bear a

close resemblance to humans in that they exhibit a rapid upstroke, a long plateau period and fast repolarization (Kompella et al., 2021). Other organisms, such as mice, are not useful for AP comparison due to their extremely rapid HR (around 600 bpm) and APs, as well as expression differences in ion channel profiles (Kompella et al., 2021). APD in cardiac cells refers to the duration of the electrical impulse that triggers the contraction of the heart. APDs are often regulated by ion channels. APD is a useful measurement as any alteration in APD often suggests underlying changes to ion channels are occurring in the heart. Furthermore, disruptions in the balance of ion channels may lead to cardiac arrhythmias (Incardona et al., 2004, 2005).

In this study, phenanthrene caused shortening of both APD50 and APD75. For APD50, phenanthrene concentrations as low as 50 µg/L saw significant decreases whereas only high concentrations (110 µg/L) induced a significant decrease for APD75. The shortening of APDs with increased HR indicated restitution was occurring. The data revealed both medium and high doses of phenanthrene yielded APD50 cycles that were on average around 40 – 60 % faster than lower concentrations. These shorter APD50 values corresponded to previously reported HR increases for these treatments. Likewise, APD75 saw an association between shortened APD and HR. Distinctly, 110 µg/L phenanthrene elicited the fastest HR resulting in the shortest APD75. As well, the findings showed phenanthrene-induced alterations to APD were capable of reversal as APD was increased when hearts were removed from the drug and exposed to the methanol control. This may indicate that short acute exposures to phenanthrene may not elicit permanent heart damage in organisms but further experimentation is required.

There is evidence in the literature that supports phenanthrene's potential for reducing APDs in fish (Kompella et al., 2021; Ainerua et al., 2020). Phenanthrene concentrations around 535 µg/L reduced APD50 and APD90 in zebrafish (Kompella et al., 2021). Another study observed APD50 shortening in Brown trout (*Salmo trutta*) only at high phenanthrene concentrations (5347 µg/L), below which phenanthrene had prolonged effects on APD (Ainerua et al., 2020). This current study did not observe this latter effect but agrees with reports of phenanthrene's reduction of APD. Also, the findings indicate phenanthrene's capability at reducing APD at even lower concentrations (50 and 110 µg/L). Very few studies have documented the potential reversal of phenanthrene's heart effects through drug washout. One study observed zebrafish hearts exposed to 535 – 1782 µg/L of phenanthrene saw partial recoveries of both APD50 and APD90 following a 10 min drug

washout (Ringer's solution) (Kompella et al., 2021). Likewise, this study saw a drug washout effect; given that phenanthrene concentrations used were 10 x lower than Kompella et al. (2021), this finding is expected and further emphasizes the reversible nature of phenanthrene exposure.

The literature also provides evidence that phenanthrene may prolong APD in fish in some cases. This suggests that phenanthrene's cardiotoxicity may differ across species. Previous studies report both APD50 and APD90 were significantly longer with increasing phenanthrene concentrations (891 - 4456 µg/L) in bluefin and yellowfin tuna cardiomyocytes (Brette et al., 2017). This finding was expected as the authors also reported bradycardia which consequently caused APD lengthening due to restitution. The authors previously reported similar results across a crude oil exposure (∑TPAH: 15 – 61 µg/L) known to contain a high proportion of tricyclic PAHs (Brette et al., 2014). In both studies, prolonged APDs led to delayed heart electrical conduction (Brette et al., 2014; Brette et al., 2017). However, while PAHs appeared to prolong APD50 and APD90, they exerted the opposite effect on APD10 which yielded shortened APDs (Brette et al., 2014). This indicates that initial repolarization may not be as affected by phenanthrene as the latter portion of the APD. Variation in APDs across studies are likely attributed to the broad range of phenanthrene concentrations used. Brette et al. (2017) used concentrations almost 10 x higher than this current study and observed prolonged APDs. Comparatively, this study's lower test concentrations saw a shortening effect on APD.

Is it important to assess the potential implications alterations to APD may have on the mechanisms of cardiac conduction. During repolarization, the membrane re-establishes the electrochemical gradient in order to allow a new AP to be stimulated (Wei et al., 2023). APD50 is a critical step as it is the onset of muscle relaxation, allowing the heart to prepare for the next contraction. If APD50 is prolonged, the heart's repolarization phase is delayed, resulting in slower heart rates and an increased risk of arrhythmias, such as ventricular tachycardia or fibrillation (Wei et al., 2023). While no arrythmias were observed in this study during phenanthrene exposure, it is highly probable arrythmias could develop from prolonged exposure. Cardiac arrythmias can compromise pumping efficiency, ultimately leading to deleterious effects on heart function and overall cardiovascular health (Incardona et al., 2004, 2005; Brette et al., 2017).

Despite the variation in reports on phenanthrene's effects on APD, there is a general understanding that changes in APD are associated with the changes in various voltage-gated ion channels (Tsai et al., 2011). Studies have reported on phenanthrene's role in altering ion levels through disrupting the regulation of these channels. The underlying physiological mechanism behind bradycardia is attributed to the inhibition or blocking of either the rapid or slow-activating delayed rectifier potassium channels (I_{Kr} and I_{Ks}, respectively) (Tsai et al., 2011; Brette et al., 2017). For eg., I_{Kr} inhibition coincided with prolonged APD90 in brown trout cardiomyocytes exposed to phenanthrene (Ainerua et al., 2020). Comparatively, shortened APD50 aligned with inhibited L-type calcium channel (I_{CaL}) currents. This effect on the I_{CaL} channel was also affirmed in a similar study using isolated zebrafish cardiomyocytes (Kompella et al., 2021). However, unlike Ainerua et al. (2020), Kompella et al. (2021) observed I_{Kr} inhibition alongside APD50 shortening. As I_{Kr} is primarily associated with APD prolongation, the shortening effect on APD observed is most likely predominantly driven by I_{CaL} inhibition that was occurring simultaneously. The effect of ion channels on APD is complex as studies suggest the variation on the strength of I_{CaL} inhibition may determine the impact on APD (Brette et al., 2017; Ainerua et al., 2020). While studies that observed APD prolongation report phenanthrene caused around 30 % inhibition of I_{CaL} (Brette et al., 2017; Ainerua et al., 2020), a study observing APD shortening reported phenanthrene caused upwards of 60 % inhibition (Kompella et al., 2021). Therefore, it can generally be surmised that phenanthrene causes APD shortening if inhibition to the I_{CaL} current is stronger than inhibition to the I_{Kr} current.

3.4.3. Calcium transient

CTs describe the changes in cytosolic calcium concentration, which is tightly regulated and necessary for facilitating excitation-contraction coupling (Brette et al., 2014). CT is a measure of the efficiency of the heart's calcium cycling and sarcomere activity (Rayani et al., 2018). Often CaTD is a parameter measured in cardiotoxicity studies. CaTD50 refers to the time it takes for the cell to reach 50 % decay during repolarization (Clusin, 2008). The CT is triggered when calcium is freed from the sarcoplasmic reticulum (SR), stimulating heart contraction (Rayani et al., 2018). However, under abnormal conditions such as the influence of a toxicant, the SR releases calcium sporadically, causing uncontrollable depolarizations of the membrane which lead to arrythmias (Rayani et al.,

2018). Therefore, controlled calcium release is imperative for normal heart contraction and calcium cycling.

Phenanthrene significantly reduced CaTD with both CaTD50 and CaTD75 shortened by more than 50 % at phenanthrene concentrations as low as 10 µg/L. A significant difference in CaTDs was not seen between treatments; however, all treatments measured significantly faster transients than the methanol washout. The literature shows shorter CaTD50s in zebrafish have been associated with elevated diastolic Ca^{+2} due to the incomplete restoration of Ca^{2+} ions (Rayani et al., 2018). For healthy cardiac conduction Ca^{2+} concentration is several fold higher in systole compared to diastole (Eisner et al., 2017). Therefore, the shortening effect on CaTD observed herein may have allowed for only a partial recovery period, hence disrupting the resting potential and Ca^{2+} ion levels. Exposure to the methanol washout showed hearts were capable of increasing their CaTDs indicating the chemical effects were reversible and did not appear to elicit permanent damage in calcium cycling.

Recent studies have reported phenanthrene is responsible for decreasing CT in fish species (Brette et al., 2017; Ainerua et al., 2020). Across a multi-PAH exposure, phenanthrene (891 µg/L) was the only compound that significantly reduced CaT amplitude and delay in Pacific Mackerel, yellowfin and bluefin tuna (Brette et al., 2017). Phenanthrene induced a significant increase in the time between decaying CTs. Time to decay was considered as time leading to 37 % decay in the peak (Brette et al., 2017). Increased CaT decay led to decreased influx of Ca^{2+}. This literature finding was in contrast to this current study which observed a significant decrease in CaTD. Rather, the observed shortened CaTDs coincided with the previously reported shortened APDs (Kompella et al., 2021; Ainerua et al., 2020). While CaT amplitude was not measured, based on a literature understanding of calcium dynamics in cardiac physiology it can be inferred that CaTD reduction would result in elevated diastolic Ca^{+2} levels (Rayani et al., 2018).

The mechanisms behind CT are fundamentally influenced by several ion channels. The L-type Ca^{2+} channels (I_{CaL}) are vital in triggering the release of calcium to start excitation-contraction coupling (Kompella et al., 2021). This influx of Ca^{2+} causes the SR to also release Ca^{2+} ions (Brette et al., 2014). Calcium through the T-type Ca^{2+} channels (I_{CaT}) and I_{CaL} channels depolarize the membrane, leading to the plateau phase of an AP (Kompella et al., 2021). There is an additional current from the sodium-calcium exchanger

(NCX1) that expels 1 Ca^{2+} ion from the cytosol for every influx of 3 Na^{+} ions into the cell during the repolarization phase of the heart (Rayani et al., 2018). This process reverses with NCX1 acting in reverse-mode during depolarization. Once the heart is in repolarization, the CT returns to a resting state by rebalancing Ca^{2+} levels (Brette et al., 2014). This recovery period in which the I_{CaL} channels are inactive occurs in approximately 96 msec in zebrafish (Rayani et al., 2018).

Studies suggest that phenanthrene alters CTs by primarily disrupting ion channeling (Brette et al., 2017). CaT reduction is believed to be resultant of decreased influx through the I_{CaL} channels or decreased Ca^{2+} efflux from the SR (Brette et al., 2017). Phenanthrene exposure studies that have observed APD shortening have observed I_{CaL} inhibition (Kompella et al., 2021; Ainerua et al., 2020). Comparatively, phenanthrene exposure studies that have reported APD prolongation and CaT delay observed inhibition of the I_{Kr} channel (Incardona, 2017; Brette et al., 2017). Therefore, this suggests any alterations to APs directly impact ion channeling and can influence Ca^{2+} cycling.

Abnormal ion channeling is often symptomatic of HR changes that affect CaTD as a result of restitution. In the current study, phenanthrene increased HR, leading to a subsequent decrease in CaTD. Studies show that as a result to changing HR, both altered CaTD or APD responses can lead to cardiac impairment (Wei et al., 2023). Prolonged CaTD50 can result in increased cytosolic Ca^{2+} that overstimulates the NCX current, generating an inward depolarization current. (Wei et al., 2023). This condition is known as delayed after depolarization (DAD) and occurs during the plateau period of the heart. This disturbance does not allow the heart to fully rest and can weaken it over time. Ventricular tachycardia also elicits APD and CaTD changes which can lead to ion channeling disturbances (Wei et al., 2023). Inactive Na^{+} and Ca^{2+} channels may be abnormally activated during prolonged APDs, causing increased depolarization (Wei et al., 2023). Comparatively, the shortened APD and CaTD observed in this current study is most likely associated with I_{CaL} inhibition (Kompella et al., 2021; Ainerua et al., 2020).

Ventricular dynamics in CaTD have been characterized as rate-dependent in zebrafish (Rayani et al., 2018). Studies that controlled for HR by stimming zebrafish hearts to set frequencies revealed fish with higher HRs exhibited rapidly shorter CaTDs. CaTD50 decreased by more than 50 % in zebrafish that exhibited a 64 % increase in HR (Rayani

et al., 2018). Similarly, this study observed an inverse relationship between increasing HR and decreasing CaTD.

Research behind phenanthrene-induced calcium channel inhibition using well documented calcium channel inhibitors in bluefin and yellowfin tuna (Brette et al., 2017) show the same calcium reduction following phenanthrene exposure as when hearts were pre-exposed to calcium channel inhibitors. Prior to phenanthrene exposure, ryanodine (2468 µg/L) prevented calcium release from the SR followed by thapsigargin (1302 µg/L) which prevented uptake. I_{CaL} amplitude decreased with increasing phenanthrene concentration (891 and 4456 µg/L), ultimately leading to bradycardia (Brette et al., 2017). This indicated hearts actively use SR Ca^{2+} stores for EC coupling and phenanthrene may disrupt the ability to acquire adequate calcium (as seen by the decreased Ca^{2+} amplitude). Conversely, the current study observed phenanthrene caused tachycardia. These differences are most likely attributed to concentration differences as Brette et al. (2017) utilized phenanthrene concentrations at least 8-fold higher than the current study.

Cardiac functionality appears to be closely related to morphology. This study previously reported phenanthrene induced significant PE in zebrafish embryos (see ch 2.3.3). The literature shows cardiac impairment may be associated with teratogenic effects like PE (Incardona et al., 2004). Incardona et al. (2004) assessed Troponin T, a protein needed for proper sarcomere function and compared it to phenanthrene exposure in zebrafish. When troponin T was selectively knocked out in cardiomyocytes, knockouts exhibited similar abnormalities to phenanthrene-treated embryos (at 9981 µg/L) which displayed PE by 48 h and spinal curvature by 3 dpf (Incardona et al., 2004). Since troponin T specifically targets the heart and no other tissues, this finding indicates morphological defects are a consequence of cardiac impairment. Similarly, phenanthrene's induction of these morphological defects also appears to be associated with earlier cardiac impairment. This current study utilized whole-hearts for analysis which limited the ability to observe morphological heart defects in adults. Given the observed PE reported earlier in this study, these findings suggest adults displaying impaired cardiac function may also display PE.

3.5. Conclusion

In this study, in situ exposure of phenanthrene to adult zebrafish (*Danio rerio*) hearts was shown to induce cardiotoxicity below previously reported concentrations. Use of both in

situ heart exposures and OM techniques enabled accurate assessment of cardiac endpoints (APD, CaTD and HR). For this reason, in situ heart exposures are recommended over whole-organism exposures when calculating precise cardiac parameters to elucidate the mechanisms of the heart. The results provided insight into phenanthrene's cardiotoxic effects in fish. Reported HR increases aligned with a recent study's report on phenanthrene's stimulatory HR effects in zebrafish embryos (Zhang et al., 2023). When weighing this finding against evidence in the literature supporting phenanthrene-induced bradycardia in fish, it can be deduced that high phenanthrene concentrations (> 800 µg/L) cause bradycardia, while lower concentrations (≤ 110 µg/L) cause tachycardia. Reported HR increases aligned with shortened APDs which reflected restitution was occurring. As HR increased, hearts underwent rapid repolarization, consequently leading to shorter APDs and CaTDs. This indicates phenanthrene's capability of altering cardiac demands, and potentially inducing stress on the heart under acute exposure conditions.

This study is the first to examine the acute cardiotoxic effects of phenanthrene in adult cannulated zebrafish (*Danio rerio*) hearts using the contractile inhibitor mavacamten. Up until recently, blebbistatin was primarily used as a contractile inhibitor in teleost heart studies (Santini et al., 2020). The application of mavacamten in this study was shown to be effective as heart quiescence was achieved in a relatively short time (< 30 min) and maintained during acute exposure (< 2 h). This study recommends the use of mavacamten in future teleost cardiotoxicity studies.

Evidence for reversal of cardiac effects indicates phenanthrene does not irreversibly bind to the heart. As long as the natural perfusion ability of the heart is maintained, it is believed phenanthrene can be successfully washed out in an attempt to return the heart to its normal state. Reversal of cardiotoxic effects carries significant environmental implications for cardiac recovery. It suggests fish undergoing acute exposure to phenanthrene may not incur permanent cardiotoxic alterations if removed from its contaminated environment. Furthermore, it suggests fish may be able to avoid the exacerbation of cardiotoxic effects that could lead to impaired heart function or worse, lethality. Regardless, phenanthrene's ability to cause significant cardiotoxic effects in zebrafish should be cause for concern. Notably, this study utilized very low phenanthrene concentrations which poses the question if reversal of cardiotoxic effects is seen at higher concentrations. Future research should focus on assessing cardiac recovery over a larger range of phenanthrene

concentrations and exposure durations to better understand exposure risks to phenanthrene. Longer exposures could lead to cardiac damage which could deleteriously impact both individuals and populations.

3.6. General Conclusion

This study investigated the impact of phenanthrene, a prominent PAH and priority pollutant, on zebrafish embryonic development and adult cardiac function. The research reflects an environmentally-relevant exposure scenario as realistic concentrations and PD techniques were employed to explore the sublethal effects of phenanthrene. The study revealed that phenanthrene exposure led to dose-dependent increases in mortality during the embryonic development phase, with notable impacts on teratogenesis, including yolk and pericardial edema and tail kinking. Importantly, pericardial and yolk edema demonstrated the potential for reversibility. Particularly, evidence for pericardial edema reversal suggests phenanthrene exposure prior to heart development may not induce permanent cardiac effects as long as perfusion ability is maintained. Furthermore, the study assessed cardiotoxicity through in vitro analysis of adult cannulated hearts, revealing significant alterations in APD and CaTD, indicative of disrupted cardiac electrophysiology and calcium handling. These effects were associated with an increase in HR, suggesting potential proarrhythmic consequences.

These findings provide valuable insights into the understanding of phenanthrene's toxicity in fish. For one, they underscore the significance of considering both acute and developmental toxicity when assessing the ecological impact of PAH-contaminated environments. The literature has shown an organism’s susceptibility to a chemical varies drastically based on life stage, species type and chemical dosage. For instance, embryonic development in fish is highly sensitive to environmental stressors. Therefore, this study suggests evaluating PAH toxicity across both early and late life stages to fully assess the sublethal toxicity of PAH in fish. Previous research has primarily focused on the developmental impacts of phenanthrene on aquatic species; however, this study's emphasis on cardiotoxicity in zebrafish contributes a novel dimension to the comprehension of the health risks associated with phenanthrene exposure. This study suggests incorporating cardiotoxicity as an additional endpoint in PAH risk assessment to account for potential adverse cardiovascular effects. While in situ tests were employed for precise cardiac measurements in this study, whole organism exposures are more practical

in methodology and environmental relevance for PAH risk assessment. Therefore, whole organism exposures should be used to assess HR as a cardiotoxic endpoint for risk assessment, while situ tests can be applied to examine further cardiac endpoints.

Overall, the research demonstrates that phenanthrene exerts significant sublethal effects on both early and late teleost life stages. While these stages were assessed separately with distinct exposures, existing literature suggests that sublethal effects arising during embryogenesis may lead to chronic effects in adults (Incardona et al., 2004; Sørhus et al., 2023). Importantly, the study highlights the reversibility of both teratogenic and cardiotoxic effects at both embryonic and adult life stages, respectively. The degree of reversibility appears to be linked to phenanthrene's potency and the level of exposure.

This study contributes to the aquatic toxicology knowledge of phenanthrene, facilitating environmental assessment, monitoring, and risk evaluation. The absence of cardiac toxicology endpoints in existing literature underscores the need for effective assessment measures. Ultimately, this research can be used to mitigate phenanthrene contamination in aquatic environments, safeguarding both fish populations and overall ecosystem health.

3.7. References

Abdel-Shafy, H. I., & Mansour, M. S. M. (2016). A review on polycyclic aromatic hydrocarbons: Source, environmental impact, effect on human health and remediation. *Egyptian Journal of Petroleum*, *25*(1), 107–123. https://doi.org/10.1016/j.ejpe.2015.03.011

Ainerua, M. O., Tinwell, J., Kompella, S. N., Sørhus, E., White, K. N., van Dongen, B. E., & Shiels, H. A. (2020). Understanding the cardiac toxicity of the anthropogenic pollutant phenanthrene on the freshwater indicator species, the brown trout (Salmo trutta): From whole heart to cardiomyocytes. *Chemosphere (Oxford)*, *239*, 124608. https://doi.org/10.1016/j.chemosphere.2019.124608

Brette, F., Machado, B., Cros, C., Incardona, J. P., Scholz, N. L., & Block, B. A. (2014). Crude Oil Impairs Cardiac Excitation-Contraction Coupling in Fish. *Science (American Association for the Advancement of Science)*, *343*(6172), 772–776. https://doi.org/10.1126/science.1242747

Brette, F., Shiels, H. A., Galli, G. L. J., Cros, C., Incardona, J. P., Scholz, N. L., & Block, B. A. (2017). A Novel Cardiotoxic Mechanism for a Pervasive Global Pollutant. *Scientific Reports*, *7*(1), 41476. https://doi.org/10.1038/srep41476

Butler, J. D., Parkerton, T. F., Letinski, D. J., Bragin, G. E., Lampi, M. A., & Cooper, K. R. (2013). A novel passive dosing system for determining the toxicity of phenanthrene to early life stages of zebrafish. *The Science of the Total Environment*, *463-464*, 952–958. https://doi.org/10.1016/j.scitotenv.2013.06.079

Butler, J. D., Parkerton, T. F., Redman, A. D., Letinski, D. J., & Cooper, K. R. (2016). Assessing Aromatic-Hydrocarbon Toxicity to Fish Early Life Stages Using Passive-Dosing Methods and Target-Lipid and Chemical-Activity Models. *Environmental Science & Technology*, *50*(15), 8305–8315. https://doi.org/10.1021/acs.est.6b01758

Canadian Council on Animal Care. (2020). CCAC guidelines: Zebrafish and other small, warm-water laboratory fish. https://ccac.ca/Documents/Standards/Guidelines/CCAC_Guidelines-Zebrafish_and_other_small_warm-water_laboratory_fish.pdf

Clusin, W. T. (2008). Mechanisms of calcium transient and action potential alternans in cardiac cells and tissues. *American Journal of Physiology - Heart and Circulatory Physiology*, *294*(1), 1–10. https://doi.org/10.1152/ajpheart.00802.2007

Hicken, C.E., Linbo, T.L., Baldwin, D.H., Willis, M.L., Myers, M.S., Holland, L., Larsen, M., Stekoll, M.S., Rice, S.D., Collier, T.K., Scholz, N.L., Incardona, J.P., 2011. Sublethal exposure to crude oil during embryonic development alters cardiac morphology and reduces aerobic capacity in adult fish. *Proceedings of the National Academy of Science*. *108*: 7086-7090.

Incardona, J. P., Collier, T. K., & Scholz, N. L. (2004). Defects in cardiac function precede morphological abnormalities in fish embryos exposed to polycyclic aromatic hydrocarbons. *Toxicology and Applied Pharmacology*, *196*(2), 191–205. https://doi.org/10.1016/j.taap.2003.11.026

Incardona, J. P., Carls, M. G., Teraoka, H., Sloan, C. A., Collier, T. K., & Scholz, N. L. (2005). Aryl Hydrocarbon Receptor-Independent Toxicity of Weathered Crude Oil during Fish Development. *Environmental Health Perspectives*, *113*(12), 1755–1762. https://doi.org/10.1289/ehp.8230

Incardona, J. P., Carls, M. G., Day, H. L., Sloan, C. A., Bolton, J. L., Collier, T. K., & Scholz, N. L. (2009). Cardiac Arrhythmia Is the Primary Response of Embryonic Pacific Herring (Clupea pallasi) Exposed to Crude Oil during Weathering. *Environmental Science & Technology*, *43*(1), 201–207. https://doi.org/10.1021/es802270t

Incardona, J.P., Carls, M.G., Holland, L., Linbo, T.L., Baldwin, D.H., Myers, M.S., Peck, K.A., Tagal, M., Rice, S.D., Scholz, N.L. (2015). Very low embryonic crude oil exposures cause lasting cardiac effects in salmon and herring. *Scientific Reports. 5*: 13499. DOi: 10.1038/srep13499

Incardona, J. P., & Scholz, N. L. (2016). The influence of heart developmental anatomy on cardiotoxicity-based adverse outcome pathways in fish. *Aquatic Toxicology*, *177*, 515–525. https://doi.org/10.1016/j.aquatox.2016.06.016

Incardona, J. P. (2017). Molecular Mechanisms of Crude Oil Developmental Toxicity in Fish. *Archives of Environmental Contamination and Toxicology*, *73*(1), 19–32. https://doi.org/10.1007/s00244-017-0381-1

Kompella, S. N., Brette, F., Hancox, J. C., & Shiels, H. A. (2021). Phenanthrene impacts zebrafish cardiomyocyte excitability by inhibiting IKr and shortening action potential duration. The Journal of General Physiology, 153(2), 1. https://doi.org/10.1085/JGP.202012733

Fossa, A. A. (2017). Beat-to-beat ECG restitution: A review and proposal for a new biomarker to assess cardiac stress and ventricular tachyarrhythmia vulnerability. *Annals of Noninvasive Electrocardiology*, *22*(5), e12460–n/a. https://doi.org/10.1111/anec.12460

Lin, E., Shafaattalab, S., Gill, J., Al-Zeer, B., Craig, C., Lamothe, M., Rayani, K., Gunawan, M., Li, A. Y., Hove-Madsen, L., & Tibbits, G. F. (2020). Physiological phenotyping of the adult zebrafish heart. *Marine Genomics*, *49*, 100701–100701. https://doi.org/10.1016/j.margen.2019.100701

McGruer, V., Tanabe, P., Vliet, S. M. F., Dasgupta, S., Qian, L., Volz, D. C., & Schlenk, D. (2021). Effects of Phenanthrene Exposure on Cholesterol Homeostasis and Cardiotoxicity in Zebrafish Embryos. *Environmental Toxicology and Chemistry*, *40*(6), 1586–1595. https://doi.org/10.1002/etc.5002

Nemtsas, P., Wettwer, E., Christ, T., Weidinger, G., & Ravens, U. (2010). Adult zebrafish heart as a model for human heart? An electrophysiological study. *Journal of Molecular and Cellular Cardiology*, *48*(1), 161–171. https://doi.org/10.1016/j.yjmcc.2009.08.034

Panakova, D., Werdich, A.A. and Macrae, C.A. (2010). Wnt11 patterns a myocardial electrical gradient through regulation of the L-type Ca2+ channel. *Nature (London)*, *466*(7308), 874–878. https://doi.org/10.1038/nature09249

Rayani, K., Lin, E., Craig, C., Lamothe, M., Shafaattalab, S., Gunawan, M., Yueh Li., A., Hove-Madsen, L., Tibbits, G.F., 2018. Zebrafish as a model of mammalian cardiac function: Optically mapping the interplay of temperature and rate on voltage and calcium dynamics. *Progress in Biophysics and Molecular Biology*. 1-23. https://doi.org/10.1016/j.pbiomolbio.2018.07.006

Renegar, D. A., Turner, N. R., Riegl, B. M., Dodge, R. E., Knap, A. H., & Schuler, P. A. (2017). Acute and subacute toxicity of the polycyclic aromatic hydrocarbon 1-methylnaphthalene to the shallow-water coral Porites divaricata: Application of a novel exposure protocol. *Environmental Toxicology and Chemistry*, *36*(1), 212–219. https://doi.org/10.1002/etc.3530

Santini, L., Palandri, C., Nediani, C., Cerbai, E., & Coppini, R. (2020). Modelling genetic diseases for drug development: Hypertrophic cardiomyopathy. *Pharmacological Research*, *160*, 105176–105176. https://doi.org/10.1016/j.phrs.2020.105176

Sørhus, E., Nakken, C. L., Donald, C. E., Ripley, D. M., Shiels, H. A., & Meier, S. (2023). Cardiac toxicity of phenanthrene depends on developmental stage in Atlantic cod (Gadus morhua). *The Science of the Total Environment*, *881*, 163484–163484. https://doi.org/10.1016/j.scitotenv.2023.163484

Strykowski, J. L., & Schech, J. M. (2015). Effectiveness of Recommended Euthanasia Methods in Larval Zebrafish (Danio rerio). *Journal of the American Association for Laboratory Animal Science*, *54*(1), 81–84.

Tsai, C.-T., Wu, C.-K., Chiang, F.-T., Tseng, C.-D., Lee, J.-K., Yu, C.-C., Wang, Y.-C., Lai, L.-P., Lin, J.-L., & Hwang, J.-J. (2011). In-vitro recording of adult zebrafish heart electrocardiogram — A platform for pharmacological testing. *Clinica Chimica Acta*, *412*(21), 1963–1967. https://doi.org/10.1016/j.cca.2011.07.002

Wallace, C.K., Bright, L.A., Marx, J.O., Andersen, R.P., Mullins, M.C., Carty, A.J., 2018. Effectiveness of Rapid Cooling as a Method of Euthanasia for Young Zebrafish (*Danio rerio*). J Am Assoc Lab Anim Sci. 57(1): 58-63. https://www.ncbi.nlm.nih.gov/pmc/articles/PMC5875099/

Wei, X., Yohannan, S. and Richards, J.R. (2023). Physiology, cardiac repolarization dispersion and reserve. In: StatPearls [Internet]. Treasure Island (FL): StatPearls Publishing; 2023 Jan-. Available from: https://www.ncbi.nlm.nih.gov/books/NBK537194/

Zakaria, Z. Z., Benslimane, F. M., Nasrallah, G. K., Shurbaji, S., Younes, N. N., Mraiche, F., Da'as, S. I., & Yalcin, H. C. (2018). Using Zebrafish for Investigating the Molecular Mechanisms of Drug-Induced Cardiotoxicity. *BioMed Research International*, *2018*, 1642684–10. https://doi.org/10.1155/2018/1642684

Zhang, Y., Chen, Y., Xu, K., Xia, S., Aihaiti, A., Zhu, M., & Wang, C. (2023). Exposure of embryos to phenanthrene impacts the cardiac development in F1 zebrafish larvae and potential reasons. *Environmental Science and Pollution Research International*, *30*(18), 52369–52379. https://doi.org/10.1007/s11356-023-26165-4

Appendix A.

Methodology Figures

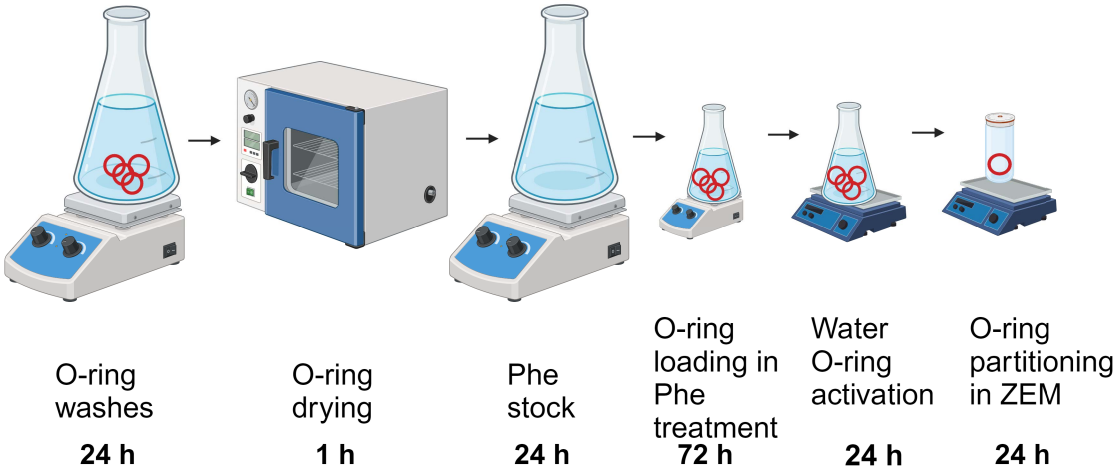

Figure A.1. **Silicone O-ring preparation for passive dosing exposure showing various stages: O-ring solvent washes [ethyl acetate (1x), methanol (3x), and distilled water (3x)] and drying, phenanthrene (Phe) stock preparation, O-ring loading in Phe treatments, water O-ring activation and O-ring partitioning into ZEM (zebrafish embryo medium).**

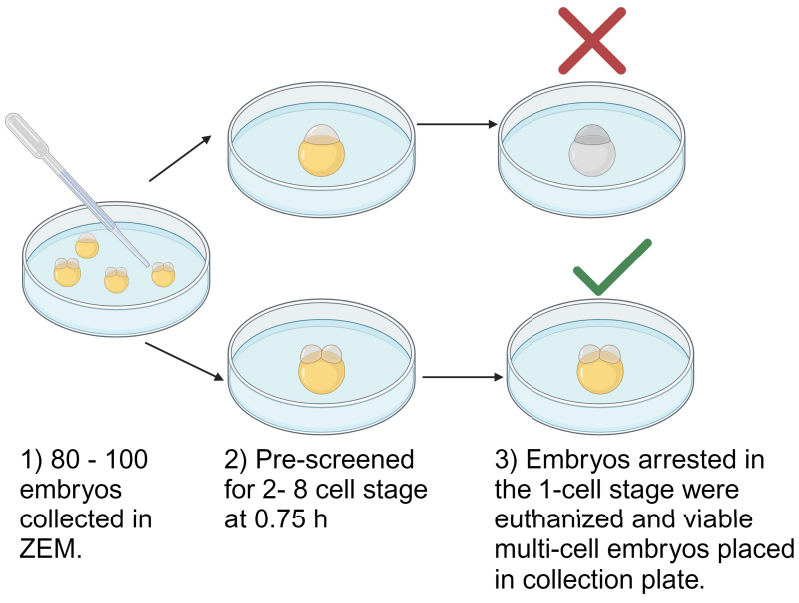

Figure A.2. **Experimental design for pre-screening process of *Danio rerio* embryos at 0.75 hpf. Embryo selection and exposures done in accordance of OECD guidelines (2013).**

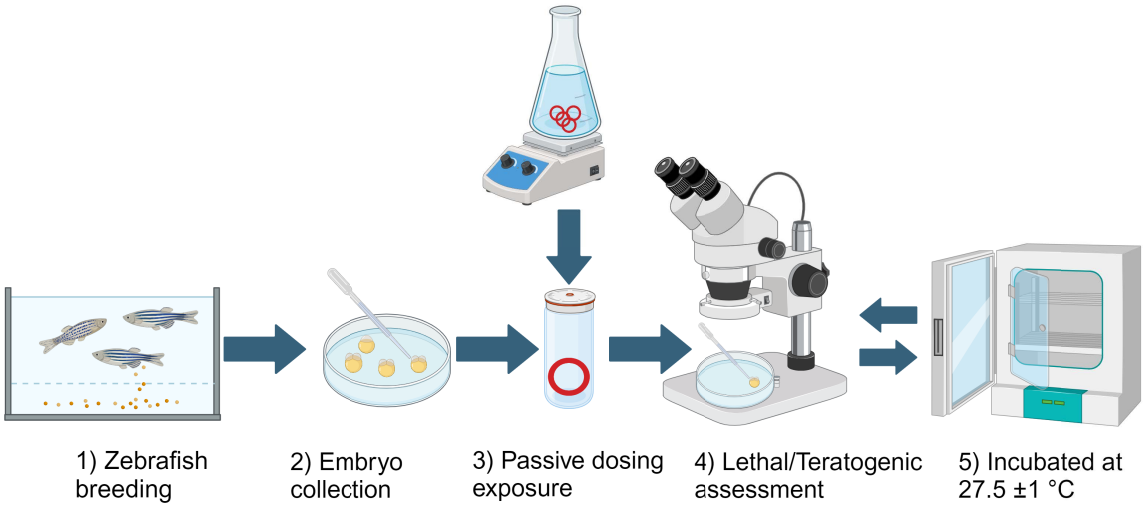

Figure A.3. **Design for acute 5-d passive dosing (PD) exposure of *Danio rerio* embryos to phenanthrene-loaded O-rings. Embryos selected from 2:1 female: male breeding ratio were individually exposed in glass scintillation vials by PD and assessed daily for lethal and teratogenic effects under a stereomicroscope. Treatments were incubated (27.5 ±1 °C) over exposure.**

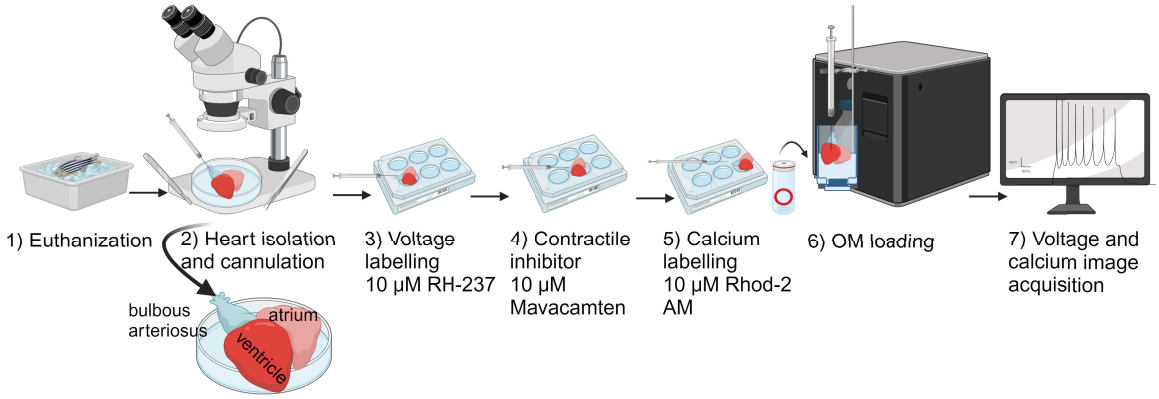

Figure A.4. **Late life stage (LLS) in-vitro exposure design for adult *Danio rerio* hearts for the assessment of phenanthrene cardiotoxicity. Treatments prepped through passive dosing and hearts cannulated (34-gauge needle syringe) and run on an optical mapping (OM) rig for potentiometric measurements of voltage and calcium transient.**

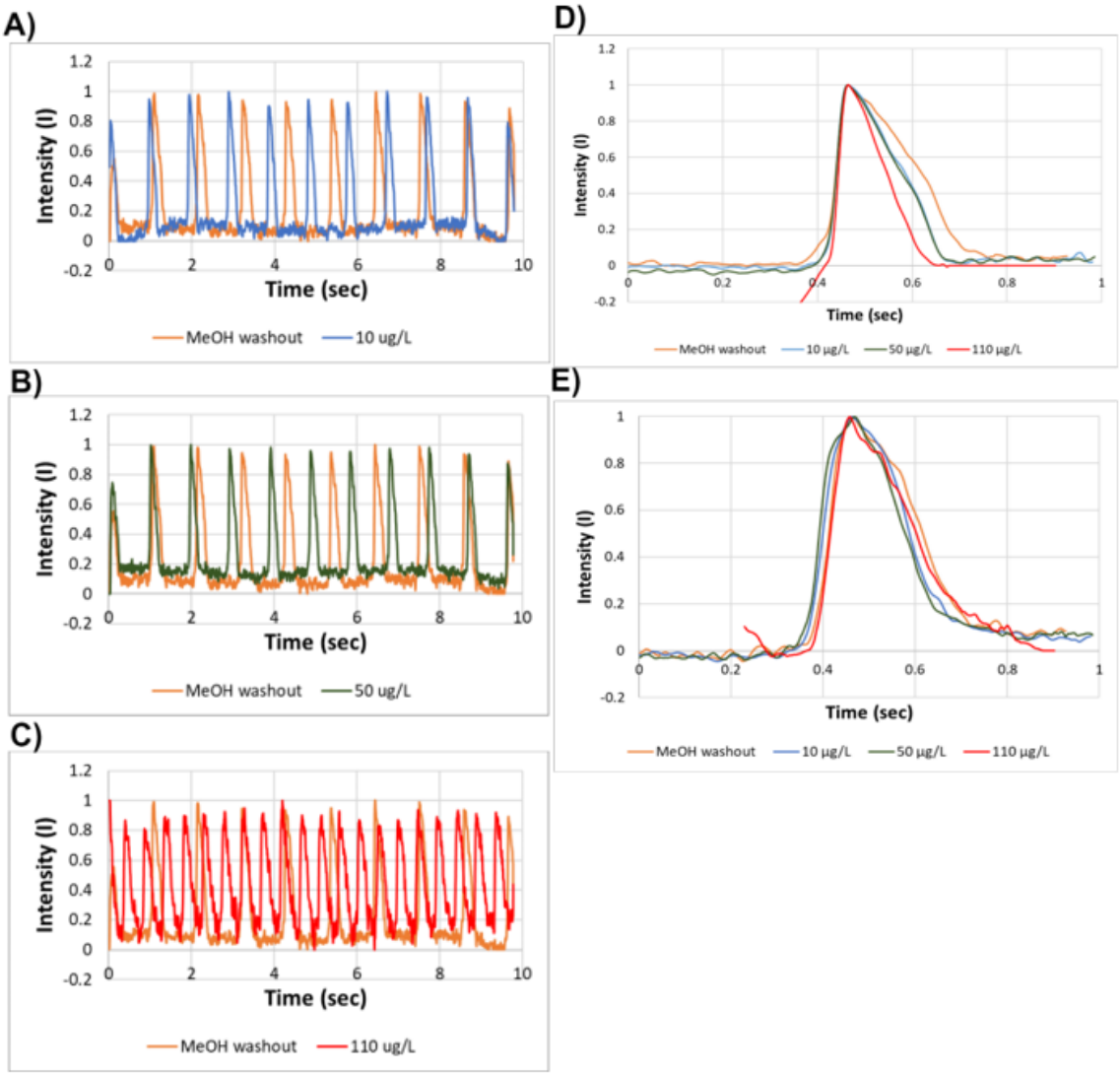

Figure A.5. **Sample voltage and calcium transient traces of isolated adult *Danio rerio* hearts computed from IDL software. All values are normalized to a control heart exposed to methanol (100 %). Hearts exposed to phenanthrene (10, 50, 110 µg/L) yielded intensity traces showing heartrate (A-C), action potential duration (D) and calcium transient duration (E).**

Appendix B.

Phenanthrene O-ring Example Calculation

Table B.1. Passive dosing O-ring parameters used for phenanthrene target concentrations (50, 110, 150, 200, 275, and 350 µg/L) for loading rings. Partitioning calculations based off of Renegar et al. (2017) equation (Equation 2.1.)

Phe Conc (µg/L)	K(MeOH-Pdms)	# Rings	Ring density	Mass of 1 Ring	Total ring mass	V O-ring (mL)	V MeOH (mL)	K(Pdms-Water)	V(Water) (mL)	Target C(mg/L)	mg per L MeOH
50	2.69	12	1.09	0.37	4.42	4.06	200	7585.78	20	0.05	1029.23
110	2.69	12	1.09	0.37	4.42	4.06	200	7585.78	20	0.11	2264.31
150	2.69	12	1.09	0.37	4.42	4.06	200	7585.78	20	0.15	3087.70
200	2.69	12	1.09	0.37	4.42	4.06	200	7585.78	20	0.20	4116.93
275	2.69	12	1.09	0.37	4.42	4.06	200	7585.78	20	0.28	5660.78
350	2.69	12	1.09	0.37	4.42	4.06	200	7585.78	20	0.35	7204.63

Equation B.1. The derivation of the phenanthrene (Phe) stock concentration (C1) used for serial dilutions in methanol for the preparation of Phe target concentrations (50, 110, 150, 200, 275, and 350 µg/L). K values were obtained from Huntsman (2022). O-ring loading and partitioning equation based on Renegar et al. (2017).

$$C_{MeOH} = \left(K_{MeOH\text{-}PDMS} + \frac{[V_{PDMS}]}{[V_{MeOH}]}\right) \times \left(K_{PDMS\text{-}Water} + \frac{[V_{Water}]}{[V_{PDMS}]}\right) \times C_{Target}$$

$$C_{MeOH} = \left(0.43 + \frac{[4.06]}{[200]}\right) \times \left(3.88 + \frac{[20]}{[4.06]}\right) \times 0.35$$

C = 7204.63 mg/L

C1 = 7.204 g/L

Table B.2. Target phenanthrene (Phe) stock volumes (V1) used for serial dilutions of stock (350 µg/L) in methanol for the preparation of Phe target concentrations (50, 110, 150, 200, 275, and 350 µg/L). C1 is the initial concentration of phenanthrene stock in methanol (g/mL) and C2 the target dilutant concentration based on the Renegar et al. (2017) partitioning equation.

Phe Conc (µg/L)	C1 (g/mL)	C2 (g/mL)	V1 (mL)	V2 (mL)
275	7.20	5.66	157	200
200	7.20	4.12	114	200
150	7.20	3.09	86	200
110	7.20	2.26	63	200
50	7.20	1.03	29	200

Appendix C.

Teratogenicity Figures

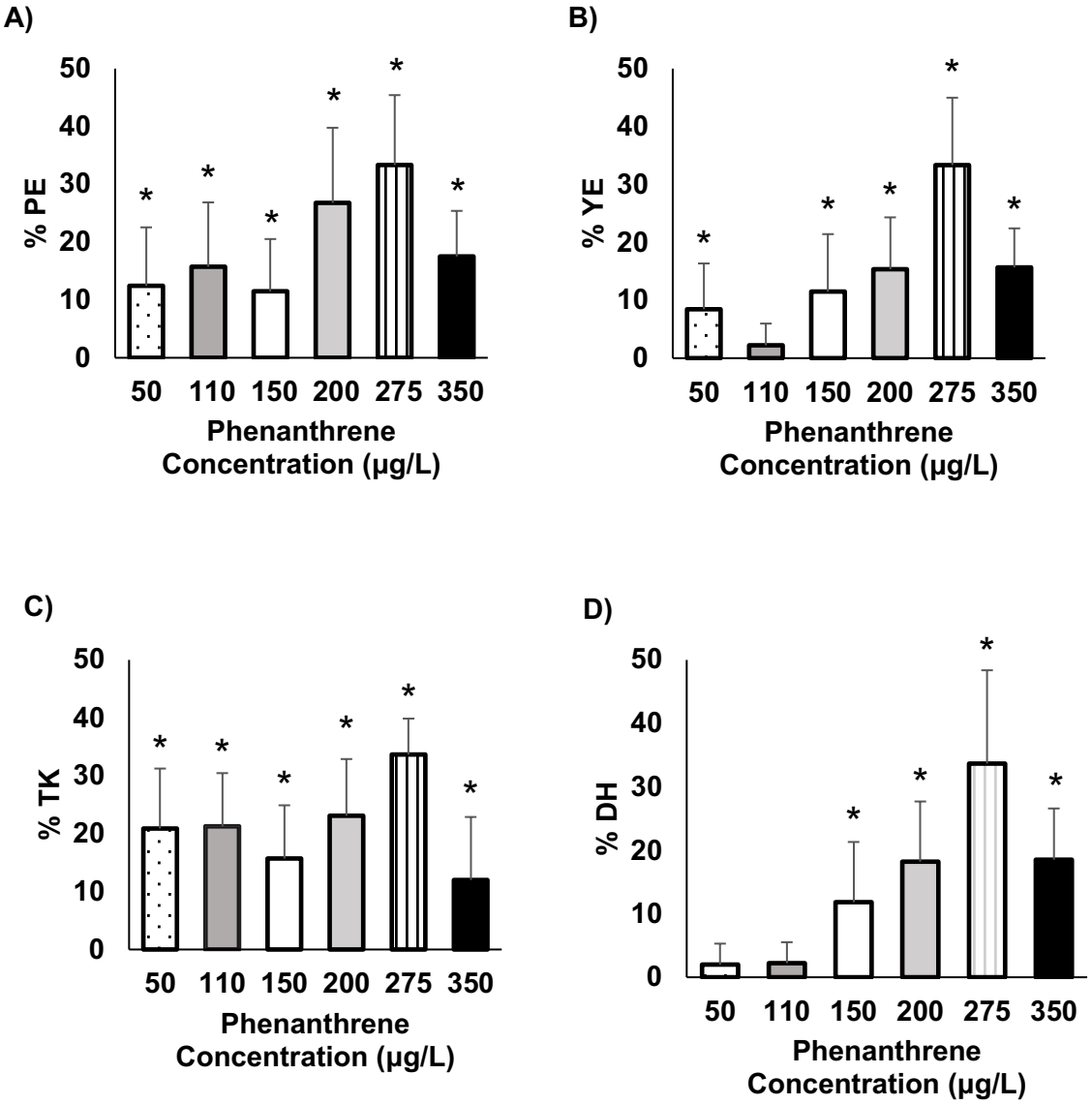

Figure C.1. **Day 5 % effects for PE (A), YE (B), TK (C) and DH (D) in *Danio rerio* survivors across all phenanthrene treatment concentrations. Each column represents the normalized mean % for the respective effect. Values were normalized to the methanol control. Error bars represent standard error values at the 95 % confidence level. Asterix denote significant difference between treatments ($p < 0.05$). Total sample size over the 5 runs yielded 350 embryos (50 per treatment).**

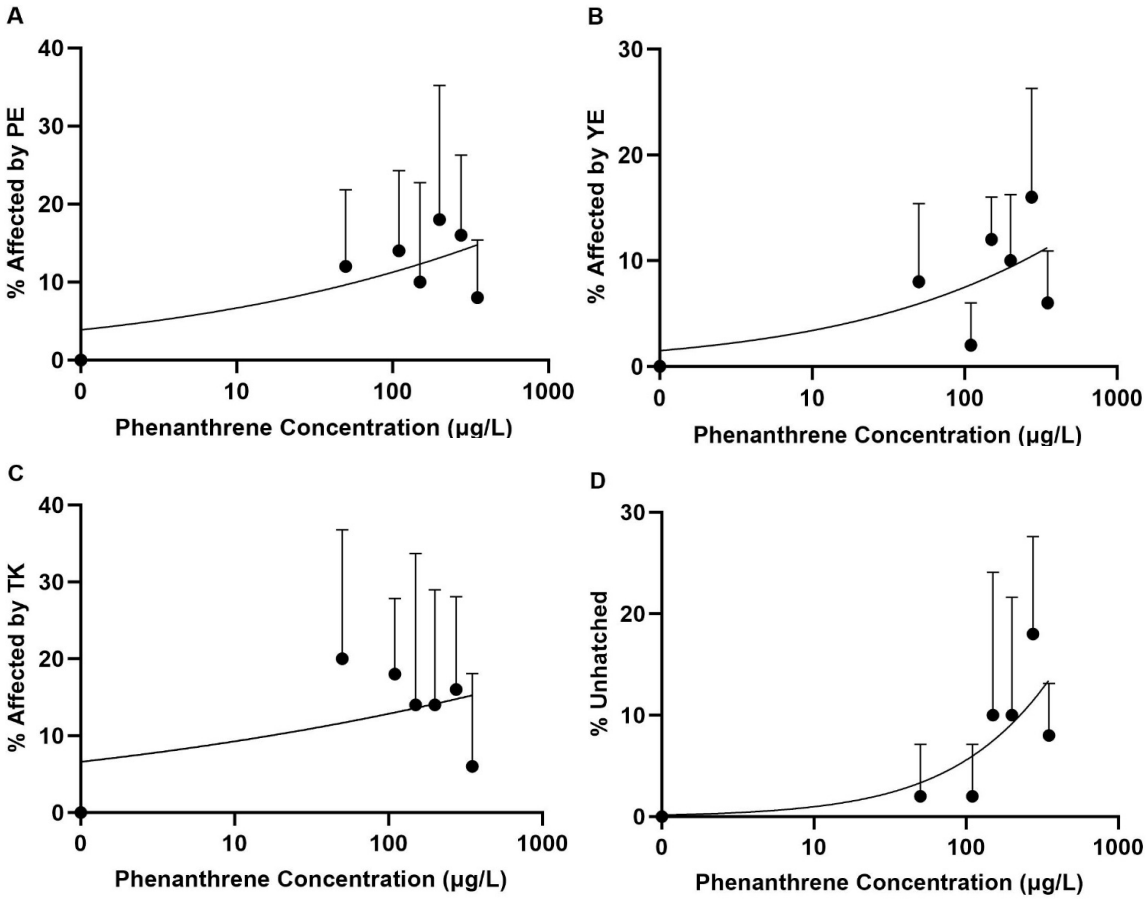

Figure C.2. **Phenanthrene concentration – effects curves for *Danio rerio* embryos at 5 d. 120-h EC10 values in order of the teratogenic effects PE, YE, TK and DH reported as follows: 58.4 µg/L (A), 122 µg/L (B), 16.9 µg/L (C) and 226 µg/L (D). Each point represents the normalized mean % mortality for a respective treatment concentration. Values were normalized to the methanol control. Error bars represent standard error values at the 95% confidence level. Total sample size over the 5 runs yielded 350 embryos (50 per treatment).**

Appendix D.

Cardiotoxicity Summary Data

Table D.1. Summary data for phenanthrene cardiotoxic effects in adult *Danio rerio* hearts: action potential duration (APD), calcium transient duration (CaTD) and heartrate (HR). Mean % values were normalized to a methanol control (100 %) and reported at the 95 % confidence interval. P-values for the fixed effect test for the effect of concentration on each cardiac parameter are also included. (*n* = 14 – 15).

Phenanthrene Concentration (µg/L)	HR		APD50		APD75		CaTD50		CaTD75	
	% Mean	2 SE	% Mean	2 SE	% Mean	2 SE	% Mean	2 SE	% Mean	2 SE
10	87.9	18.7	117.2	18.6	116.6	18.4	112.2	29.0	116.6	30.1
50	113.1	18.7	96.5	18.6	99.3	18.4	101.6	29.0	102.9	30.1
110	169.7	19.3	73.7	19.1	76.1	18.9	89.2	30.0	94.8	31.1
0 (MeOH washout)	80.8	19.3	133.7	19.1	117.3	18.9	176.2	30.0	175.2	31.1
Fixed effect test (concentration)	P < 0.0001		P < 0.0001		P = 0.0017		P = 0.0001		P < 0.0005	